Marine and Petroleum Geology 107 (2019) 527–554

Contents lists available at ScienceDirect

Marine and Petroleum Geology

journal homepage: www.elsevier.com/locate/marpetgeo

Review article

# A review of the nature and origin of limestone microporosity

Mohammed S. Hashim*, Stephen E. Kaczmarek

*Department of Geological and Environmental Sciences, Western Michigan University, Kalamazoo, MI, 49008, USA*

ARTICLE INFO

*Keywords:*
Review
Microporosity
Limestone
Micrite
Carbonate Diagensis
Reservoir Characterization
Lime Mud
Stabilization

ABSTRACT

Limestone microporosity is ubiquitous and extensively developed in most Phanerozoic limestones. From an economic perspective, microporosity is important because it contributes substantially to the carbonate pore system, which can host significant volumes of water and hydrocarbons. Therefore, determining the presence and distribution of limestone micropores is necessary for accurate hydrocarbon estimations, reservoir characterization, and fluid flow simulations. From an academic standpoint, microporosity is important because its genesis is intimately linked with the mineralogical stabilization of metastable sediments, a fundamental process in carbonate diagenesis.

Many types of micropores contribute to what has been referred to as microporosity, but the vast majority is hosted among low-magnesium calcite (LMC) microcrystals that are present in limestone matrix and allochems. Geochemical, textural, and mineralogical data from natural settings and laboratory experiments indicate that LMC microcrystals are diagenetic in origin. More specifically, these data support a diagenetic model of mineralogical stabilization that involves dissolution of precursor sediments dominated by aragonite and high-magnesium calcite (HMC) minerals, and precipitation of LMC microcrystal cements. The stabilization process is inferred to take place in the meteoric, marine, and burial diagenetic realms. Although it has not been directly observed, carbon and oxygen isotopes, as well as trace element data suggest that LMC microcrystals form during burial diagenesis in marine-like fluids.

Evidence suggests that porosity is not generated during this dissolution-precipitation process, but rather inherited from the precursor sediments. The final arrangement of the micropores in a limestone, however, depends on the precise diagenetic pathway. LMC microcrystals exhibit a range of microcrystalline textures that are classified on the basis of crystal morphology and size. The three main textural classes - granular (framework), fitted (mosaic), and clustered - have been recognized across a wide range of ages, depositional settings, burial depths, and precursor types, and are characterized by distinct petrophysical properties, such as porosity, permeability, and pore-throat size.

Observations from modern sediments also support the hypothesis that LMC microcrystals develop from aragonite and HMC dominated lime mud. The origin of lime mud has been extensively studied but still highly debated. Of particular interest to the discussion of microporosity are proposed secular variations in the dominant mineralogy of carbonate sediments through the Phanerozoic. Microporous limestones comprised of LMC microcrystals are equally abundant during times of aragonite seas and calcite seas, which suggests that no special mineral precursor is required. Microporous textures are also observed in deep marine chalks where micropores are hosted between chalk constituents. Unlike shallow marine limestones, deep marine sediments start out as mostly LMC therefore mineralogical stabilization is not a significant process in chalk diagenesis.

## 1. Introduction

Porosity is perhaps the most important petrophysical property of a carbonate rock. Pore abundance (storage capacity) and connectivity (permeability) are routinely used to characterize limestone reservoirs in terms of economic value, and as a means of assessing diagenetic alteration (Lucia, 2007; Moore and Wade, 2013). Whereas conventional porosity models focus on the macroscopic pores located between larger carbonate allochems (Archie, 1952; Choquette and Pray, 1970), new research shows that most carbonates host vastly more complicated pore systems, particularly at the micrometer scale (Lucia, 1995; Lønøy, 2006).

Limestone microporosity refers to the abundance of micrometer-size pores common in a wide variety of ancient limestones (Wright et al.,

* Corresponding author.
*E-mail address:* mohammed.s.hashim@wmich.edu (M.S. Hashim).

https://doi.org/10.1016/j.marpetgeo.2019.03.037
Received 24 January 2019; Received in revised form 28 March 2019; Accepted 29 March 2019
Available online 11 April 2019
0264-8172/ © 2019 Elsevier Ltd. All rights reserved.

**Table 1**
Non-exhaustive list of studies that investigated limestone microporosity organized by geologic age. All studies are in marine limestones, unless otherwise noted.

| Age | Location | Altered Material | Reference |
|---|---|---|---|
| Holocene | Bahamas | Aragonite Mud | Steinen (1982) |
| Pleistocene | Barbados | Aragonite Mud | Steinen (1978) |
| Pleistocene and Oligocene | Enewetak Atoll, Marshall Islands | Matrix, Coral, Halimeda, Mollusks | Saller and Moore (1989) |
| Miocene–Pleistocene | Bahamas | Matrix | Lucia (2017) |
| Miocene–Pleistocene | Bahamas | Matrix & Allochems | Lucia and Loucks (2013) |
| Neogene | Bahamas | Matrix | Melim et al. (2002) |
| Miocene (lacustrine) | Spain | Matrix | Volery et al. (2010a) |
| Miocene | Spain | Matrix | Wright et al. (1997) |
| Oligocene–Pleistocene | Florida, U.S.A., Bahamas, Mexico, Italy | Matrix | Lasemi and Sandberg (1984, 1993) |
| Eocene | Tunisia | Nummulite, Red Algae | Loucks et al. (1998) |
| Eocene | Florida, U.S.A. | Matrix | Maliva et al. (2009) |
| Paleogene (lacustrine) | Spain | Matrix | Arribas et al. (2004) |
| Paleocene | Spain | Matrix | da Silva et al. (2009) |
| Cretaceous – Holocene | Ontong Java Plateau, Pacific Ocean | Chalk | Borre and Fabricius (1998) |
| Cretaceous & Miocene | U.A.E., Indonesia, Iran | Matrix | Moshier (1989a,1989b) |
| Cretaceous & Paleogene | North Sea | Chalk | Fabricius et al. (2008) |
| Cretaceous | U.A.E. | Matrix | Budd (1989) |
| Cretaceous | Oman, Middle East | Matrix | Al-Awar and Humphrey (2000) |
| Cretaceous | U.A.E. | Matrix | Cox et al. (2010) |
| Cretaceous | Belgium, France, UK | Chalk | Descamps et al. (2017) |
| Cretaceous | Middle East | Matrix | Deville de Periere et al. (2011) |
| Cretaceous | Albania | Matrix | Dewever et al. (2007) |
| Cretaceous | Belgium, England, France | Chalk | Faÿ-Gomord et al. (2016) |
| Cretaceous | U.A.E. | Matrix | Flügel (2004) |
| Cretaceous | Egypt | Chalk | Holail and Lohmann (1994) |
| Cretaceous | U.S.A. | Matrix, Allochems | Loucks et al. (2017) |
| Cretaceous | Oman, Bahrain, Iraq, Qatar, Syria, Saudi Arabia | Matrix | Volery et al. (2009) |
| Cretaceous | U.A.E. | Peloids, Skeletal Fragments | Morad et al. (2019) |
| Cretaceous | U.A.E. | Peloids | Morad et al. (2018) |
| Cretaceous | Texas, U.S.A. | Matrix, Peloids | Perkins (1989) |
| Cretaceous | Texas, U.S.A. | Peloids, Forams, Intraclasts | Van Simaeys et al. (2017) |
| Cretaceous | Texas, U.S.A. | Matrix | Longman and Mench (1978) |
| Cretaceous | Texas, U.S.A. | Matrix, Peloids, Forams, Mollusks, Red Algae | Loucks et al. (2013) |
| Cretaceous | Nova Scotia, Canada | Chalk | Ings et al. (2005) |
| Cretaceous | France | Matrix, Peloids, | Fournier and Borgomano (2009) |
| Cretaceous | France | Matrix, Peloids | Richard et al. (2007) |
| Jurassic & Cretaceous | U.A.E. | – | Marzouk et al. (1998) |
| Jurassic & Cretaceous | Iraq, U.A.E. | Matrix | Lambert et al. (2006) |
| Jurassic & Cretaceous | France, Switzerland | Matrix | Joachimski (1994) |
| Jurassic & Cretaceous | France | Matrix | Volery et al. (2010b) |
| Jurassic | France | Matrix | Brigaud et al. (2010) |
| Jurassic | France | – | Humbert (1976) |
| Jurassic | France | Matrix, Micritized Grains | Carpentier et al. (2015) |
| Jurassic | France | Matrix | Loreau (1972) |
| Jurassic | Germany | Matrix | Munnecke et al. (2008) |
| Jurassic | U.K. | Ooids, Micritized Bioclasts | Heasley et al. (2000) |
| Jurassic | U.K. | Ooids | Sellwood and Beckett (1991) |
| Jurassic | Saudi Arabia | Peloids, Matrix, Forams, Ooids | Cantrell and Hagerty (1999) |
| Jurassic | Saudi Arabia | Matrix and Grains | Clerke et al. (2008) |
| Jurassic | Spain | Matrix | Coimbra et al. (2009) |
| Jurassic | Texas, U.S.A. | Ooids | Ahr (1989) |
| Jurassic | Texas, U.S.A. | Ooids | Dravis (1989) |
| Permian & Cretaceous | Middle East | – | Tavakoli and Jamalian (2018) |
| Permian | U.S.A. | Matrix, Ooids, Pisolites, Micritized Intraclasts | Pittman (1971) |
| Carboniferous | Canada | Matrix, Allochems | Njiekak et al. (2018) |
| Devonian – Paleogene | U.S.A., Canada, Middle East, Europe, North Africa | Matrix, Peloids, Ooids, Forams, Corals, Red Algae, Green Algae, Stromatoporoids, Bivalves, Brachiopods, Echinoderms | Hasiuk et al. (2016) |
| Devonian–Oligocene | U.S.A., Canada, Middle East, South America, Southeast Asia, Europe, North Africa | Matrix, Peloids, Ooids, Forams, Corals, Red Algae, Green Algae, Stromatoporoids, Bivalves, Brachiopods, Echinoderms | Kaczmarek et al. (2015) |
| Devonian – Carboniferous | The Caspian Sea, Kazakhstan | Matrix, Micritized Grains | Dickson and Kenter (2014) |
| Devonian | Canada | Stromatoporoid, Peloids | Kaldi (1989) |
| Devonian | Canada | Stromatoporoid, Peloids | Al-Aasm and Azmy (1996) |
| Silurian & Pliocene | Bahamas, Sweden | Matrix | Munnecke et al. (1997) |
| Ordovician | Canada | Matrix | Oldershaw (1972) |

1997; Fabricius, 2007). Microporosity has been reported in Phanerozoic limestone reservoirs throughout the Middle East, North Africa, Southeast Asia, the Caspian region, North America, South America, and Europe (Table 1). In many of these reservoirs, microporosity constitutes a significant proportion of the total pore system (e.g., Kaczmarek et al., 2015; Van Simaeys et al., 2017). It is therefore essential to understand the occurrence and distribution of microporosity in limestone reservoirs (Fullmer et al., 2014).

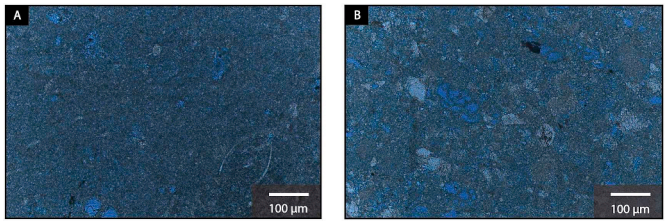


**Fig. 1.** Thin section photomicrographs of Cretaceous-age limestones from Middle East. The blue haze appearance characterizes microporous areas within the matrix, whereas the lighter blue areas characterize macropores.

Microporosity is an important research topic for several economic reasons. First, limestone micropores can host significant volumes of oil and gas, particularly when the hydrocarbon column is thick enough to overcome the entry pressure of the small pore throats (Illing et al., 1967; Pittman, 1971). More commonly perhaps, micropores are filled with bound, immobile water that is detected on resistivity log responses, leading to erroneous hydrocarbon estimations (Kieke and Hartmann, 1974; Keith and Pittman, 1983; Cantrell and Hagerty, 1999). The distribution of microporosity in a reservoir must be considered for accurate volumes and fluid flow simulations of both hydrocarbon reservoirs and groundwater aquifers (Akbar et al., 2000; Harland et al., 2015).

Historically, much of what we know about limestone microporosity comes from studies by the oil and gas industry. In fact, microporosity was originally inferred by geologists trying to explain limestone reservoirs exhibiting high porosities but abnormally low permeabilities (Archie, 1952; Clerke et al., 2008; Clerke, 2009a,b). Amongst carbonate petrographers, microporosity is commonly implicated by the presence of the "blue haze" observed in blue epoxy-impregnated petrographic thin sections (Fig. 1) (Saller and Moore, 1989; Cantrell and Hagerty, 1999). More recently, advanced electron imaging techniques has permitted high-resolution characterization of these small pores (see review by Milliken and Curtis, 2016). These analyses reveal that microporosity can take on a wide variety of forms, including microporous grains and matrix, microvugs, microchannels, and micropores between equant and fibrous cement crystals (Moshier, 1987; Moshier, 1989a; Al-Aasm and Azmy, 1996; Cantrell and Hagerty, 1999, Figs. 2 and 3). Additionally, microporosity is also observed in dolomites (e.g., Slowakiewicz et al., 2016; Perri et al., 2017). This paper, however, reviews limestone microporosity only.

In addition to its economic importance, detailed examination of the microcrystals associated with limestone micropores may shed light on mineralogical stabilization; a fundamental process in carbonate diagenesis. In fact, the first observations of limestone microporosity came from investigations focused on the origin and diagenesis of lime mud (Gee et al., 1932; Bathurst, 1958, 1959b; Folk, 1959, 1965, 1974).

Microporosity was the focus of a technical session on "Reservoir Diagenesis and the Evolution of Micro- and Macro-Pore Networks in Carbonate Rocks" at the 1987 SEPM conference hosted in Austin, Texas. Seven of the papers presented at that conference were published in a 1989 special issue of *Sedimentary Geology* (edited by C.R. Handford, R.G. Loucks, and S.O. Moshier) devoted to the topics of limestone microporosity and lime mud diagenesis. The studies included in this volume (Ahr, 1989; Budd, 1989; Dravis, 1989; Kaldi, 1989; Moshier, 1989a, 1989b; Perkins, 1989; Saller and Moore, 1989) not only established a number of foundational observations that still hold true today, they also set the tone for research on this topic for the following three decades. The major findings in this volume can be summarized as follows: (1) The majority of limestone microporosity is attributed to micropores hosted between LMC microcrystals (e.g., Budd, 1989; Moshier, 1989a); (2) LMC microcrystals occur both in matrix and allochems in a wide variety of shallow marine limestones (Ahr, 1989; Budd, 1989; Moshier, 1989a); (3) LMC microcrystals are diagenetic products formed

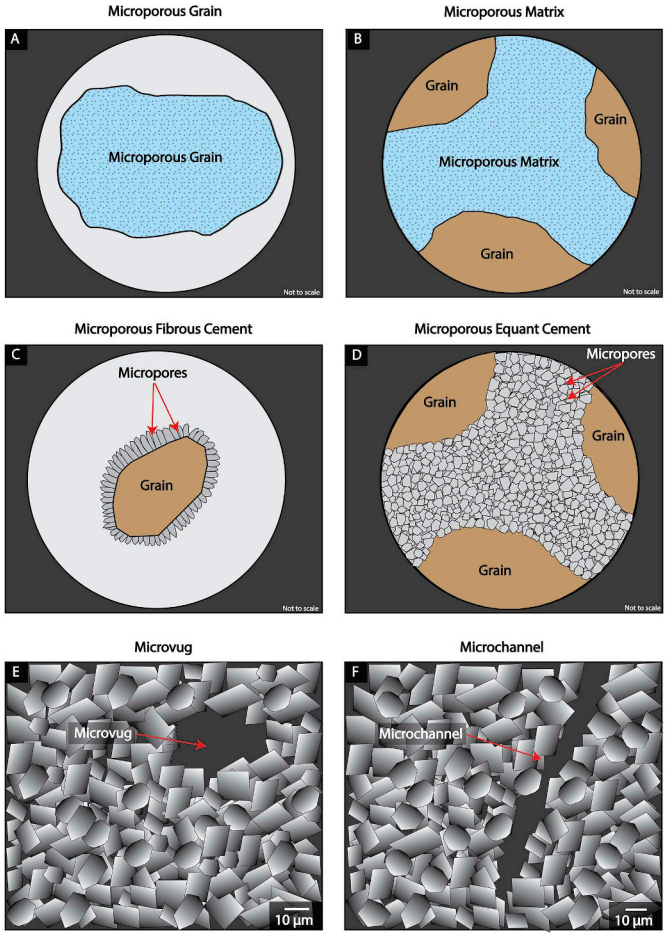


**Fig. 2.** Schematic illustration of the different micropore types in limestones as they appear under light microscope (A, B, C, and D) and under SEM (E and F). A) Microporous grain characterized by blue haze appearance. The Micropores are hosted among LMC microcrystals within the grain. B) Microporous matrix characterized by blue haze appearance, where the micropores are hosted between LMC microcrystals in the matrix. C) Micropores hosted between fibrous cement crystals. D) Micropores hosted between equant cement crystals. E) Microvug occurs among LMC microcrystals. F) Microchannel within matrix.

during mineralogical stabilization of metastable carbonate sediments (Budd, 1989; Moshier, 1989a; Saller and Moore, 1989); (4) Variations in LMC microtexture are linked to porosity and permeability attributes (Moshier, 1989a). Although these studies revolutionized how carbonate geologists think about the nature and genesis of limestone microporosity, they naturally raised a number of important questions: (1) What is the mineralogy and texture of the precursor sediment? (2) How many different types of LMC microcrystals exist? (3) What are the depositional and diagenetic conditions that promote microporosity development? (4) What type of LMC microcrystal result from the process of mineralogical stabilization? (5) What is the role of the different diagenetic processes, such as dissolution, compaction, and cementation in modifying the texture of LMC microcrystals?

Since 1989, significant advancements have been made in our understanding of limestone microporosity, particularly in terms of the questions listed above. Therefore, the current review is intended to supplement the review by Moshier (1989a), and to discuss new scientific understanding since publication of the seminal *Sedimentary Geology* volume. The goal of this review is to serve as both an entry point for geoscientists and engineers interested in learning about limestone microporosity, as well as an in-depth reference guide for those looking to learn about the developments during the past three decades. The review uses as a focal point the concept of a diagenetic origin of LMC

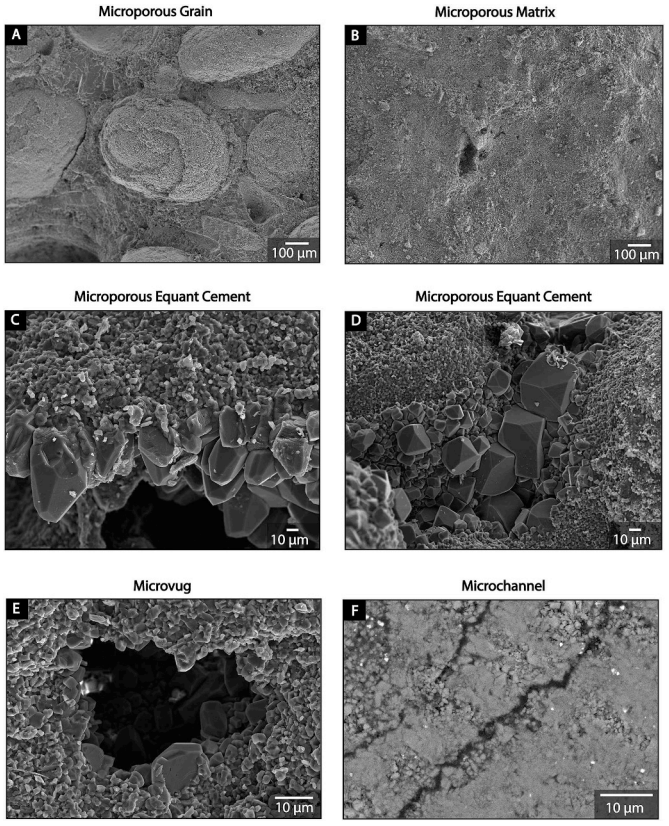


**Fig. 3.** SEM photomicrographs showing various micropore types (illustrated in Fig. 2). A) Microporous grain (an ooid) where micropores are hosted within LMC microcrystals in a Cretaceous-age limestone from Europe. B) Microporous matrix where micropores are hosted within LMC microcrystals in a Cretaceous-age limestone from Europe. C) Micropores hosted within equant cement crystals (spar) in a Devonian-age limestone from Canada. D) Another example of micropores hosted within cement crystals in Jurassic limestone from USA. E) SEM photomicrograph showing a microvug within a matrix of LMC microcrystals in a Devonian limestone from Alberta, Canada. F) SEM photomicrograph of a thin section showing a microchannel within matrix in a Cretaceous-age limestone from France.

microcrystals that host the majority of micropores. Important terminology will be discussed followed by a review of precursor sediments in terms of their origin, mineralogy, and texture prior to diagenetic alteration. To accomplish this objective, the origins of modern lime mud and carbonate allochems will also be discussed as well as the proposed secular variations of the dominant carbonate depositional mineralogy throughout the Phanerozoic. An overview of LMC microcrystals and associated micropores is also provided, with special attention given to the various textural classification schemes and the relationship between texture and petrophysical properties. Lastly, the diagenetic processes responsible for transforming metastable lime mud and grains into a more stable collection of LMC microcrystals will be discussed.

## 2. Definitions and terminology

As is the case with any subject that has been studied by researchers from a variety of disciplines, the literature on limestone microporosity is rife with confusing, and sometimes contradictory terminology. For example, in addition to microporosity and microporous, the terms chalky, earthy, pinpoint, and intramicrite porosity are commonly used in the petroleum geology literature to describe limestone rocks exhibiting high porosity but low permeability (Archie, 1952; Choquette and Pray, 1970; Moshier, 1989a). The term microporosity has also been used to describe zones with “low resistivity pay” as well as the fraction of porosity associated with pores falling below the resolution of a standard thin section (Pittman, 1971; Budd, 1989; Cantrell and Hagerty, 1999). Therefore, no set definition exists for microporosity.

Some workers have used pore and pore throat size to define microporosity, though the definitions of these metrics vary greatly in literature (Fig. 4). Pores have been defined as small as 0.02–2 µm (Loucks and Ulrich, 2015) to as big as 5–62 µm (Al-Awar and Humphrey, 2000). Similarly, pore throat radii have been defined as small as 0.3 µm (Skalinski and Kenter, 2015) to as large as 50 µm (Tonietto et al., 2014). The disagreement in definitions has largely resulted from workers relying on different tools and techniques of investigation, as well as different study purposes. For example, Archie (1952) used the term “invisible pores” to refer to pores < 10 µm in diameter. In their classification of porosity in carbonate rocks, Choquette and Pray (1970) defined micropores as pores with < 62.5 µm (1/16 mm). Pittman (1971) defined micropores as voids measuring < 1 µm in at least one dimension, whereas Coalson et al. (1985) chose an upper size limit of 5 µm. Based on fluid flow and reservoir performance, Moshier (1989a) argued that a value of 62 µm is too high and a value of 5 µm is too low. Moshier (1989a) considered a range of 5–10 µm in diameter for micropores. Most recently, general agreement has been reached that the term micropore should be used for pores with a diameter < 10 µm or those hosted between < 10 µm microcrystals (Cantrell and Hagerty, 1999; Lønøy, 2006; Deville de Periere et al., 2011; Loucks et al., 2013; Kaczmarek et al., 2015; Hasiuk et al., 2016).

The last source of confusion lies in how microcrystals are defined. Micrite, a contraction of “microcrystalline calcite” is the term introduced by Folk (1959) to refer to microcrystalline ooze (i.e., lime mud) ranging between 1 and 4 µm. Folk (1959) intended to the term micrite to provide a quantitative term to describe rocks that consist almost entirely of microcrystalline calcite as seen under the

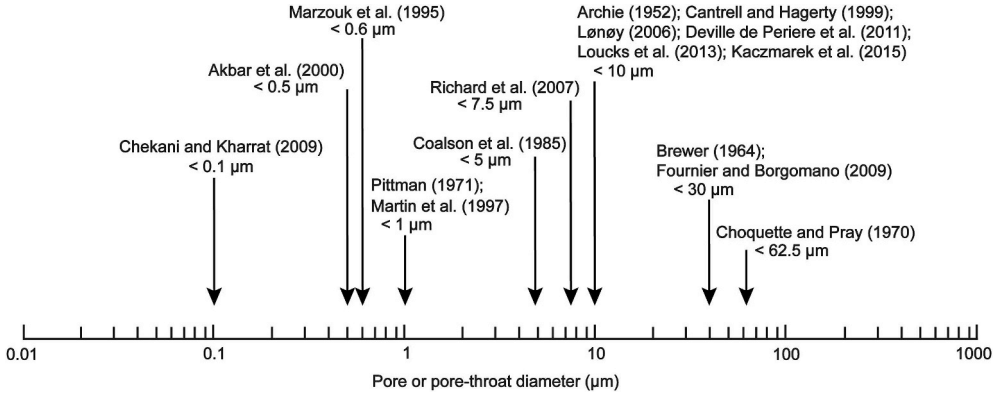


**Fig. 4.** The various micropore definitions in literature. The horizontal axis is a logarithmic scale representing pore or pore-throat diameter in micrometers, and the arrows refers to the upper size limit used by different authors.

petrographic microscope, and to replace older terms such as calcilutite (Grabau, 1904) and lithographic limestone, which were loosely used to refer to microcrystalline calcite. However, Folk (1959, 1962) stated that the presence of micrite indicates a low energy depositional environment. Therefore, the term micrite also has a genetic meaning, in addition to a descriptive one. Micrite was subsequently redefined by Leighton and Pendexter (1962) to include consolidated mud and unconsolidated ooze of either chemical or mechanical origin measuring less than 30 μm. The upper size limit of micrite (i.e. lime mud), has been modified several times. For example, Dunham (1962) proposed using 20 μm and Elf-Aquitai (1975) proposed using 10 μm as upper size limits for micrite. Bathurst (1964) also used the term micrite to refer to microcrystalline aragonite. Bathurst (1966) described the formation of a micrite envelope through the process of micritization. These envelopes consist of aragonite cement and imply no information about the depositional environment (Milliman et al., 1985). Consequently, for most authors, micrite is used as a descriptive, non-genetic term to refer to micrometer-sized carbonate particles. Microspar, another term introduced by (Folk, 1959), refers to LMC crystals (5–15 μm) that form via recrystallization (aggrading neomorphism) of micrite. Although important in a historical context, the terms micrite and microspar, have become increasingly confusing and equivocal. To avoid further confusion, these terms will be used only when necessary. Instead, the term "microcrystal" will be used herein to refer to micrometer-size carbonate crystals measuring $\leq$10 μm consistent with the global study of microporous limestone reservoirs by Kaczmarek et al. (2015).

## 3. Precursor sediments

The prevailing interpretation is that the vast majority of limestone microporosity is associated with diagenetically altered matrix and allochems (Fig. 5). To provide the reader with a fuller appreciation for the mineralogical, textural, and geochemical alterations that are inferred to have taken place during the diagenetic transformation from carbonate sediments to ancient limestones, the following discussion is provided. The purpose of the discussion is to examine the origin of these sediments and to fully characterize modern sediments from the perspective of their origin, mineralogy, texture, and geochemistry. Deep marine chalks will be discussed separately in section 6, because they follow a distinct diagenetic pathway compared to shallow marine sediments (Scholle, 1977; Fabricius, 2007).

### 3.1. Lime mud

Lime mud in modern carbonate environments includes a heterogeneous assortment of fine sediments mainly composed of metastable carbonate minerals (aragonite and high-Mg calcite (HMC)). These sediments are produced through physical, chemical, and biological processes, and are characterized by a wide variety of textures. Lime muds have been historically classified into two broad genetic classes, automicrite (i.e. autochthonous micrite), which is formed in situ, and allomicrite (i.e. allochthonous micrite), which is formed elsewhere and is transported to the site of deposition (Flügel, 2013). These classes should not be confused with diagenetic micrite, which is also referred to as psuedomicrite (Flügel, 2013). The source, mineralogy, textures, and petrophysical properties of lime mud are discussed below.

#### 3.1.1. Source

Lime mud forms in marine and non-marine environments across various settings and conditions, and is a major constituent of recent and ancient carbonate sediments (Mathews, 1966; Flügel, 2013). It has been postulated that lime mud originates from several organic and inorganic processes. The degree to which these processes contribute to the overall volume of sediment, as well as the origin and composition of lime mud constituents, have been debated for more than a century (Vaughan, 1917; Lowenstam, 1963; Bathurst, 1975; Steinen et al., 1988; Shinn et al., 1989; Milliman et al., 1993; Turpin et al., 2008, 2011, 2014; Purkis et al., 2017; Trower et al., 2019). Initially, most workers considered carbonate mud as "chemical" sediments that precipitate directly from sea water (e.g., Vaughan, 1917; Smith, 1940; Newell, 1955; Cloud et al., 1962). Vaughan (1917) suggested that chemical precipitation is possible based on the observation that ocean water is supersaturated with respect to various carbonate mineral phases, as well as the understanding that a number of organic and inorganic factors, such as bacterial activity, increased concentration due to evaporation, and elevated temperature, help facilitate precipitation. Later experimental work by Gee et al. (1932) supported the chemical precipitation hypothesis by demonstrating that aragonite needles could precipitate inorganically from artificial sea water. The inorganic model was subsequently challenged by a series of studies that showed the range of oxygen and carbon isotopic measurements from aragonite needles in the Bahamas were similar to those measured in codiacean algae (*Halimeda* and *Penicillus*), oolites, and grapestones (Lowenstam, 1955, 1963; Lowenstam and Epstein, 1957). Lowenstam (1955) reported that the abundance of aragonite needle-producing algae was similar to muddy sediments comprised of aragonite needles in several modern carbonate environments. Based on the similarity between the production rate of mud-secreting organisms and rate of mud accumulation, an organic origin was postulated for lime mud in Florida (Stockman et al., 1967), in Discovery Bay, Jamaica (Land, 1979), and in the bight of Abaco (Neumann and Land, 1975). A number of authors, however, argued against the algal source model based on the observation that algal populations were insufficient to account for the vast mud accumulations in the Bahamas (Newell and Rigby, 1957; Cloud et al., 1962; Queen,

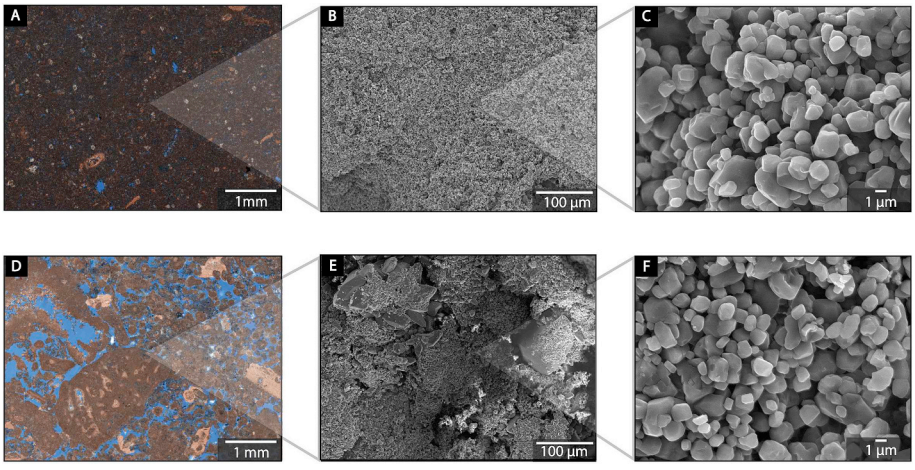


**Fig. 5.** Thin section and SEM photomicrographs of a Cretaceous-age limestone reservoir from the Middle East showing the major type of micropores in limestones that is hosted within LMC microcrystals at different scales. A) Thin section photomicrograph of a microporous mud-dominated limestone. B & C) SEM photomicrographs at different magnification of the sample shown in A, illustrating the microporosity-hosting LMC microcrystals. D) Thin section photomicrograph of a microporous grain-dominated limestone from the same reservoir as in A. E & F) SEM photomicrographs at different magnification of the sample shown in D, illustrating that grains are also characterized by similar LMC microcrystals that host micropores. Modified after Kaczmarek et al. (2015).

1977; Steinen et al., 1988; Shinn et al., 1989).

The algal model has also been challenged based on geochemical and textural evidence. Milliman (1974), for example, documented that the Sr content of aragonite produced by green algae ranges 0.8–0.9% in contrast to the 0.95–1.0% observed in inorganically precipitated aragonite in ooids, grapestones, and pellets. These data suggested to Milliman (1974) that the inorganic component of the lime mud in the Bahamas was a larger contributor to the bulk mud fraction than the algal component. Scanning electron microscope (SEM) observations presented by Loreau (1982) showed that approximately 60–75% of the aragonite produced by *codiacean* algae is in the form of equidimensional nanograins and ~25–40% are short aragonite needles. Both forms, importantly, are fundamentally different from the longer aragonite needles that are observed in the lime mud of the Bahamas (Milliman et al., 1993; Gischler et al., 2013).

Patches of suspended lime mud called “whitings” have also been implicated as a source of modern carbonate mud. Some evidence suggests that whitings represent intermittent occurrences of in situ abiotic (Cloud et al., 1962; Shinn et al., 1989; Milliman et al., 1993; Purkis et al., 2017), or biotic (Robbins and Blackwelder, 1992; Riding, 1993; Yates and Robbins, 1998) aragonite precipitation from seawater. Other evidence, however, suggests that whitings are re-suspended bottom sediments caused by agitation of the water (Broecker and Takahashi, 1966; Boss and Neumann, 1993; Dierssen et al., 2009). Published geochemical data are more consistent with the suspension hypothesis (Broecker and Takahashi, 1966; Morse et al., 1984, 2003; Shinn et al., 1989; Morse and Mackenzie, 1990; Bustos-Serrano et al., 2009). Morse et al. (1984), for example, cited the observed similarities in various chemical parameters such as pH, total alkalinity, and total $CO_2$ measured in water within and adjacent to whitings to argue against direct precipitation from seawater. He reasoned that direct precipitation should result in observable changes in water chemistry, especially a reduction in the total alkalinity value. Shinn et al. (1989) showed that the oxygen isotopic composition of suspended sediments in whitings were not in equilibrium with the surrounding waters from which they are assumed to precipitate, suggesting that the sediments associated with whitings were re-suspended bottom sediments. Shinn et al. (1989) also compared $\delta^{14}C$ from sediments in whitings with those from modern coral and bottom sediments. Sediments in whitings values range between −60 and +23‰, modern coral measured +111 to +149‰, and bottom sediments measured −31‰. Accordingly, Shinn et al. (1989) suggested mixing occurred between old and new carbon sources.

Numerous authors have pointed out that the major deficiency of the sediment suspension model is that it lacks a robust mechanism to explain how bottom sediments become suspended (e.g., Shinn et al., 1989; Larson and Mylroie, 2014). Initially, sediment suspension was postulated to occur via agitation by bottom feeding fish. Despite employing numerous techniques, such as side-scan sonar, fathometer imaging, shrimp trawls, rotenone, remote video, and direct scuba observations, Shinn et al. (1989) concluded that there is no relationship between fish and whitings, an observation also made earlier by Cloud et al. (1962) and Gebelein (1974). Shinn et al. (1989) also observed that whitings occur equally over rocky, sandy, and muddy substrates suggesting re-suspension was unlikely.

Shinn et al. (1989) compared bottom sediments with those suspended in whitings in the Bahamas and found subtle differences in mineralogy and texture. On average, bottom sediments were composed of 91% aragonite, 8% HMC, and 1% LMC, whereas suspended sediments were composed of 86% aragonite, 12% HMC, 2% LMC, and trace amounts of inorganic non-carbonate material (Shinn et al., 1989). Bottom sediments were characterized as rectangular to hexagonal aragonite needles with partially rounded crystal terminations and measuring 0.25 μm by 2–3 μm. Also observed within the bottom sediments were agglutinated grains composed of bundles of similarly oriented aragonite needles. In contrast, suspended sediments consisted of randomly oriented aggregates of aragonite needles, and single aragonite needles some of which exhibited blunt crystal terminations (Shinn et al., 1989). Macintyre and Reid (1992) reported that crystal morphologies in sediments suspended in whitings were similar to Bahamian bottom sediments, although both were morphologically distinct from those associated with algae. Whitings and bottom sediments were characterized by pointed ends and poorly developed crystal faces, whereas algal needles were generally blunt ended with well-developed crystal faces (Macintyre and Reid, 1992). Based on these morphological observations, Macintyre and Reid (1992) suggested that Bahamian bottom sediments and those suspended in the whitings near Andros Island were not of algal origin.

The direct precipitation model has been strengthened by a wide range of geochemical evidence. Robbins and Blackwelder (1992) observed that various organic compounds, such as protein and amino acids, analyzed from suspended sediments in whitings were different from those in bottom and algal sediments. Some of these organic materials were found to be associated with planktonic algae. Robbins and Blackwelder (1992) proposed a model of biologically induced precipitation whereby planktonic algae facilitate precipitation of aragonite by providing nucleation sites and via $CO_2$ removal by their photosynthesis. A biological origin for whitings was argued against by Friedman (1993), who suggested that, although Bahamian whitings might be biological in origin, whitings elsewhere are not. Unlike the Bahamas, whitings in the Dead Sea occur only once every few years, and coincided with annual temperature maxima (Neev, 1963). Morse et al. (2003) later argued that aragonite precipitation via planktonic algae catalysis is incapable of explaining why whitings are rare occurrences because planktonic algae are ubiquitous in the oceans. Boss and Neumann (1993) analyzed satellite images of the Bahamas and demonstrated that the distribution of whitings is not random, but rather more concentrated in areas where hydrodynamic energy was higher and lime mud bottom sediments were more abundant. These observations led them to propose a mechanism by which bottom sediments were re-suspended by turbulent bottom currents. Based on a correlation between the distribution of whitings and hydrodynamic movements of water as observed from satellite imagery and hydrodynamic modeling, Purkis et al. (2017) recently hypothesized that Florida currents facilitate inorganic aragonite precipitation by bringing fresh, $CaCO_3$-rich off bank waters onto the platform top.

Some authors have suggested that sediments in whitings represent a combination of directly precipitated and re-suspended bottom sediments (Shinn et al., 1989; Morse and Mackenzie, 1990; Morse et al., 2003; Bustos-Serrano et al., 2009). This model reconciles the textural and mineralogical observations that support the direct precipitation model and geochemical data that suggest a source of sediments other than direct precipitation. Shinn et al. (1989) proposed that one type of whitings occur after regional storms redistribute agitated bottom sediments, whereas a second type has been proposed to occur locally and represent direct precipitation from sea water. Morse and Mackenzie (1990) and Morse et al. (2003) proposed that re-suspended sediments act as nucleation sites for $CaCO_3$ precipitation. This model, which they called “The Hip-Hop'n model”, explains geochemical data including the similarities in $C^{14}/C^{12}$ between bottom sediments and whiting sediments, as well as the faster rate of $CaCO_3$ removal from seawater in whitings area compared to areas where whitings are absent (Broecker and Takahashi, 1966; Morse et al., 1984, 2003). On the basis of similar geochemical observations (pH, total alkalinity, total $CO_2$, and $CaCO_3$ removal from seawater), Bustos-Serrano et al. (2009) proposed a similar mechanism whereby $CaCO_3$ precipitation occurs on re-suspended sediments to explain whitings in Little Bahama Bank.

The genetic origin of whitings is still debated (e.g., Purkis et al., 2017). According to the direct precipitation model, sediments in whitings may be considered autochthonous. Autochthonous lime mud may also form in microbialites (Burne and Moore, 1987; Reitner, 1993; Perri et al., 2017). Microbialite is a term introduced by Burne and Moore (1987) to describe “organosedimentary deposits formed from

interaction between benthic microbial communities and detrital or chemical sediments." The exact mechanism by which biological carbonate precipitation occurs is poorly understood (Perri et al., 2018), but one form of precipitation is attributed to macromolecules that bind cations such as $Ca^{2+}$ and $Mg^{2+}$ (Reitner, 1993; Reitner et al., 2000; Perri et al., 2018). Autochthonous mud may also be produced through the biological activities and metabolic processes of bacteria, cyanobacteria, algae, fungi (Burne and Moore, 1987; Flügel, 2013), and possibly viruses (Perri et al., 2018). In this case, biological precipitation is linked to photosynthesis and bacterial activities that mediate the chemistry of the surrounding fluids (e.g., remove $CO_2$) and thus facilitate $CaCO_3$ precipitation (Flügel, 2013). Biological precipitation of carbonates has been categorized into three broad classes: microbial metabolism, cell surface reaction, and physical microbial presence (see review by Kaczmarek et al., 2017).

Although the contribution of biological autochthonous mud to the sediment budget has not been quantitatively documented (Riding, 1993), it has been postulated that cyanobacterial-induced mud was a larger portion of the sedimentary budget during the Precambrian, prior to the evolution of eukaryotes (Golubic et al., 2000). Because a wide range of eukaryotic organisms deplete ocean water of $CaCO_3$, and prior to their evolution, Precambrian oceans were likely more saturated with respect to the various carbonate minerals, and "much closer to a state of spontaneous carbonate precipitation" as stated by Golubic et al. (2000). Textural criteria for distinguishing autochthonous carbonate mud include biolaminated structures, clotted peloidal fabrics, and/or cryptocrystalline textures (Flügel, 2013). That being said, biologically mediated autochthonous mud is likely to disintegrate and disperse (Golubic et al., 2000), in which case, the origin of sediments is more challenging to interpret.

Production of lime mud via abrasion of sand-size allochems was a model originally proposed by Sorby (1879), and recently tested by Trower et al. (2019) using physical abrasion experiments. They observed that the abrasion of ooids produced mud composed of 1–2 μm needles, whereas skeletal grains produced a more heterogenous assortment of needles and nanograins. Morphologically, mud produced from ooids and skeletal grains was similar to natural lime mud. Accordingly, Trower et al. (2019) argued that abrasion could be an important mechanism for mud production. They further suggested that this mechanism could compensate for the lower rates of inorganic and organic production, particularly in the Precambrian prior to the evolution of carbonate producing eukaryotes. One limitation of this conclusion, however, is that inorganic and organic production of sand-sized material is still required in this model.

Although most studies of lime mud production have focused on the Caribbean and Florida (Gischler et al., 2013, Table 1), the process has also been investigated in Hawaii (e.g., Thorp, 1936), the Dead Sea (Neev, 1963), Persian Gulf (Wells and Illing, 1964), Red Sea (Ellis and Milliman, 1985), French Polynesia (Debenay et al., 1999), the Maldives (Gischler et al., 2013) and Great Barrier Reef (Gischler et al., 2013). Based on the morphology, $\delta^{13}C$, and Sr, Gischler et al. (2013) suggested that the majority of the lime mud was biogenic and was derived from breakdown of skeletal grains and the disintegration of codiacean algae. This agrees in general with many other studies that also concluded a biological source of lime mud in shallow marine, tropical settings (e.g., Andrews et al., 1997; Debenay et al., 1999; Gischler and Zingeler, 2002; Perry et al., 2011; Salter et al., 2012; Flügel, 2013). The origins of lime mud in temperate (cool water) environments has received less attention. In one study, O'Connell and James (2015) investigated Spencer Gulf, South Australia, a temperate, shallow water marine environment. Using SEM, O'Connell and James (2015) showed that the majority of the silt-size sediments (4–63 μm) were comprised of the skeletal remains of benthic organisms such as bivalves, foraminifer, ascidian spicules, echinoderms, and rhodoliths. Clay-size particles (< 4 μm) were mainly composed of sheets, blades, and needles of aragonite, LMC, and HMC, but were still interpreted to form through the physical and chemical breakdown of skeletal material via maceration, which refers to disintegration of skeletons into their microscopic structural elements (*sensu,* Alexandersson, 1979). This interpretation was based on the observation that the microscopic structural elements of the skeletons were also characterized by sheets, blades, and needles (O'Connell and James, 2015).

### 3.1.2. Mineralogy

Modern case studies have demonstrated that lime mud is composed of metastable aragonite and HMC, as well as LMC to a lesser extent (Friedman, 1964; Bathurst, 1975). The relative abundances of these minerals vary by geographic location. For example, the Bahamas tends to be dominated by aragonite (Cloud et al., 1962; Husseini and Matthews, 1972; Milliman, 1974), whereas lime muds in Red Sea, as well as Shark Bay, Australia, and along the northeastern coast of Yucatan, Mexico are dominated by HMC (Logan and Cebulski, 1970; Milliman and Müller, 1973). Mathews (1966) reported that lime mud from Honduras is composed of 49% aragonite, 44% HMC, and 7% LMC. Steinen (1978) estimated the mineralogy of modern, tropical, shallow-water lime muds in Barbados to be 60–95% aragonite, 5–40% HMC, and 0–10% LMC. O'Connell and James (2015) found that, in the modern, temperate, shallow-water environment of Spencer Gulf in Australia, the fine sediments are composed of 23–31% aragonite, 17–40% LMC, and 29–52% HMC. Gischler et al. (2013) calculated a global average for mineralogical composition of modern lime mud as 82.5% aragonite, 12.6% HMC, and 3.7% LMC based on data from Belize, Bahamas, Florida, the Maldives, French Polynesia, and Great Barrier Reef. These authors also observed that mineralogical composition of lime mud differs by geographic location. In the Great Barrier Reef, offshore Australia and the Maldives, for example, lime mud is characterized by elevated HMC content (up to 25%), whereas in the Bahamas HMC is 2.3% only. In all the six locations examined, aragonite is the dominant mineralogy. Fig. 6 illustrates mineralogical differences between modern lime mud from U.S. Virgin Islands, which is dominated by aragonite, and ancient limestones, which are dominated by LMC.

Some studies reported bulk mineralogical data for lime mud for all particles < 62.5 μm (e.g., Logan and Cebukski, 1970; Husseini and Matthews, 1972; Milliman and Müller, 1973; Milliman, 1974), whereas others split the mud into multiple fractions (e.g., Pilkey, 1964; Reid et al., 1992; Andrews et al., 1997; Gischler and Zingeler, 2002; Gischler et al., 2013). Only a few studies (e.g., Pilkey, 1964; Reid et al., 1992; Andrews et al., 1997; Gischler and Zingeler, 2002) report mineralogical data for small size fractions (< 10 or < 4 μm), primarily because it is more difficult to isolate fine particles in quantities large enough to accurately determine mineralogy. This is important because mineralogical composition has been observed to vary with crystal size. According to Hoffmann (1983) and Andrews et al. (1997), aragonite content increases in the smaller size fraction, whereas Mathews (1966) reported the same to be true of HMC. Despite a wide range of materials and locations studies, the order of decreasing relative abundance in modern carbonate muds appears to be aragonite, HMC, and LMC.

### 3.1.3. Texture

Investigating the textural attributes of lime mud has been challenging due to the small particle size (Bathurst, 1975). Initially, crystal size and shape were described using a binocular microscope (e.g., Gee et al., 1932; Wood, 1941). The advent of the SEM in the 1940's allowed for more detailed characterization. Many authors have described the textural characteristics of carbonate muds from modern depositional environments (e.g., Folk, 1965; Mathews, 1966; Loreau, 1982; Macintyre and Reid, 1992; Reid and Macintyre, 1998; Gischler and Zingeler, 2002; Gischler et al., 2013). Folk (1965) reported crystal sizes for various synthetic and natural lime mud samples from earlier studies (e.g., Gee et al., 1932; Cloud et al., 1962; Newell and Rigby, 1957; Hathaway and Robertson, 1961; Hoskin, 1963). Folk (1965) showed that these muds

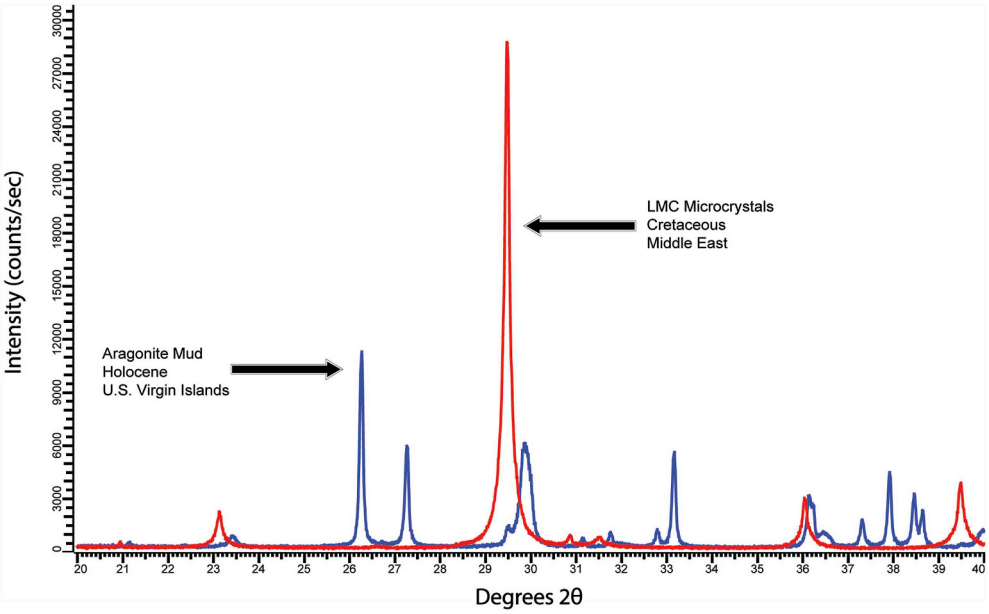


**Fig. 6.** XRD diffractograms of modern lime mud from U.S. Virgin Islands (blue) and microcrystals in matrix of Cretaceous-age limestone from Middle East (red). The modern carbonate mud is composed of 95.2% aragonite, 4.07% HMC, and 0.73% LMC, whereas the microcrystals in the ancient limestone are composed of ~100% LMC.

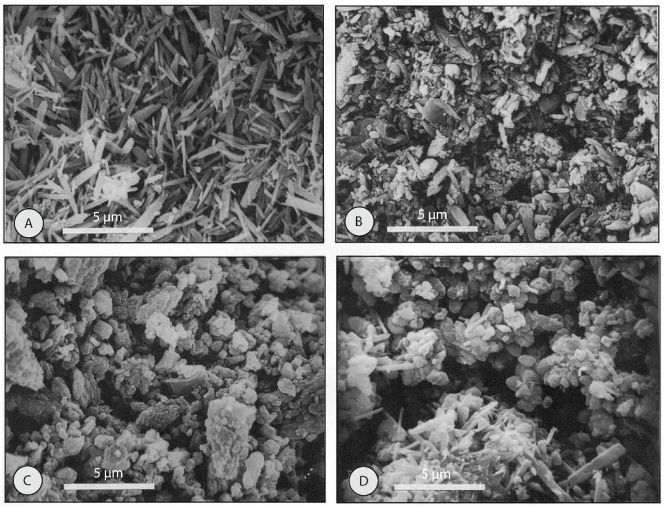


**Fig. 7.** SEM photomicrographs of carbonate mud from different modern environments showing the variability in mineralogy and texture. A) Lime mud composed mainly of aragonite needles from the Bahamas. B) Aragonite and HMC lime mud from Florida. C) Lime mud composed of HMC nanograins from the Bahamas. D) HMC cement with some detrital aragonite from coral reef in Florida. Modified after Lasemi and Sandberg (1993).

were composed of elongated aragonite needles measuring 0.1–0.8 by 0.5–4 µm. A subsequent study by Mathews (1966) described lime mud from Honduras as a collection of randomly oriented granular to irregular crystals measuring < 4 µm. More recently, Gischler et al. (2013) described lime muds from various modern environments around the world. They observed that the grain-size fraction < 4 µm is dominated by various grain morphologies such as needles, nanograins, and platelet of coccoliths. Aragonite needles were found to be either short needles (2–4 µm) with irregular crystal faces and pointed ends, or longer (up to 10 µm) needles with regular, six-sided crystal faces (Gischler et al., 2013). Nanograins are < 1 µm equidimensional but anhedral (Gischler et al., 2013). Lime mud constituents vary in morphology and abundance from one location to another (Lasemi and Sandberg, 1993; Gischler et al., 2013). Fig. 7 illustrates the various textures exhibited by lime muds from different modern environments. These observations on lime mud textures from modern environments highlight the stark differences with textures exhibited by lime muds in ancient limestones (compare Figs. 7 and 9).

### 3.1.4. Petrophysical properties of lime mud

Lime muds are observed to have high porosities and low permeabilities (Bathurst, 1975; Enos and Sawatsky, 1981; Kominz et al., 2011; Flügel, 2013). In Holocene carbonate sediments from Florida and the Bahamas, Enos and Sawatsky (1981) reported that the muddiest sediments, which they defined as very fine grained wackestones, are characterized by the highest porosities (70.5%) but the lowest permeabilities (0.87 md) among sediments exhibiting a range of depositional textures, which they described as grainstone, packstone, and wackestone. Similar porosity and permeability ranges have been observed for lime mud from Ocean Drilling Program (ODP) data (Kominz et al., 2011).

## 3.2. Carbonate grains

Carbonate grains are classified on the basis of their origin (Bathurst, 1975; Flügel, 2013). Skeletal carbonate grains are skeletons or skeletal fragments of carbonate-secreting organisms (Flügel, 2013). Non-skeletal carbonate grains include coated grains, peloids, grain aggregates, and clasts (Folk, 1959; Bathurst, 1975; Tucker, 2009). Grains respond differently to diagenesis and microporosity development based on their mineralogy and microtexture (Budd, 1989, 1992; Cantrell and Hagerty, 1999). Therefore, the mineralogy and microstructure of carbonate grains will be discussed.

### 3.2.1. Mineralogy

Marine exoskeletons are most commonly comprised of the carbonate minerals aragonite, LMC, and HMC (Lowenstam and Weiner, 1989). Phosphates, silica, and iron oxides are also common, and they follow carbonate minerals in abundance (Lowenstam and Weiner, 1989). Some organisms form monomineralic skeletons (e.g., scleractinian coral), whereas others can be polymineralic (e.g., foraminifera). Fig. 8 is a summary of most common carbonate-producing organisms and their corresponding mineralogy. Modern non-skeletal allochems, such as ooids, also exhibit a variety of mineral compositions. In marine settings and saline lakes, ooids are mostly aragonite (Kahle, 1974; Sandberg, 1975), but HMC ooids also exist. Land et al. (1979), for example, reported Holocene HMC ooids from Baffin Bay, Texas. LMC ooids, in contrast, tend to occur more commonly in lakes, streams,

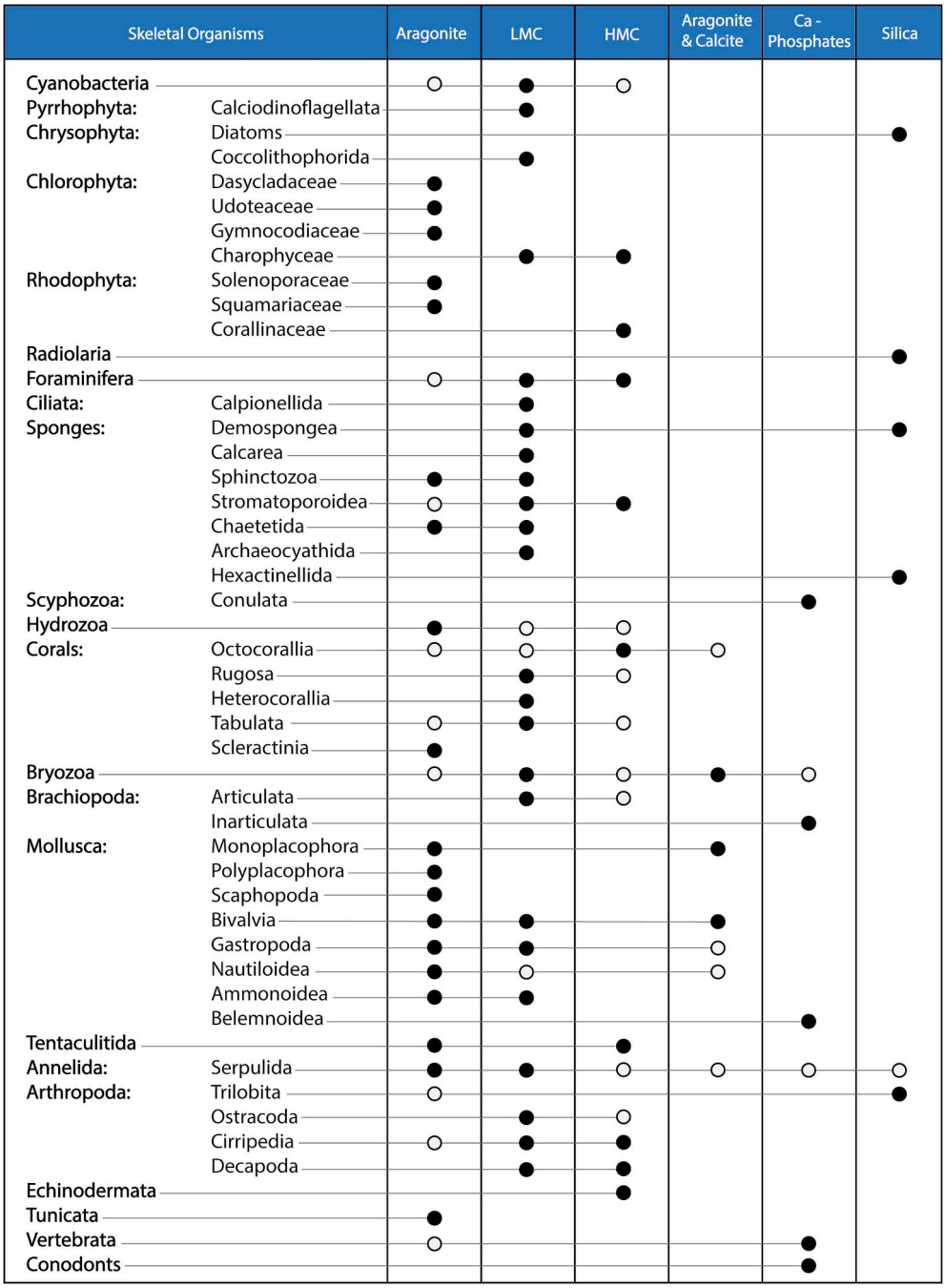


**Fig. 8.** Primary skeletal mineralogy of some common organisms in carbonates. Black circles refer to the dominant mineralogy, whereas less common mineralogy is indicated by open circles. Modified after Flügel (2013).

caves, and calcareous soils (Geno and Chafetz, 1982). Pisoids have been reported to be both aragonite and HMC (Scholle and Kinsman, 1974; Ferguson and Ibe, 1982). Non-marine pisoids tend to be LMC (Chafetz and Butler, 1980). The mineralogy of peloids, grain aggregates, and intraclasts commonly reflects the composition of the materials they are made from (Flügel, 2013).

### 3.2.2. *Microstructure*

Microstructure refers to the internal texture of carbonate allochems (Horowitz and Potter, 2012), which has been investigated using a variety of methods, including standard thin section petrography (e.g., Horowitz and Potter, 2012) and SEM (e.g., Flügel, 2013; Gannon et al., 2017). Most of what we know about the skeletal microstructures of carbonate-producing organisms comes from descriptions of modern fauna that have not been affected by diagenesis yet (e.g., Bathurst, 1975; Budd and Hiatt, 1993; Flügel, 2013; Gannon et al., 2017). Although they are easily altered by diagenesis (Stearn et al., 1999), the primary skeletal microstructures in some well-preserved ancient carbonates have been documented (e.g., Wendt, 1990; Roniewicz, 1996; Stanley, 2003). Still, the nature of microstructure is highly debated. For example, more than 14 distinct wall microstructures have been reported in Paleozoic stromatoporoids (Stearn et al., 1999), leading to general uncertainty about which types are primary and which are diagenetic (Horowitz and Potter, 2012).

The internal microstructure of non-skeletal carbonate allochems has also been described in detail by various authors (Bathurst, 1975;

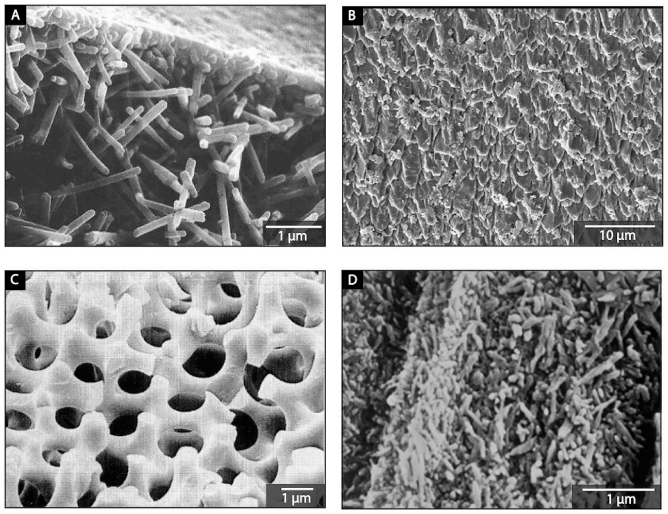


**Fig. 9.** SEM photomicrographs showing microstructure of some organisms. A) Halimeda *incrassata* (green algae) with microstructure characterized by randomly oriented needles and equant crystals. Modified after Lowenstam and Weiner (1989). B) Microstructure of *Tridacna gigas* (Mollusk) composed of shield-like aragonite crystals. Modified after Gannon et al. (2017). C) Test of the sea urchin *Paracentrotus lividus* (echinoderm). Modified after Scholle and Ulmer-Scholle (2003). D) SEM photomicrograph an acid etched section of aragonitic ooid showing the tangentially oriented and randomly distributed aragonite needles. Modified after Scholle and Ulmer-Scholle (2003).

Sandberg, 1975; Simone, 1980; Flügel, 2013) and will be reviewed only briefly here for context. Concentric ooids consist of tangentially arranged needles, or concentric layers of nano-grains (Loreau and Purser, 1973; Sandberg, 1975; Simone, 1980). Radial ooids, in contrast, consist of radial crystals arranged perpendicular to the surface (Simone, 1980; Tucker, 2009; Flügel, 2013). Superficial ooids consist of a single cortex around a central nucleus (Tucker, 2009). Evidence suggests that ooid microstructure is controlled by environmental conditions as well as original mineralogy (Rusnak, 1960; Simone, 1980; Flügel, 2013). For example, tangential ooids are often aragonite, whereas radial-fibrous ooids can be either HMC or aragonite (Flügel, 2013). Pisoids generally exhibit tangential or radial internal microstructures, similar to ooids, but are characterized by more closely spaced laminae (Flügel, 2013). Peloids, by definition, lack internal structure, and are composed of microcrystalline material (Tucker, 2009).

A number of microstructure types for carbonate allochems have been identified. Flügel (2013), for example, categorized the internal microstructure of modern allochems into ten major types based on crystal size, morphology, and orientation. Four different microstructures from various organisms are presented in Fig. 9. It can be observed that the green algae *Halimeda Incrassata* has a microstructure characterized by randomly oriented needles and equant crystals (Fig. 9A), whereas the internal microstructure of *Tridacna gigas* mollusk is composed of shield-like aragonite crystals (Fig. 9B). For detailed descriptions of the most common skeletal microstructures, the reader is referred to reviews by Horowitz and Potter (2012), Majewske (1974), Carter (1990), and Flügel (2013).

## 4. Microporosity and microcrystals in ancient limestones

Dozens of limestone reservoir studies spanning the Ordovician to the Quaternary, and from all around the world, have documented the occurrence of limestone micropores in rocks representing various depositional environments and burial depths (Table 1). Micropores have been observed both in marine limestones (e.g., Budd, 1989; Perkins, 1989; Holail and Lohmann, 1994; Al-Aasm and Azmy, 1996; Neilson et al., 1998; Loucks et al., 2013), as well as in lacustrine limestones (e.g., Wright et al., 1997; Arribas et al., 2004; Volery et al., 2010a). The most common form of microporosity in ancient limestones is attributed to the micropores hosted between LMC microcrystals (Moshier, 1989a; Cantrell and Hagerty, 1999; Kaczmarek et al., 2015). As such, the remainder of this review will focus on this particular type of microporosity.

LMC microcrystals occur in what is identified petrographically as matrix, and in association with most carbonate allochems (Moshier, 1989a; Cantrell and Hagerty, 1999; Kaczmarek et al., 2015). Accurate characterization of LMC microcrystals has proven important because the morphology (size, shape) and arrangement (orientation, organization) of these microcrystals dictate the geometry of the associated pore spaces, and thus the petrophysical properties of the rock (Deville de Periere et al., 2011; Kaczmarek et al., 2015).

Various methods have been employed to study LMC microcrystals and the associated micropores. High porosity - low permeability intervals detected on wireline logs have long been interpreted to indicate the presence of microporosity (Pittman, 1971; Cantrell and Hagerty, 1999; Clerke et al., 2008). Early characterization studies utilized plane light microscopy methods to investigate LMC microcrystals and micropores (e.g., Gee et al., 1932; Bathurst, 1959b; Folk, 1959; Jodry, 1972). Carbonate petrologists routinely use the presence of the “blue haze” in standard blue epoxy-impregnated petrographic thin sections to infer the presence of abundant micropores (Fig. 1) (Saller and Moore, 1989; Jameson, 1994; Cantrell and Hagerty, 1999). Because most petrographic microscopes are incapable of resolving the µm-size particles (Pittman, 1971; Lasemi and Sandberg, 1983; Flügel, 2013), carbonate petrologists now routinely apply more advanced imaging techniques. SEM, for instance, in combination with other analytical tools, such as TEM, AFM, porosimetry, and MICP has allowed micropores to be more precisely characterized in terms of pore size, pore-throat size, shape, and connectivity (e.g., Flügel et al., 1968; Pittman, 1971; Longman and Mench, 1978; Lambert et al., 2006; Clerke et al., 2008; Deville de Periere et al., 2011; Milliken and Curtis, 2016). Pore casts techniques have also been used to characterize the geometry and distribution of micropores (e.g., Pittman, 1971; Budd, 1989; Moshier, 1989a; Cantrell and Hagerty, 1999).

### 4.1. Description of LMC microcrystals

LMC microcrystals are described based on various physical attributes, such as size, morphology, and type of boundaries between crystals. In fact, these attributes have been used to classify LMC microcrystals into various textural classes (e.g., Moshier, 1989a; Lambert et al., 2006; Clerke et al., 2008; Deville de Periere et al., 2011; Kaczmarek et al., 2015). Crystal size distribution data show that LMC crystal diameters generally range between 1 and 10 µm (e.g., Pittman, 1971; Longman and Mench, 1978; Budd, 1989; Kaldi, 1989; Loucks et al., 2013; Kaczmarek et al., 2015). Based on data from a global study of 12 microporous limestone reservoirs spanning Devonian to Paleogene in age, Kaczmarek et al. (2015) reported that 99% of LMC microcrystals measure 0.5–9 µm with a mode of ~2.0 µm. Data published by Folk (1965), Flügel et al. (1968), Loreau (1972); Folk (1974), Kaldi (1989), Lasemi and Sandberg (1993), Cantrell and Hagerty (1999), Lambert et al. (2006), Richard et al. (2007), Munnecke et al. (2008), Volery et al. (2009), Deville de Periere et al. (2011) and Loucks et al. (2013) are generally consistent with this range.

Despite the narrow range in LMC microcrystal sizes, a broad range of morphologies is observed. A variety of terms have been used to describe crystal morphology including euhedral, subhedral, anhedral, rhombic, scalenohedral and rounded. Euhedral refers to crystals with well-defined crystal faces, subhedral refers to crystals with moderately defined faces, and anhedral refers to crystals with poorly defined faces (Friedman, 1965). Terms such as idiotopic, hypidiotopic, and xenotopic are also used to describe fabrics in which the majority of crystals are euhedral, subhedral, and anhedral, respectively (Friedman, 1965).

Euhedral crystals have also been referred to as rhombic (e.g., Ahr, 1989), and subhedral crystals have been referred to as polyhedral (e.g., Pittman, 1971; Dravis, 1989), and rounded (e.g., Lambert et al., 2006). LMC microcrystals are commonly equidimensional, meaning that their X-Y-Z dimensions are relatively similar. However, elongated crystals, which are referred to as scalenohedral have also been reported (e.g., Longman and Mench, 1978; Saller and Moore, 1989; Deville de Periere et al., 2011).

### 4.2. Textural classifications

Numerous studies have used the physical attributes of LMC microcrystals as the basis for classification (e.g., Moshier, 1989a; Lambert et al., 2006; Deville de Periere et al., 2011; Kaczmarek et al., 2015). Moshier (1989a) recognized two major textural classes: a porous framework texture characterized by euhedral crystals with clearly distinguished crystal boundaries, and a non-porous mosaic texture characterized by anhedral crystals with curvilinear or straight crystal boundaries. In their investigation of Mesozoic carbonate reservoirs in the Middle East, Lambert et al. (2006) distinguished three main textural classes: rounded, micro-rhombic, and compact anhedral. Deville de Periere et al. (2011) used the type of crystal contacts to classify LMC microcrystals into two major textural classes: porous textures defined by point or partially coalescent contacts, and tight textures defined by fully coalescent or fused contacts. Porous textures were further classified based on crystal morphology into rounded, subrounded, scalenorhombohedral, and polyhedral, whereas tight textures were divided into anhedral compact and fused (Deville de Periere et al., 2011). Most recently, Kaczmarek et al. (2015) proposed a classification that was based on a broad study of 12 microporous limestone reservoirs that span a wide range of basins, geological ages, burial depths, and depositional environments. Kaczmarek et al. (2015) proposed three major textural classes - granular, clustered, and fitted - which were identified based on qualitative and quantitative descriptions of individual microcrystals in terms of shape and orientation, and description of intercrystalline boundaries in terms of edge density, edge length, and geometry. Granular texture was described as a loose framework of randomly oriented LMC microcrystals. The clustered texture was characterized by rough and lumpy crystals with irregular contacts. The fitted texture was described as a compact mosaic of LMC microcrystals with interlocking boundaries. Subclasses were also proposed to account for observed variations within each class. The granular texture, for example, was subdivided into granular euhedral and granular subhedral based on the morphology of individual crystals in the limestone. Fig. 10 summarizes the various LMC microcrystal textural classifications.

The aforementioned microcrystal classes account for the vast majority of LMC microcrystals observed in ancient limestones (Kaczmarek et al., 2015), yet additional textures have been reported (Kaldi, 1989; Al-Aasm and Azmy, 1996). For example, “incipient and immature” textures were observed in stromatoporoids in Kee Scarp, Canada, where euhedral LMC microcrystals are arranged in a uniform manner with consistent 60° and 120° angles between crystals (Fig. 11) (Kaldi, 1989; Al-Aasm and Azmy, 1996).

### 4.3. Petrophysical properties

Micropores can constitute the sole pore type in a rock (e.g., Loucks et al., 2013), but more often coexist with other macro pore types (e.g., Cox et al., 2010). In microporous limestones, where nearly all the porosity is attributed to micropores, porosities range from 2 to 35% and permeabilities range from < 0.01 to > 100 mD (Ahr, 1989; Budd, 1989; Moshier, 1989a, 1989b; Perkins, 1989; Al-Aasm and Azmy, 1996; Lambert et al., 2006; Deville de Periere et al., 2011).

In grain-dominated carbonates, grain size has been shown to exert the dominant control on petrophysical properties (Lucia, 1995; Melim et al., 2001a,b; Moore and Wade, 2013). In microporous carbonates, however, petrophysical properties are controlled not only by crystal size, but also by the morphology of crystals (e.g., Moshier, 1989a; Lambert et al., 2006; Deville de Periere et al., 2011; Kaczmarek et al., 2015). Moshier (1989a) described microcrystal textures in Miocene limestones from North Sumatra, Indonesia. He reported that limestones characterized by the mosaic texture had porosity values below 5%. In contrast, limestones characterized by the crystal-framework texture had 15–30% porosity. Deville de Periere et al. (2011) identified three distinct petrophysical classes – C, F, D – in Cretaceous microporous limestone reservoirs in the Middle East. Class C was characterized by the highest average porosities (> 20%), permeabilities (0.2–190 md), and pore throat radii (~0.5 μm). Class F was characterized by intermediate reservoir qualities (3–35%, < 10 md, < 0.5 μm), and Class D by the poorest reservoir qualities (< 10%, < 1 md). No pore throat radii values were reported for Class D. Kaczmarek et al. (2015) also documented a similar variety of petrophysical types in their global survey of microporous marine limestones. In their classification, Type I corresponds to the granular-subhedral texture and is characterized by highest porosities, permeabilities, and pore throat radii (> 20%, 1–20 md, 0.7 μm). Type II includes the granular-euhedral and the clustered textures and is characterized by intermediate reservoir quality (10–20%, 0.1–1.0 md, 0.2 μm). Type III is associated with the fitted textures and is characterized by the lowest reservoir quality (< 10%, 0.1 md, 0.06 μm). Petrophysical types I, II, and III of Kaczmarek et al. (2015) are loosely correspond to classes C, F, and D of Deville de Periere et al. (2011), respectively. Fig. 12 summarizes the petrophysical types recognized by Kaczmarek et al. (2015) and their associated microcrystalline textures and petrophysical properties. Porosity and permeability relationships in micropore dominated limestone reservoirs exhibit a log-linear trend (Fig. 13) (Lønøy, 2006; Kaczmarek et al., 2015; Van Simaeys et al., 2017) similar to that observed in crystalline dolomites (Lucia, 2007; Loucks and Ulrich, 2015). Along this trend, the major textural classes have distinct porosity and permeability values, and thus they plot in different zones.

Capillary pressure measurements on LMC microcrystals produce curves that have been interpreted to indicate well sorted and fine-skewed pore-throat size distributions (Archie, 1952). More recently, Kaczmarek et al. (2015) described their pore-throat size distributions as narrow and fine-skewed, indicating pore throat sizes that are uniform but skewed toward smaller pore radii. Pore throat radii distributions from Deville de Periere et al. (2011), Kaczmarek et al. (2015), and Van Simaeys et al. (2017) show that although each textural class is characterized by a range of pore throat radii, the classes easily distinguished.

The relationship between petrophysical properties and elastic properties, such as sonic velocity, is of great importance in carbonate rocks because correlations allow for predictive relationships between petrophysical properties, wireline logs, and seismic responses. Such relationships can also improve seismic inversion and AVO analyses (Baechle et al., 2008; Brigaud et al., 2010; Janjuhah et al., 2019) as well as seismic well ties. Eberli et al. (2003) measured acoustic velocities in modern carbonate sediments and limestones from the Bahamas using experiments to simulate in-situ stress conditions of buried rocks. They found that rocks with higher interparticle or microporosity have lower velocities by over 2500 m/s compared to limestones with moldic porosity (up to 5000 m/s) (Eberli et al., 2003). Baechle et al. (2008) specifically examined the effect of microporosity on sonic velocity. They found that sonic velocities decreased as the percentage of microporosity relative to the total porosity increased (Fig. 14). For example, at a given porosity, samples with > 80% microporosity exhibit lower velocities than samples with < 50% microporosity. Although some of the samples were microporous dolomites, Baechle et al. (2008) showed that microporosity was related to lower velocities regardless of lithology.

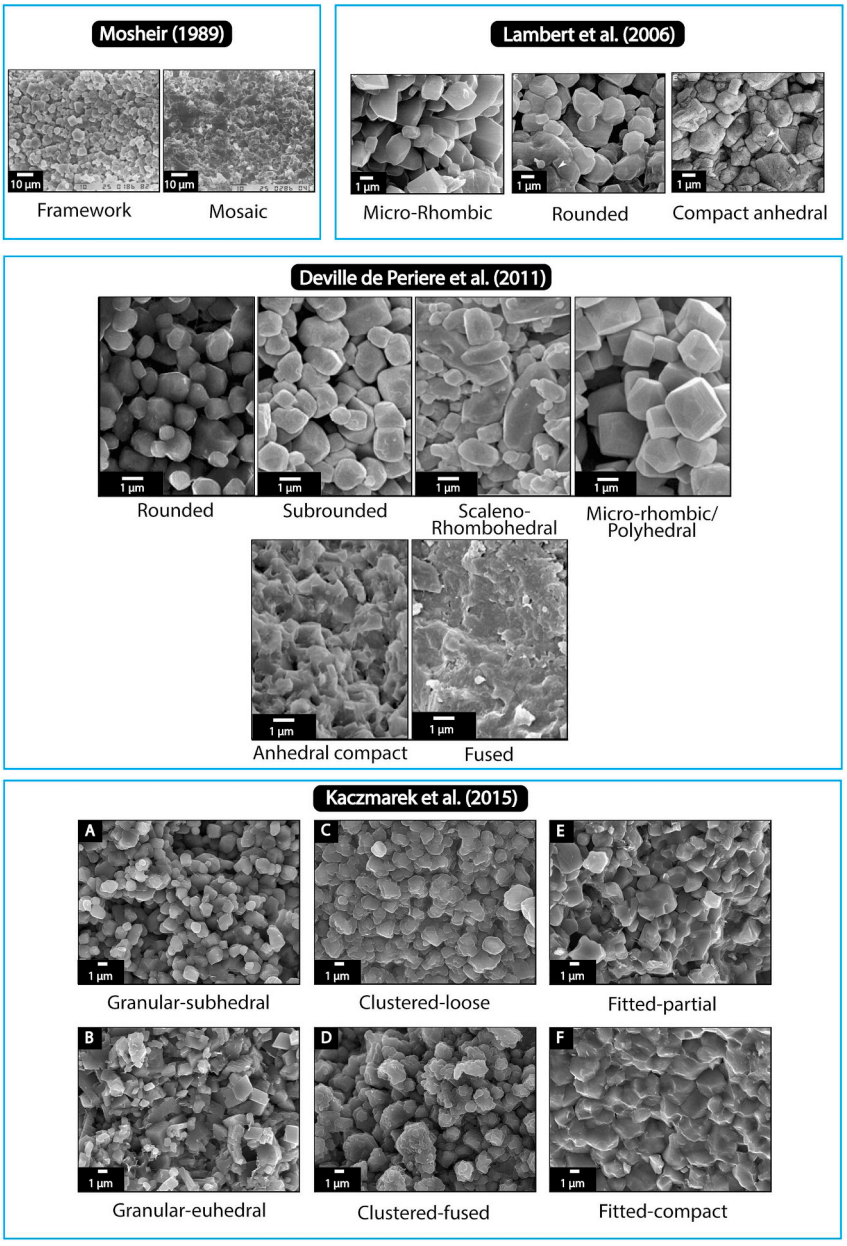


**Fig. 10.** Summary of the main textural classifications of LMC microcrystals. Mosaic texture identified by Moshier (1989a,1989b) corresponds to the fused texture of Deville de Periere et al. (2011), and fitted compact of Kaczmarek et al. (2015). Framework texture of Moshier (1989a,1989b) corresponds to rounded texture of Lambert et al. (2006), rounded texture of Deville de Periere et al. (2011), and granular subhedral of Kaczmarek et al., (2015). Micro-rhombic texture of Lambert et al. (2006) corresponds to subrounded and micro-rhombic textures of Deville de Periere et al. (2011), and granular euhedral texture of Kaczmarek et al. (2015).

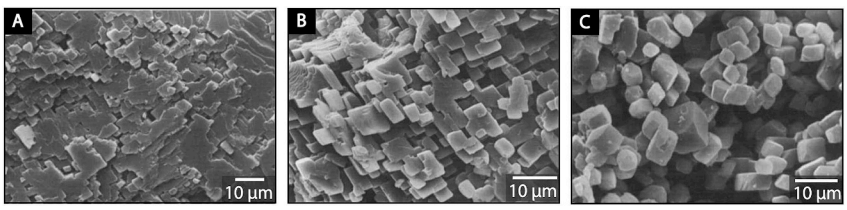


**Fig. 11.** SEM photomicrographs showing a unique texture exhibited by LMC microcrystals in stromatoporoids from Kee Scarp reef, Norman Wells, Canada. LMC microcrystals can be seen to develop 60° and 120° cleavage traces. Modified After Kaldi (1989).

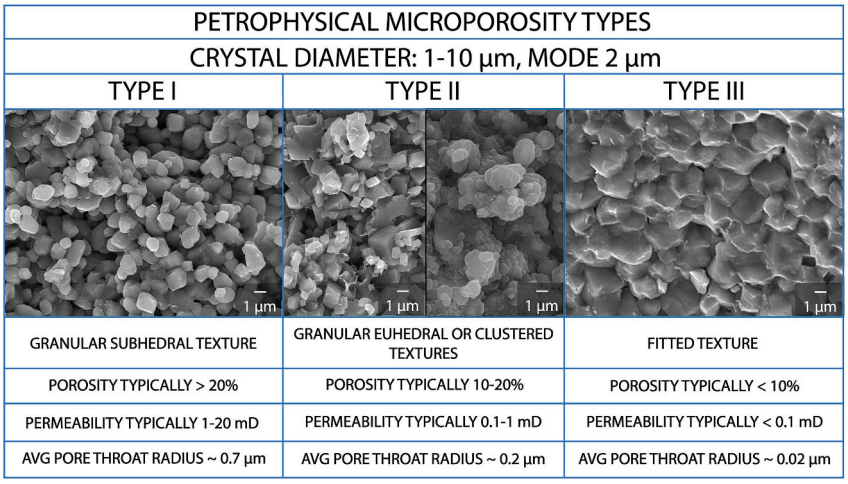


**Fig. 12.** The three petrophysical types proposed by Kaczmarek et al. (2015). Each type is associated with certain microcrystalline texture and petrophysical properties. Modified after Kaczmarek et al. (2015).

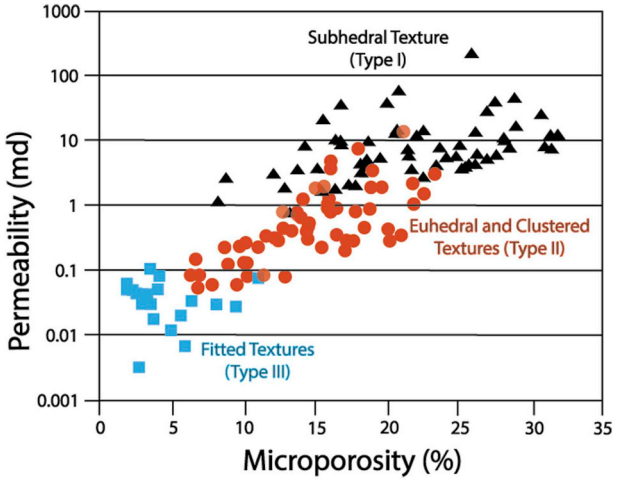


**Fig. 13.** Porosity-permeability cross plot showing log-linear relationship in microporosity dominated limestones. Data compiled from Deville de Periere et al. (2011), Kaczmarek et al. (2015), and Van Simaeys et al. (2017). Data points are color coded based on the dominant microcrystalline texture observed in SEM photomicrographs and the petrophysical types identified by Kaczmarek et al. (2015) (black triangles = granular subhedral texture (type I), red circles = granular euhedral and clustered-loose textures (type II), blue squares = fitted textures (type III).

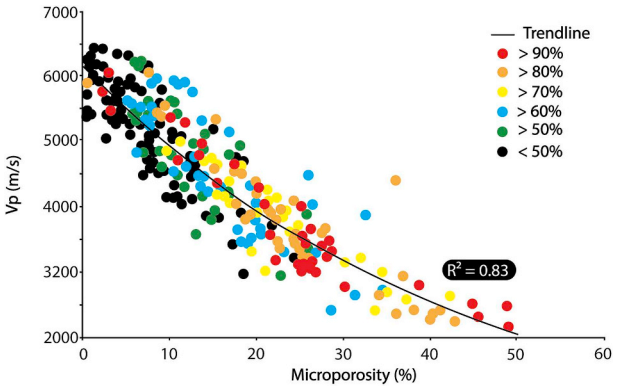


**Fig. 14.** Cross plot showing an inverse relationship between percent microporosity and sonic velocity (Vp). Modified after Baechle et al. (2008).

## 5. Origin of microporosity and LMC microcrystals

The microcrystals that host the majority of micropores in limestones are invariably LMC, whereas modern sediments are predominantly aragonite and HMC (Fig. 6). Texturally, the LMC microcrystals observed in ancient limestones also differ significantly from the materials that comprise modern carbonate sediments (compare Fig. 7 and 9 with 10) (Moshier, 1989a). Geochemically, LMC microcrystals are also dissimilar to modern carbonate sediments in terms of Sr and Mg content (e.g., Carpenter et al., 1991; Hasiuk et al., 2016). Together, these observations suggest that the transformation from the heterogeneous, mineralogically unstable assortment of carbonate sediments observed in modern carbonate settings to the homogeneous, stable assortment of microcrystals observed in ancient limestones is a common diagenetic process (Bathurst, 1975; Longman and Mench, 1978; Ahr, 1989; Budd, 1989; Moshier, 1989a; Loucks et al., 2013; Kaczmarek et al., 2015; Hasiuk et al., 2016).

### 5.1. Mineralogy of precursor sediments

One important aspect of the diagenetic origin of LMC microcrystals is the mineralogy of the precursor sediments (Lasemi and Sandberg, 1984, 1993; Wiggins, 1986; Moshier, 1987; Coimbra et al., 2009; Volery et al., 2009). Investigating precursor mineralogy is important because of the proposed hypothesis regarding secular variations in the dominant carbonate depositional mineral throughout the Phanerozoic (Sandberg, 1983). In modern marine environments, ooids are composed of aragonite exhibiting concentric (tangential) microtexture, whereas ancient ooids are composed of LMC exhibiting predominately radial textures (Kahle, 1974; Sandberg, 1975). Using modern ooids as an analogue, ancient LMC ooids were interpreted to have been stabilized from originally aragonite ooids with concentric microtexture (e.g., Eardley, 1938; Purdy et al., 1964; Carozzi, 1962; Loreau, 1969; Bathurst, 1972). Radial ooids from the Great Salt Lake in Utah, for example, were interpreted as originally aragonite with tangential microtexture that later stabilized to LMC with radial microtexture (e.g., Eardley, 1938; Carozzi, 1962; Bathurst, 1972). However, the proposed textural alteration (tangential to radial) associated with aragonite to LMC stabilization is at odds with observed textures in LMC replacing known skeletal aragonites (Sanders and Friedman, 1967; Sandberg, 1975). Shells composed originally of aragonite typically alter to coarse LMC crystals (Sandberg et al., 1973). Similar textural alterations were also observed in Pleistocene ooids whose original mineralogy was interpreted to be aragonite (Sandberg, 1975). Accordingly, Sandberg

(1975) re-evaluated ooids from Great Salt Lake and observed that their mineralogy is actually aragonite not LMC, and interpreted the radial texture as depositional not diagenetic. Based on these mineralogical and textural relationships, Sandberg (1975, 1983) argued that the original mineralogy in many ancient ooids exhibiting radial texture must have been LMC. This interpretation challenged the existing paradigm about the mineralogy of ancient carbonate sediments and questioned the veracity of using modern sediments as ancient analogues.

Sandberg (1983) also used the aforementioned observations to propose that secular variations in non-skeletal carbonate mineralogy occurred during the Phanerozoic. More specifically, that there were times when aragonite and HMC were favored and other times when LMC was more favored. He called these times "aragonite seas" and "calcite seas," respectively (*sensu* Milliken and Pigott, 1977). The mineralogical oscillations were subsequently shown to broadly correlate with eustatic sea level changes, climatic trends, and seawater Mg/Ca ratio (Mackenzie and Pigott, 1981; Hardie, 1996).

Several mechanisms have been proposed to explain mineralogical variations through the Phanerozoic. Among the most likely causes are changes in atmospheric $pCO_2$ (Mackenzie and Pigott, 1981; Sandberg, 1983, 1985; Wilkinson and Given, 1986) and changes in seawater Mg/Ca ratio (Sandberg, 1975; Wilkinson, 1979; Hardie, 1996). Hardie (1996) presented data showing how the dominant mineralogy of evaporites also changed in conjunction with non-skeletal carbonate mineralogy (Zharkov, 1984; Hardie, 1990). Hardie (1996) reasoned that, although $pCO_2$ may affect carbonates directly, it clearly cannot explain the observed variation in evaporite mineralogy. He thus concluded that changes in Mg/Ca ratio of sea water driven by changes in the rate of ocean crust production is the more likely control on carbonate mineral oscillations during the Phanerozoic. The secular variation in seawater Mg/Ca ratios is extensively reviewed in Ries (2010).

It is important to note that Sandberg (1975, 1983) proposed secular variations in mineralogy for non-skeletal carbonates only. More recent experiments by Ries (2006) and Ries et al. (2006) showed that major aragonite-producing organisms in modern environments such as codiacean algae and scleractinian corals, switched partially to LMC production at slower rates when put in artificial sea water with lower Mg/Ca ratios (Mg/Ca = 2.5 or 1) compared to modern seawater (Mg/Ca = 5.2). Based on these observations, it is reasonable to assume similar variations in lime mud mineralogy also occurred throughout geologic time, since lime mud originates from the degradation of various skeletal materials (Lowenstam, 1955, 1963; Lowenstam and Epstein, 1957; Swinchatt, 1965; Stockman et al., 1967; Neumann and Land, 1975; Sandberg, 1975; Gischler et al., 2013) as well as precipitates inorganically from seawater (Vaughan, 1917; Smith, 1940; Newell, 1955; Cloud et al., 1962; Milliman, 1974; Loreau, 1982; Milliman et al., 1993).

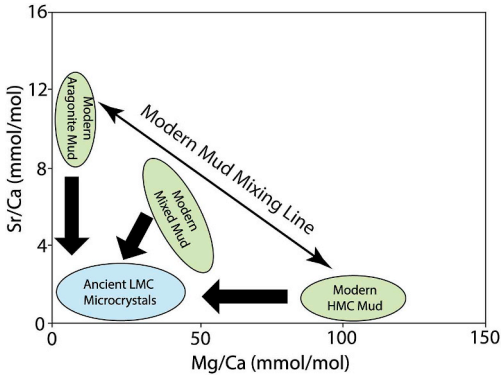


**Fig. 15.** Conceptual diagram showing Sr/Ca and Mg/Ca contents of modern lime mud and ancient LMC microcrystals. Aragonite dominated mud tends to be richer in Sr/Ca, whereas HMC dominated mud tends to be richer in Mg/Ca. Ancient stabilized mud is characterized by lower Sr/Ca and Mg/Ca ratios. Modified after Hasiuk et al. (2016).

Assuming secular variations in the dominant mineralogy of carbonate sediments has occurred (Sandberg, 1983), some studies have postulated a similar trend in the mineralogy of lime mud, the inference being that during times of "calcite seas" carbonate mud is dominated by LMC rather than aragonite and HMC (Moshier, 1987, 1989b; Volery et al., 2009). Moshier (1989b) observed that LMC microcrystals in a Lower Cretaceous limestone in Middle East have low Sr and Mg contents (Sr 148 ppm and Mg 1010 ppm), which he interpreted to reflect the primary signature of LMC dominated sediments. However, based on a compilation of published and new data, Hasiuk et al. (2016) later showed, that the Sr and Mg concentrations in a wide variety of ancient LMC microcrystals are lower than both modern biotic and abiotic calcites precipitated directly from seawater (Fig. 15). This observation led Hasiuk et al. (2016) to argue that LMC microcrystals do not preserve their primary chemical signature with respect to Sr and Mg contents, and therefore low Sr content does not necessarily indicate an LMC precursor.

Based on observations from Cretaceous microporous limestone reservoirs in the Middle East, Volery et al. (2009) more recently suggested that precursor sediments must have been dominated by LMC because they were deposited during times of "calcite seas". Volery et al. (2009) further claimed that "low-Mg calcite muds are a necessary prerequisite for the formation of microporous limestones". Microporous limestones have been observed, however, in limestones deposited during times of "aragonite seas" as well as "calcite seas". Examples from times of "aragonite seas" are Carboniferous: Dickson and Kenter (2014), Permian: Pittman (1971), Pliocene and Early Miocene: Lucia (2017), Miocene: Moshier (1989a), and examples from times of "calcite seas" are Silurian: Munnecke et al. (1997), Devonian: Kaldi (1989), Jurassic: Cantrell and Hagerty (1999), Cretaceous: Volery et al. (2009).

The vast majority of researchers agree that precursor sediments in ancient marine environments were likely to be dominated by aragonite and HMC, similar to sediments in modern marine settings. This consensus is based in large part on published observations from natural environments and laboratory experiments that show aragonite and HMC lime muds transform to LMC microcrystals similar to those observed in ancient limestones (e.g., Bathurst, 1975; Steinen, 1978; Steinen, 1982; McManus and Rimstidt, 1982; Lasemi and Sandberg, 1984; Papenguth, 1991; Lasemi and Sandberg, 1993; Lucia and Loucks, 2013; Lucia, 2017). In addition to the marine sediments, studies, such as Volery et al. (2010a) showed that lacustrine deposits, interpreted to have LMC precursor, now host LMC microcrystals with textures undistinguishable from LMC microcrystals in marine deposits with aragonite and HMC precursors (e.g., Wright et al., 1997; Arribas et al., 2004; Volery et al., 2010a). Deep ocean chalks that form from accumulated LMC coccolith debris also exhibit LMC microcrystals similar to marine and lacustrine limestones (Fabricius, 2007; Faÿ-Gomord et al., 2016). These observations indicate no unique mineral assemblage is required for the development of LMC microcrystals and associated micropores.

### 5.2. Transformation mechanism

A variety of mechanisms have been proposed to explain the diagenetic origin of LMC microcrystals. Bathurst (1958) suggested that transformation of aragonite mud to LMC microcrystals proceeds by grain growth. Grain growth is a dry transformation whereby intercrystalline boundaries migrate causing crystal enlargement (Bathurst, 1958, 1961). This mechanism was adopted from the metallurgy literature where growth of some metals takes place in dry conditions (e.g., Fullman, 1952). Bathurst (1964) later abandoned this idea, based on the understanding that diagenetic environments are always assumed to be wet (Bathurst, 1964; Bathurst, 1975 p. 480). Hathaway and Robertson (1961) investigated experimentally how natural aragonite needles in Bahamian sea water changed under burial conditions

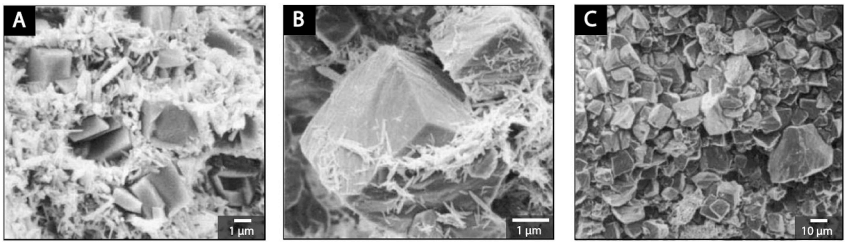


**Fig. 16.** SEM photomicrographs showing rhombic LMC microcrystals within Holocene aragonite mud from the Bahamas. A) Rhombic crystals of calcite within aragonitic sediments. B) LMC microcrystals have grown around and engulfed aragonite needles. C) Interlocking LMC microcrystals free of aragonite sediment. Modified after Steinen (1982).

equivalent to 10–20 km depth (up to 400 °C and 50,000 psi). They observed conversion of aragonite needles to LMC with the retention of the needle shape, although needle terminations became blunted. LMC needles subsequently converted to equidimensional LMC microcrystals. Informed by the experiments of Hathaway and Robertson (1961), Folk (1965) speculated that the transformation process starts with the conversion of larger µm-long aragonite needles to LMC while retaining their needle shape. In contrast, smaller aragonite needles were proposed to fully dissolve with the $CaCO_3$ re-precipitating as LMC overgrowths on the larger LMC needles, thus producing equidimensional LMC crystals.

To explain the formation of larger LMC microcrystals (i.e., microspar), Folk (1965) proposed a process that he called aggrading neomorphism whereby smaller LMC microcrystals grow into larger LMC microspar. "Neomorphism" was used by Folk (1965) as a general term of ignorance encompassing all transformations between one mineral and itself or a polymorph. Folk (1974) proposed that aggrading neomorphism was inhibited by the presence of Mg in the solution, which formed a "cage" around LMC microcrystals preventing crystal growth. Only after Mg was removed from the system, by fresh water for instance, could micrite recrystallize to microspar via aggrading neomorphism (Folk, 1974; Longman, 1977; Longman and Mench, 1978).

Ostwald ripening (Ostwald, 1887), also referred to as grain coarsening, is another process invoked to explain the growth of LMC microcrystals. Ostwald ripening is similar to aggrading neomorphism. In fact, these terms have been used synonymously in the literature (e.g., Dewever et al., 2007; Richard et al., 2007; Carpentier et al., 2015). What distinguishes Ostwald ripening from aggrading neomorphism (*sensu* Folk, 1965) is that the thermodynamic drive for Ostwald ripening comes from minimization of surface free energy of the system via dissolution of smaller crystals and growth of larger ones (Morse and Casey, 1988). Some authors restrict the use of Ostwald ripening to recrystallization where there is no change in mineralogy (e.g., Morse and Casey, 1988; Volery et al., 2010b; Carpentier et al., 2015). Lucia (2017) used the term Ostwald ripening more broadly to refer to recrystallization or mineralogical inversion from one mineral to another (e.g., aragonite to LMC). To avoid confusion, Volery et al. (2010b) introduced the new term "Hybrid Ostwald Ripening" to describe Ostwald ripening involving a change in mineralogy and restricted Ostwald ripening to recrystallization where no mineralogical change occurred. Recently, Ostwald ripening has been proposed by numerous authors to explain the formation of LMC microspar in limestones (Dewever et al., 2007; Richard et al., 2007; Volery et al., 2010a; Léonide et al., 2014; Carpentier et al., 2015; Morad et al., 2018). Evidence in support of Ostwald ripening includes LMC microcrystals size bimodality observed in limestones where smaller crystals are more rounded and interpreted to indicate dissolution, whereas larger crystals are more euhedral and were interpreted to indicate overgrowth (Volery et al., 2010b; Carpentier et al., 2015). Schultz et al. (2013) conducted recrystallization experiments at 23 °C, 100 °C and 200 °C, where LMC submicron crystals with surface area of 11.8 $m^2/g$ observed to grow to ~2 µm in solution saturated with respect to LMC (i.e., at equilibrium). Schultz et al. (2013) attributed the crystal coarsening to Ostwald ripening.

The number of studies that have examined the rates of conversion from aragonite to LMC are numerous (e.g., MacDonald, 1956; Clark, 1957; Fyfe and Bischoff, 1965; Davis and Adams, 1965; Taft, 1967; Bischoff and Fyfe, 1968; Bischoff, 1969; Berner, 1975; Perdikouri et al., 2008), but those that directly investigated textural changes during this process are limited. A handful of case studies in natural environments have been published (Steinen, 1978, 1982; Ahr, 1989; Perkins, 1989; Al-Aasm and Azmy, 1996; Deville de Periere et al., 2011; Loucks et al., 2013; Lucia, 2017), and there are even fewer laboratory-based experimental studies (Moshier and McManus, 1986; Papenguth, 1991). Steinen (1978) examined Pleistocene marine carbonate sediments in Barbados and observed that sediments in the mixing zone are characterized by 65% aragonite, 15–20% HMC, and 10–20% LMC. Microporosity, estimated visually, was 35–40%, and grain size ranges between < 0.1 to ca. 15 µm. In contrast, sediments residing in fresh water (above the mixing zone) are characterized by 100% LMC. Microporosity in these sediments is < 15%. Crystal sizes were bimodal, with small crystals measuring between 0.5 and 2.0 µm, and larger crystals 3–8 µm. The larger crystals were faceted and formed patches or clusters that grew in pore spaces (secondary molds). Steinen (1978) proposed that the larger LMC microcrystals (i.e., microspar) formed, not by aggrading neomorphism, but by a cementation process associated with mineralogical stabilization in fresh water. That is, aragonite and HMC precursor sediments dissolve, and equant LMC microcrystals precipitate as cement crystals into existing pore space. The decrease in microporosity associated with mineralogical stabilization was also interpreted to indicate the introduction and precipitation of carbonates as cement. Later, Steinen (1982) examined Holocene aragonitic mud in the fresh water zone beneath hammocks on the tidal flats of west Andros Island, Bahamas. He observed large (5–15 µm) pitted LMC microcrystals within aragonitic lime mud that appeared to engulf adjacent aragonite needles. Steinen (1982) concluded that LMC microcrystals formed by precipitation as cement crystals among aragonite needles. The precipitation step was proposed to be followed by aragonite dissolution and reprecipitation as LMC. Further cementation and/or compaction, it was argued, is required to produce fitted (mosaic) textures similar to those observed in ancient limestones (Steinen, 1982). Fig. 16 shows rhombic LMC microcrystals among Holocene aragonitic mud from the Bahamas (after Steinen, 1982).

The findings of Steinen (1978, 1982) were later supported by the observations from laboratory experiments reported in a GSA conference abstract by McManus and Rimstidt (1982) and later published by Moshier and McManus (1986) and Moshier (1989a). These experiments, which involved the conversion of aragonite to LMC at 50°–100 °C and 1 bar, were intended to mimic shallow burial diagenesis of aragonite-dominated lime muds (Moshier and McManus, 1986). The experimental conditions more accurately resemble sedimentary conditions than the earlier experiments by Hathaway and Robertson (1961), which were conducted at high temperatures and pressures (up to 400 °C and 3447 bar). McManus and Rimstidt (1982) reported that aragonite needles sequentially transformed to equant LMC crystals (2–15 µm in diameter) suggesting that mineralogical conversion took place by passive dissolution of aragonite and precipitation of LMC cement crystals (Fig. 17).

The only other laboratory study to examine the conversion of metastable carbonate to LMC from the textural standpoint was a Ph.D. dissertation completed under the guidance of Philip Sandberg. In this

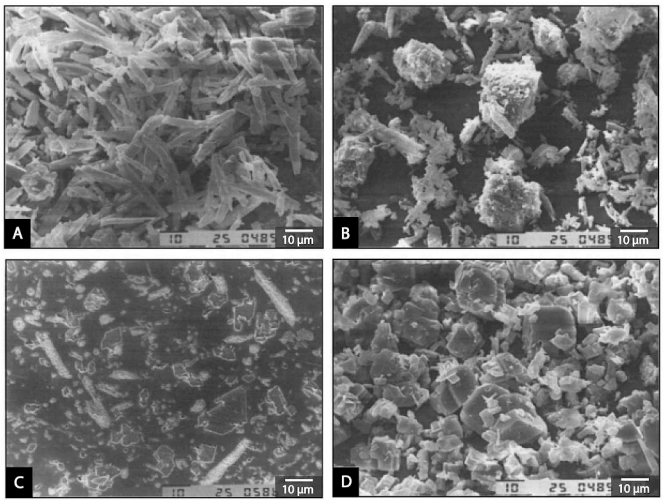


**Fig. 17.** SEM photomicrographs illustrating the conversion of synthetic aragonite needles to LMC microcrystals in stabilization experiments in distilled water at 50 °C conducted by McManus and Rimstidt (1982). A) Texture of the reactant that is composed of 95% synthetic aragonite and 5% reagent grade LMC. B) Experimental result after conversion of 50% of aragonite to LMC. C) Polished and etched SEM photomicrograph of experimental result after conversion of 50% of aragonite to LMC. D) Experimental result after conversion of 100% of aragonite to rhombic LMC microcrystals. Modified after Moshier (1989a).

study, Papenguth (1991) conducted dozens of open and closed system experiments to evaluate lime mud stabilization. Papenguth (1991) used a variety of carbonate precursors, including natural lime mud collected from the Bahamas and Florida, artificial mud prepared from pulverizing modern skeletal material, and fine-grained carbonate precipitates formed in the laboratory. Papenguth (1991) observed that lime mud stabilization to LMC occurs by dissolution of the reactant and precipitation of LMC rhombic cement crystals. Further, it was observed that after complete transformation of aragonitic lime mud to LMC microcrystals, no further change in LMC crystal size occurred, which argues against the role of aggrading neomorphism in LMC stabilization. The main drawback of this study is the general lack of experimental control. More specifically, multiple variables were change between experiments, thus complicating any attempt to evaluate individual controls on the process and outcomes of mineralogical stabilization.

Lasemi and Sandberg (1984, 1993) observed pitted surfaces in LMC microcrystals, which they interpreted as relics formed by dissolution of aragonite needles, and elevated Sr concentrations in larger LMC microspar as evidence against aggrading neomorphism. They reasoned that if aggrading neomorphism was responsible for the transformation of LMC microcrystals to larger LMC microspar, then aragonite relics would have been obliterated during this secondary recrystallization process. Instead, Lasemi and Sandberg (1984, 1993) proposed that LMC microcrystals (micrite and microspar) form during a single step, and that the mineralogy of the precursor sediments is what controls the crystal size. Relatively large (4–9 µm) crystals that engulf aragonite relics, with higher Sr concentrations, and rough or pitted crystal surfaces, were also interpreted by Lasemi and Sandberg (1984) to reflect an aragonite dominated precursor. In contrast, relatively small (2–4 µm) crystals that lack aragonite relics, with lower Sr concentrations, and smooth surfaces, were interpreted to reflect an LMC dominated precursor. In a later study, Munnecke et al. (1997) compared Pliocene carbonates from the Bahamas to Silurian limestones from Sweden. Pitted microspar surfaces were interpreted by Munnecke et al. (1997) as evidence of dissolution of aragonite precursors, consistent with the interpretation of Lasemi and Sandberg (1984, 1993) that microspar crystals form as cements during dissolution-precipitation and not by aggrading neomorphism.

Recently, Lucia and Loucks (2013) and Lucia (2017) examined the transformation process from aragonite mud to LMC microcrystals in the Neogene limestones of the Clino well from the Bahamas. Bulk mineralogy was reported to be 0–25% aragonite, 73–91% LMC, and 0–66% dolomite. Lucia and Loucks (2013) observed a change in texture and mineralogy with depth from a heterogeneous mixture of metastable sediments to a more homogeneous assortment of LMC. Based on the observation that porosity remained constant through the interval examined, they concluded that stabilization is a local dissolution-precipitation process taking place in a closed system without introduction of additional carbonate from an outside source. However, Lucia and Loucks (2013) observed several examples where sediments dominated by LMC microcrystals had lower porosity values, which they attributed to additional cementation. The findings of Lucia and Loucks (2013) suggest that the pore space observed in microporous limestones is inherited from the initial muddy carbonate sediments, which have long been known to contain an abundance of pore space (Bathurst, 1975; Enos and Sawatsky, 1981; Lucia and Loucks, 2013; Lucia, 2017). The eventual configuration of the micropores, however, is dictated by the distribution of diagenetic LMC microcrystals. Lucia (2017) also investigated the carbonates in Clino well, but focused on the formation of the smaller LMC microcrystals (i.e., micrite). He observed that the bulk mineralogy of a sample composed of minimicrite (*sensu*, Reid and Macintyre, 1998) which refers to crystals < 1 µm was a mixture of aragonite and LMC, but that the bulk mineralogy of a sample composed of crystals 1–4 µm (micrite) and > 4 µm (microspar) contained only LMC. Lucia (2017) also noted a decrease in minimicrite but an increase in micrite with depth. SEM observations also revealed that anhedral micrite crystals appeared to be aggregates of many smaller minimicrite crystals. These observations were interpreted by Lucia (2017) to reflect dissolution of aragonite and some LMC minimicrite with concomitant precipitation of LMC cement on adjacent LMC minimicrite crystals, which forms larger micrite crystals. Similar to this, microspar appeared to Lucia (2017) to form as individual micrite crystals cemented together. Lucia (2017) further measured minimicrite crystal sizes and observed no change with depth. Based on this observation, Lucia (2017) concluded that Ostwald ripening could not explain the formation of LMC microspar, because if Ostwald ripening was controlling the dissolution of minimicrite, the average crystal size of minimicrite should decrease with depth.

Dissolution has been proposed as a mechanism to explain the occurrence of microporosity in limestone (Oldershaw, 1972; Wilson, 1975; Frost et al., 1983; Harris and Frost, 1984; Harris et al., 1985; Dravis, 1989; Jameson, 1994). Oldershaw (1972) examined Ordovician limestones from Ontario, Canada and observed microporous textures to be associated with supratidal, evaporitic facies, whereas non-porous textures were observed in subtidal facies. A supratidal environment was indicated by the presence of fine-grained dolomite, and chalcedony, both observations interpreted to indicate high salinity environment. Oldershaw (1972) attributed the preservation of micropores to the early precipitation of interstitial evaporite cements that prevented the occlusion of the micropores by LMC overgrowth. The microporous textures, it was proposed, developed after the dissolution of the interstitial evaporite cements. Evaporite dissolution, however, cannot explain the occurrence of LMC microcrystals, and has been shown unsatisfactory to explain the majority of micropores (e.g., Moshier, 1989a). The vast majority of evidence suggests that LMC microcrystal development is a constructive process rather than a destructive one (Folk, 1965; Bathurst, 1975; Moshier, 1989a; Cantrell and Hagerty, 1999; Loucks et al., 2013; Hasiuk et al., 2016). The microporosity, it has been argued, is not produced during diagenesis, but rather redistributed to micropores associated with the diagenetic LMC microcrystals (Lucia and Loucks, 2013; Kaczmarek et al., 2015). In summary, data from numerous studies suggest that the transformation of aragonite and HMC dominated sediments to LMC microcrystals occurs via a dissolution–precipitation process driven by mineralogical stabilization

**Table 2**
Chemical and thermodynamic data for calcite and aragonite minerals at earth surface conditions (25 °C and 1 atm.). Data from Robie and Hemingway (1995) and Fegley (2012).

| Chemical Formula | Mineral | Crystal System | $V_m$ ($cm^3$) | $S^o_{298}$ (J $K^{-1}$ $mol^{-1}$) | $C^o_P$ (J $K^{-1}$ $mol^{-1}$) | $\Delta_f H^o_{298}$ (KJ $mol^{-1}$) | $\Delta_f G^o_{298}$ (KJ $mol^{-1}$) |
|---|---|---|---|---|---|---|---|
| $CaCO_3$ | Calcite | Trigonal | 36.94 | 91.71 | 83.47 | −1207.37 | −1128.84 |
| | Aragonite | Orthorhombic | 34.16 | 87.99 | 82.32 | −1207.43 | −1127.79 |

(Land et al., 1967; Budd, 1989; Moshier, 1989a; Al-Aasm and Azmy, 1996; Cantrell and Hagerty, 1999; Melim et al., 2002; Loucks et al., 2013; Kaczmarek et al., 2015; Hasiuk et al., 2016; Lucia, 2017). Aragonite and HMC are metastable under most surface conditions and tend to stabilize to LMC (Bathurst, 1975; Steinen, 1978; Carlson, 1983). During this process, the pore system changes from one characterized by a heterogeneous assortment of pore sizes and shapes in the interstices between grains, mud, etc. to one characterized by a narrow distribution of pore shapes and sizes in the interstices between LMC microcrystals.

### 5.3. Constraints on the stabilization process

Mineralogical stabilization as it pertains to carbonate diagenesis is a complex process. It involves various mineral reactants exhibiting a wide range in texture, size, and abundance, texturally variable products, and several diagenetic conditions that may affect reaction kinetics in various ways. These factors are discussed below with a focus on how they impact microporosity development.

#### 5.3.1. Mineralogical constraints

LMC and aragonite are two phases of calcium carbonate ($CaCO_3$). These two polymorphs have different physical, chemical, and thermodynamic properties (Table 2). Based on the thermodynamic data, LMC is more stable compared to aragonite. That is, the reaction from aragonite$_{(s)}$ to calcite$_{(s)}$ is thermodynamically favored, because $\Delta_f G_{calcite} < \Delta_f G_{aragonite}$. However, transformation of aragonite to LMC, as well as the direct precipitation of carbonate minerals from seawater, is governed by kinetic factors (Morse and Mackenzie, 1990).

In nature, carbonate minerals exhibit unique responses to mineralogical stabilization (Bathurst, 1975; Flügel, 2013; Loucks et al., 2013). Whereas aragonitic lime muds have been observed to transform to LMC microcrystals both naturally and experimentally (Steinen, 1978, 1982; McManus and Rimstidt, 1982; Lasemi and Sandberg, 1984; Papenguth, 1991), aragonite allochems are not thought to yield the microporous textures observed in ancient limestones. Instead, aragonite allochems typically undergo dissolution leading to mold formation (e.g., Friedman, 1964; Land et al., 1967), or dissolution accompanied by LMC spar precipitation (Sandberg and Hudson, 1983; Martin et al., 1986; Brand, 1989; Budd, 1989, 1992; Cantrell and Hagerty, 1999; Loucks et al., 2013). Saller and Moore (1989) proposed that LMC microcrystals do not form in aragonite skeletal grains, at least not in the open marine and mixing zone realms. In Pleistocene sediments from Enewetak Atoll, they interpreted neomorphic LMC spar cement to replace the aragonite skeletons of coral, algae, and molluscs. Aragonite grains were observed to undergo dissolution accompanied by precipitation of LMC cement crystals as overgrowth (Saller and Moore, 1989). Depleted oxygen isotope values (−5 to −9‰ VPDB) in the neomorphic spar were interpreted by Saller and Moore (1989) to indicate precipitation in a meteoric environment. Based on these observations, Saller and Moore (1989) proposed mineralogical stabilization of aragonite to neomorphic LMC spar passing through an intermediate stage characterized by intrafabric dissolution and LMC overgrowth cement.

The mechanism by which aragonite converts to LMC is controlled by kinetic and hydrologic factors (e.g., Pingitore, 1976; McManus, 1982; Carlson, 1983). McManus (1982) investigated the role of reactive surface area on the transformation of aragonite to LMC through stabilization experiments. She proposed three transformation mechanisms to explain the variability in LMC textures based on the reactive surface area available. The proposed mechanisms include passive dissolution precipitation, transformation across a chalk zone, and transformation across a thin fluid film (McManus, 1982). In experiments where fine aragonite powder was used as reactant (i.e., large reactive surface area), the conversion to LMC was texturally destructive, and thus inferred to proceed by passive dissolution-precipitation (Taft, 1967; McManus, 1982; McManus and Rimstidt, 1982; Papenguth, 1991). Conversely, when the surface area of the reactant was lower, the transformation of aragonite was proposed to proceed by thin fluid films based on the observation that the texture of the reactant is preserved (McManus, 1982; Budd and Hiatt, 1993). Transformation through thin films has not been observed in laboratory because the process requires slow reaction rates (McManus, 1982).

The lack of LMC microcrystal formation in aragonite allochems is contrasted with the observation that LMC microcrystals are commonly develop in HMC allochems (e.g., Budd, 1989; Saller and Moore, 1989; Budd, 1992; Al-Aasm and Azmy, 1996; Cantrell and Hagerty, 1999; Loucks et al., 2013). Budd (1989) observed that LMC microcrystals in the Shuaiba Formation, U.A.E., occurred most commonly in HMC dominated micritic materials, including the carbonate mud in boundstones and packstones, as well as in micritized pellets and micritized porcellaneous foraminifera. LMC microcrystals, in contrast, were absent in originally aragonite and LMC allochems, nor were they observed in echinoderms and hyaline foraminifera (Budd, 1989). The inference being that stabilities of echinoderms and hyaline foraminifera are determined by their microstructure, not their mineralogy. In Kee Scarp reefs, Canada, LMC microcrystals have been observed in stromatoporoids which interpreted to have HMC precursor, whereas corals, which interpreted to be originally aragonite were not microporous (Al-Aasm and Azmy, 1996). In their study of the Jurassic Arab Formation in Saudi Arabia, Cantrell and Hagerty (1999) reported that originally aragonitic allochems, including mollusks, corals, and dasycladacean algae, were leached, but HMC allochems were microporous. Originally LMC allochems, such as brachiopods, bryozoans, arthropods, and stromatoporoids were neither leached nor microporous, but exhibited well preserved skeletal microstructures. It is worth noting, however, that Cantrell and Hagerty (1999) inferred original grain mineralogy based on published textural observations (e.g., Chave, 1964; Purser, 1969; Johnson, 1971; Majewske, 1974; Bathurst, 1975; Sandberg, 1975; Wray, 1977; Wilkinson et al., 1985), some of which are in disagreement. For example, the original mineralogy of ooids has been

**Table 3**
Qualitative susceptibility of carbonate grains to micropore development. Based on data from[1]Budd (1989),[2]Al-Aasm and Azmy (1996),[3]Cantrell and Hagerty (1999),[4]Loucks et al. (2013), and [5]Kaczmarek et al. (2015).

| Higher Susceptibility | Lower Susceptibility |
|---|---|
| Matrix[1,2,3,4] | Echinoderms[1,3,5] |
| Micritized Grains[1,3,4] | Bivalves[5] |
| Peloids[3,4,5] | Brachiopods[3,5] |
| Ooids[3,5] | Hyaline Foraminifera[1] |
| Corals[2,5] | Stromatoporoids[3] |
| Foraminifera[2] | Ostracodes[3] |
| Stromatoporoids[2] | |
| Algae[4,5] | |

interpreted to be aragonite and HMC which suggests uncertainty in the understanding of the precursor mineralogy (Cantrell and Hagerty, 1999, Table 1). In their global survey of microporous Phanerozoic limestones, Kaczmarek et al. (2015) reported that peloids, ooids, corals, foraminifera, and algae are generally more susceptible to develop micropores than echinoderms, bivalves, and brachiopods. Loucks et al. (2013) investigated the genesis of the micropores in Pawnee Field, Texas. Based on petrographic observations, they interpreted open and cement-filled molds as dissolved aragonite allochems (e.g., bivalves), whereas HMC grains, including foraminifera, red algae, and other micritized allochems developed LMC microcrystals. Although no systematic quantitative evaluation of the relative susceptibilities of carbonate allochems has been provided, qualitative observations from the various studies are illustrated in Table 3.

The most common diagenetic pathway for unstable HMC allochems is dissolution and concurrent precipitation of LMC pore-filling cement (e.g., Land et al., 1967; Richter, 1979; Brand and Veizer, 1980; Turner et al., 1986; Budd, 1992). In rare cases, dissolution of HMC allochems lead to mold formation (Schroeder, 1979; Saller, 1984; Budd, 1992). Budd (1992) showed that moldic pores in the Bahamas and Bermuda formed as a result of HMC dissolution during exposure to meteoric fluids. Diagenetic transformation of HMC allochems occur either by incongruent dissolution (Chilingar, 1962; Friedman, 1964; Land et al., 1967; Schroeder, 1969; Gomberg and Bonatti, 1970) or congruent dissolution (Oti and Müller, 1985; Turner et al., 1986). Incongruent dissolution refers to a cation exchange process where Mg is replaced by Ca within the crystal lattice thus preserving the allochem microstructure (Friedman, 1964). This hypothesis has been disproven based on the observed textural and chemical modifications that accompany transformation of HMC to LMC (e.g., Oti and Müller, 1985; Budd and Hiatt, 1993). Congruent dissolution, in contrast, is synonymous with passive dissolution-reprecipitation and entails textural alteration/replacement (Oti and Müller, 1985).

Towe and Hemleben (1976) proposed that HMC porcellaneous foraminifera undergo mineralogical stabilization in two stages based on the observation that unaltered tests are composed of HMC needles and laths, whereas altered tests are composed of LMC needles, laths, and equant LMC crystals. In this model, the first stage involves a mineralogical change and textural preservation where HMC needles and laths convert to LMC. The second stage includes a textural change whereby the LMC laths and needles convert to equidimensional crystals. Budd and Hiatt (1993) investigated the stabilization process of Holocene porcellaneous foraminifera in the meteoric environment from the Bahamas. Based on textural observations and geochemical data, they concluded that HMC skeletons of foraminifera undergo mineralogical stabilization with no textural change. Budd and Hiatt (1993) observed that Mg loss corresponds to how long the foraminifera were subjected to meteoric fluids. To explain the observed textural retention but geochemical change, they proposed that stabilization of porcellaneous foraminifera involves incongruent intracrystal alteration via incremental dissolution-precipitation, consistent with the first stabilization stage proposed by Towe and Hemleben (1976). Budd and Hiatt (1993) did not, however, report a second stabilization stage characterized by textural alteration. It is unknown if two-step stabilization applies to other HMC skeletons because evidence of an earlier stage of alteration would be obscured in most cases (Budd and Hiatt, 1993).

Plummer and Mackenzie (1974) investigated biogenic HMC dissolution by reacting *Amphiroa r.* (coralline algae) in distilled water at 25 °C with continuous addition of $CO_2$ gas. Based on the slope changes in a plot of [Ca] and [Mg] versus the square root of time, Plummer and Mackenzie (1974) identified three stages of dissolution. Stage 1 and 2 are marked by a linear relationship between Ca and Mg, and were interpreted to reflect congruent dissolution of the HMC. Stage 3 is characterized by nonlinear relationship and was interpreted to indicate incongruent dissolution. This incongruent dissolution was further supported by comparing XRD patters of the initial and the partially dissolved material. Plummer and Mackenzie (1974) observed a reduction in the asymmetry toward more Mg-rich calcite in the partially dissolved material, which was interpreted to result from the incongruent dissolution of the higher Mg-calcite portions of *Amphiroa r.*

Oti and Müller (1985) carried out year-long experiments where HMC skeletons of *Lithothamnion* sp. (Coralline algae) reacted in distilled water with various concentrations of $CaCl_2.2H_2O$. Although they observed no shift in the (104) XRD reflection in the altered material, they did observe a decrease in the peak intensity, which was interpreted to indicate a reduction in the amount of HMC material due to replacement by LMC. Oti and Müller (1985) argued for congruent dissolution (i.e., passive dissolution-precipitation) whereby HMC dissolves and rhombic LMC microcrystals precipitate as cement. Stabilization, however, was documented only in fluids with $CaCl_2.2H_2O$ added. In these experiments, the abundance of LMC microcrystals precipitated as measured by XRD correlated with amount of $CaCl_2.2H_2O$ in the experimental fluids. In contrast, no LMC precipitated in the distilled water experiments. Oti and Müller (1985) interpreted the irregular release of Mg and Ca into solution, which had also been documented previously (Schroeder, 1969; Plummer and Mackenzie, 1974), to indicate spatial heterogeneity of Mg within the skeletons, and that Mg exists in compounds other than $MgCO_3$. Therefore, Oti and Müller (1985) suggested that more Mg is released into the solution from dissolution of the more soluble portions of skeletons (i.e., the Mg-enriched parts).

Laboratory stabilization of HMC (Oti and Müller, 1985), and aragonite in Mg-bearing fluids have been largely unsuccessful (e.g., Fyfe and Bischoff, 1965). Explanations for this include the presence of chemical inhibitors, such as Mg, $PO_4$, $SO_4$, and organic matter (Fyfe and Bischoff, 1965; Bischoff and Fyfe, 1968; Bischoff, 1969; Carlson, 1983; Papenguth, 1991). In seawater, the most significant chemical inhibitor is Mg (Carlson, 1983). It has been proposed that Mg hinders both direct precipitation of LMC (Lippman, 1960; Simkiss, 1964; Berner, 1975) and stabilization of aragonite and HMC to LMC (Taft, 1967; Bischoff and Fyfe, 1968; Berner, 1975; Carlson, 1983). Inhibition of LMC growth by Mg is thought to occur by adsorption of Mg at active growth sites and into LMC crystal structure (Berner, 1975; Carlson, 1983).

Bischoff and Fyfe (1968) observed that it took longer for LMC growth to initiate in experimental solutions with higher concentrations of Mg. Bischoff and Fyfe (1968) suggested that LMC grown in the Mg-bearing solution incorporates Mg until the concentration of Mg drops below a critical value. After this, LMC growth proceeds as it does in the Mg-free solutions. Importantly, the concentrations of $MgCl_2$ in their experiments were at least an order of magnitude lower than concentrations of $CaCl_2$. Modern seawater, it should be noted, has an Mg/Ca of ~5.0 (Lowenstein et al., 2001) so the applicability of these experiments to nature is uncertain.

LMC allochems are generally considered more stable and therefore less susceptible to diagenetic alteration in most diagenetic environments (James and Choquette, 1984; Morse and Mackenzie, 1990). Dravis (1989), however, reported that LMC grains (oyster fragments) in the Haynesville Formation, Texas, exhibited microporous textures similar to HMC allochems, such as foraminifera and red algae. This study was based on observations from thin section photomicrograph taken under blue-light fluorescence, where bright areas were interpreted to indicate the existence of micropores. No SEM photomicrographs of the oyster shells were provided so the presence of LMC microcrystals cannot be confirmed. Based on petrographic and geochemical observations, including lack of subaerial exposure, lack of meteoric cement or vuggy pores, extensive pressure solution features, and stable carbon and oxygen isotopes of LMC cements consistent with burial diagenesis, Dravis (1989) suggested that microporosity development occurred in the deep burial realm where corrosive fluids led to development of microporous textures.

#### 5.3.2. Textural constraints

The texture of precursor carbonate sediments has also been shown

to be an important control on mineralogical stabilization and subsequent microporosity development (e.g., Al-Aasm and Azmy, 1996; Cantrell and Hagerty, 1999; Loucks et al., 2013; Carpentier et al., 2015). This is especially true for allochems. Dissolution of biogenic carbonates has been shown in laboratory experiments to be influenced by fluid chemistry, as well as the mineralogy and microstructure of the allochems (Walter, 1983; Walter and Morse, 1985). Walter and Morse (1985) showed that allochem microstructure can override thermodynamic constraints of mineralogical solubility under certain chemical conditions. Dissolution experiments involving carbonate allochems were carried out in solutions where the saturation state was held constant by controlling the $[Ca^{+2}]$, $[CO_3^{-2}]$, $pCO_2$, pH, and ionic strength. In solutions undersaturated with respect to LMC, Walter and Morse and Mackenzie (1993) showed that aragonite allochems with finely crystalline microstructures, such as green algae (*Halimeda*) and gastropods, dissolve faster than HMC allochems, such as foraminifera (*Peneroplis*) (15 mol% $MgCO_3$) and red algae (18 mol% $MgCO_3$) that are more thermodynamically unstable and have a lower reactive surface area. Al-Aasm and Azmy (1996) showed that micropores associated with LMC microcrystals developed more extensively in tabular stromatoporoids than in algae. They reasoned that the open skeletal structure of stromatoporoids allowed fluids to more easily pass through the skeletal framework and thus establish a positive feedback on the rate. A microstructural control was also invoked by Cantrell and Hagerty (1999) to explain the lack of micropore development in echinoderm fragments, which are comprised of a single crystal of HMC and have relatively low reactive surface area.

Numerous studies have shown that micritized grains are more likely to exhibit microporous textures (e.g., Pittman, 1971; Ahr, 1989; Budd, 1989; Cantrell and Hagerty, 1999; Loucks et al., 2013). According to Bathurst (1966), micritization refers to the process by which the original fabric of a carbonate allochem is altered to microcrystalline carbonate. Micritization, refers specifically to alteration to aragonite or HMC only, not LMC stabilization (Alexandersson, 1972; Reid and Macintyre, 1998; Flügel, 2013). Initially, micritization was interpreted as inorganically precipitated microcrystalline carbonate in the voids left by endolithic borings by microorganisms, such as bacteria and algae (Bathurst, 1966; Alexandersson, 1972). Reid and Macintyre (2000) recognized another type of micritization where biologically induced precipitation of aragonite takes place concurrently with endolithic activity. A third type of micritization occurs via recrystallization of skeletal allochems that occurs during the life cycle of the organism and continues post mortem. This process has been shown to be widespread in shallow marine environments (Purdy, 1968; Reid and Macintyre, 1998). Reid and Macintyre (1998) documented recrystallization micritization in living *Archaias* porcellaneous foraminifer (HMC) where the original aragonite/HMC rods comprising the skeletal wall recrystallize to anhedral equant minimicrite (0.05–0.1 μm) without an associated mineralogical change. They also documented post-mortem recrystallization as a series of textural changes from skeletal rods and needles that convert to minimicrite (crystals that are < 1 μm), which then convert to pseudomicrite (crystals that measure between 0.02 and 0.05 μm) and finally micrite (1–4 μm). Although the formation of minimicrite from rods and needles involves no change in mineralogy, the formation of pseudomicrite and micrite may involve a change in mineralogy from HMC to aragonite or vice versa (Reid and Macintyre, 1998). Hover et al. (2001) reported similar observations on living and recently deceased *Peneropolid* foraminifera from Florida and the Bahamas. The elongated HMC crystal rods in the tests of living samples were observed under the SEM to be shorter and more equidimensional than in altered foraminifera (Hover et al., 2001). Using high-resolution scanning transmission analytical electron microscopy (STEM/AEM), Hover et al. (2001) observed that HMC crystals comprising the altered tests exhibited rounded terminations and more irregular shapes, which they interpreted as evidence of dissolution. The crystals comprising the altered test were also cemented together by intercrystalline material forming larger aggregates, interpreted as evidence of precipitation (Hover et al., 2001). Hover et al. (2001) also observed that average crystal lengths increased from 280 ± 9 nm in living organisms to 353 ± 15 nm in deepest interval (12–14 cm), and average crystal widths increased from 56 ± 1 nm in living specimens to 120 ± 4 nm in the deepest interval. Based on these observations, they proposed that textural alterations in *Peneropolid* foraminifera occur without mineralogical changes and is driven by Ostwald ripening.

Recrystallization processes described by Macintyre and Reid (1995), Reid and Macintyre (1998), and Hover et al. (2001) occur in shallow marine environments to living organisms and during post-mortem. Although these recrystallization processes may involve mineralogical changes from aragonite to HMC or vice versa, they are unrelated to mineralogical stabilization to LMC (Reid and Macintyre, 1998, p. 944) despite being confused with the process of mineralogical stabilization by which LMC microcrystals develop (e.g., Kaczmarek et al., 2015).

#### 5.3.3. Diagenetic environments

Geochemical and petrographic observations implicate various diagenetic environments for mineralogical stabilization of carbonate sediments. Moshier (1989b) presented geochemical data from LMC microcrystals in the Lower Cretaceous Thamama Group at Sajaa field, U.A.E. Average $\delta^{18}O$ and $\delta^{13}C$ values were −4 to −5‰ and 1.5–5‰, respectively. Trace element (Fe, Mn, Sr, Na) concentrations were depleted ($10^1$–$10^2$ ppm) relative to modern marine carbonates. Moshier (1989b) interpreted the low concentrations of trace elements as the primary signature of a precursor sediments dominated by LMC. Negative $\delta^{18}O$ values suggested to Moshier (1989b) that stabilization happened at slightly elevated fluid temperatures (~40–48 °C) corresponding to shallow burial between 530 and 815 m $\delta^{13}C$ values also became less positive with depth, which was interpreted to reflect addition of isotopically light $CO_2$ generated by anaerobic microbial activity at shallow burial depths (Irwin et al., 1977). Using a closed system model linking the observed changes in $\delta^{18}O$, porosity, and temperature, Moshier (1989b) concluded that stabilization occurred in "marine-like" fluids in the shallow burial realm.

Budd (1989) investigated Thamama Group limestones in an adjacent field to the field studied by Moshier (1989b). Despite observing low trace element concentrations and depleted $\delta^{18}O$ values, Budd (1989) proposed that two diagenetic events were required for microporosity development. The first corresponds to mineralogical stabilization to LMC by meteoric fluids in a water-buffered system, which is reflected in both the low Sr and Mg concentrations and depleted $\delta^{18}O$. The second, Budd (1989) posited, is LMC recrystallization that further reduced $\delta^{18}O$. The drive for secondary LMC recrystallization was not discussed. Budd (1989) further argued that mineralogical stabilization in marine fluids was unlikely because the high Mg/Ca ratio of seawater would inhibit LMC growth as documented in numerous studies (Fyfe and Bischoff, 1965; Bischoff and Fyfe, 1968; Bischoff, 1969; Berner, 1975; Carlson, 1983; Papenguth, 1991).

Meteoric fluids are the most commonly implicated to explain carbonate stabilization (Longman and Mench, 1978; Ahr, 1989; Budd, 1989; Perkins, 1989; Richard et al., 2007; da Silva et al., 2009; Volery et al., 2009; Volery et al., 2010b; Deville de Periere et al., 2011). Based on petrographic observations, including clay-filled karst cavities, aragonite allochem molds, and sparry calcite cements, in Cretaceous age carbonates from Iraq, Qatar, and U.A.E., Deville de Periere et al. (2011) suggested that mineralogical stabilization occurs in meteoric fluids. A gradual increase in $\delta^{13}C$ (1.1–3.5‰) in LMC microcrystals below a major unconformity was also consistent with the addition of soil carbon associated with meteoric diagenesis (Deville de Periere et al., 2011).

Insights on the diagenetic environment where mineralogical stabilization occurs have also come from investigations of the Neogene and Pleistocene limestones in the Clino and Unda cores, which are located along the western margin of the Great Bahama Bank (Melim et al., 1995, 2002, 2001a; 2001b; Melim, 1996; Melim and Masaferro, 1997;

Munnecke et al., 1997; Westphal and Munnecke, 1997; Westphal, 1998; Swart, 2000; Swart and Melim, 2000; Westphal et al., 1999b, 2000). Based on the observation that aragonite needles are commonly engulfed in LMC microcrystals, the limestones are interpreted to have an aragonitic precursor (Munnecke et al., 1997; Melim et al., 2002). Melim et al. (2002) used petrographic and geochemical data to propose a model whereby LMC cement forms at the expense of the dissolution of aragonite dominated muds. They reasoned that this process happened in seawater because the sediments showed no evidence of having been in contact with meteoric fluids. The interpretation that LMC microcrystals form in the marine realm (Melim et al., 2002) challenged the idea that stabilization does not take place in the presence of Mg, as implied by stabilization experiments performed by Fyfe and Bischoff (1965), Taft (1967), Berner (1975), and Papenguth (1991), and argued by many authors (e.g., Ahr, 1989; Budd, 1989; Perkins, 1989). One possibility is that pore-fluids were Mg-depleted. Dolomite was observed, but pore-fluids were not analyzed. Aragonite dissolution in shallow marine environments is typically unfavorable because above the aragonite compensation depth (ACD), as it is the case in Clino and Unda wells, seawater is supersaturated with respect to aragonite (Melim et al., 2002). Dissolved aragonite in wells 1007 and 1006, both of which are located downslope from Clino and Unda, was also observed earlier by Frank and Bernet (2000), who suggested that ACD was shallower during the Miocene. This requires, however, a shallowing of the ACD by more than 3000 m compared to its present-day position. The fact that Clino and Unda wells are both substantially shallower than wells 1007 and 1006, led Melim et al. (2002) to reject the hypothesis of Frank and Bernet (2000). As an alternative, they proposed that aragonite dissolution was more likely caused by undersaturated pore-fluids driven by $CO_2$ release during microbial degradation of organic matter. Aragonite dissolution, they reasoned, would have also reduced the Mg/Ca ratio of the pore-fluids, thus lessening the kinetic inhibition effect of Mg on the precipitation of LMC microcrystals.

Reuning et al. (2006) examined Pliocene sediments from the Maldives recovered from ODP Leg 115. Based on the observation that porosity decreased and the percent of LMC increased in some stratigraphic intervals, they inferred variations in the degree of LMC cementation. In these intervals, the Mg/Ca ratio of the pore-fluids was lower than seawater (Swart and Burns, 1990). Reuning et al. (2006) reasoned that these conditions favored LMC precipitation (Morse et al., 1997). Mineralogical data from ODP Hole 1127, which penetrates Southern Australian slope sediments, also show that aragonite and HMC dominate near the sea floor, whereas LMC and dolomite dominate below ~150 m (Feary et al., 2000; Rivers et al., 2012). Pore-fluid chemistry in the well shows a decrease in Mg/Ca with depth from ~5 near the sea floor, to ~4.1 at 150 m, to ~2 at 500 m (Feary et al., 2000; Rivers et al., 2012). These data taken together, suggest that the Mg/Ca ratio of solution may play a significant role in the stabilization of aragonite to LMC, which is also consistent with laboratory experiments (e.g., Taft, 1967).

Hasiuk et al. (2016) compiled a stable isotope and elemental dataset from seven hydrocarbon reservoirs and twenty-one published studies covering a wide range of geological ages, burial depths, and depositional environments. $\delta^{13}C$ values measured in LMC microcrystals were between −10‰ and +5.5‰, and $\delta^{18}O$ values were between −18‰ and +3.5‰ (Hasiuk et al., 2016). They reported that LMC microcrystals had $\delta^{18}O$ values a few per mil more negative and $\delta^{13}C$ values less than a per mil more negative compared to age-equivalent marine calcites. Further, both $\delta^{18}O$ and $\delta^{13}C$ were observed to decrease with depth along a burial trend that was modeled with a positive slope (Hasiuk et al., 2016). This isotopic trend was interpreted to indicate formation of LMC microcrystals in shallow burial environment. Data from Moshier (1989b) and Deville de Periere et al. (2011), however, show stable $\delta^{18}O$ but highly variable $\delta^{13}C$, which were interpreted to indicate stabilization in meteoric realm (Hasiuk et al., 2016). Elemental data, which showed Mg/Ca range between 6.4 and 90.4 mmol/mol, Sr/Ca 0.2–0.9 mmol/mol, Fe/Ca 0.0–29.3 mmol/mol, and Mn/Ca 0.0–1.3 mmol/mol (Fig. 15) further supported this interpretation. The trace element concentrations also co-varied with $\delta^{18}O$, and Mg/Ca decreased, but Fe/Ca increased as $\delta^{18}O$ became more depleted (Hasiuk et al., 2016). Hasiuk et al. (2016) argued that diagenetic stabilization was unlikely to occur in meteoric fluids, but rather during shallow burial in a marine setting.

### 5.4. Controls on LMC microcrystal size

LMC microcrystals have historically been classified either as micrite (1–4 μm) or microspar (5–10 μm) based on a proposed gap in crystal size distributions reported by Folk (1965). Subsequent studies, however, have failed to confirm a gap in the sizes of LMC micrite and microspar in Phanerozoic limestones (Lasemi and Sandberg, 1993; Kaczmarek et al., 2015), but instead showed unimodal crystal size distributions in the range of 1–10 μm. Based on these new data, Kaczmarek et al. (2015) avoided the terms micrite and microspar, and instead used the term microcrystal when referring to LMC crystals < 10 μm. Additionally, it has been demonstrated that both micrite and microspar form from lime mud during a one-step stabilization process, and what controls crystal size is precursor mineralogy (Lasemi and Sandberg, 1984, 1993; Papenguth, 1991; Munnecke et al., 1997). Lasemi and Sandberg (1993), showed that aragonite dominated muds produced larger LMC crystals with mean size of 5–12 μm, whereas HMC dominated muds produced smaller crystals with mean size of 1–4 μm. Papenguth (1991) also evaluated how mineralogy controlled LMC microcrystal size during stabilization experiments. Aragonite-rich muds stabilized to 5–25 μm LMC microcrystals, whereas HMC-rich muds stabilized to 1–3 μm LMC microcrystals. Precursor mineralogy is hypothesized to control the number of nucleation sites (Lasemi and Sandberg, 1984; Papenguth, 1991). The scarcity of nucleation sites in aragonite-rich muds results in coarser LMC crystals, whereas an abundance of nucleation sites in HMC-rich muds produces finer LMC crystals (Papenguth, 1991; Lasemi and Sandberg, 1993).

Another proposed control on LMC microcrystal size is the grain size of precursor sediments (Bathurst, 1961; Papenguth, 1991). Bathurst (1961) suggested that LMC microcrystal size is limited by the length of aragonite needles in the precursor sediments. An attempt was made to experimentally evaluate the influence of grain size of initial sediments on crystal size of LMC microcrystals by Papenguth (1991). HMC-rich muds were prepared by grinding up skeletons of *Goniolithon and Melobesia* (HMC algae) into two crystal size populations (< 25 μm and ≪25 μm). These muds were then reacted in $CaCl_2.2H_2O$ solutions at 200 °C for 117 days. Grain size measurements of the resultant LMC microcrystals indicate that *Goniolithon* muds with smaller crystal size (≪25 μm) stabilized to larger (3 μm) LMC microcrystals compared to muds with larger crystal size (< 25 μm) which produced smaller (1.6 μm) LMC microcrystals (Papenguth, 1991). *Melobesia* muds showed a similar trend, but the difference in crystal sizes was less significant. That is, initial grain size ≪25 μm produced crystal that measure 1.8 μm, compared to initial grain size < 25 μm that produced crystals of 1.4 μm. One comment about these experiments is that the HMC lime muds only partially transformed to LMC (maximum LMC = 54 wt%), which limits our ability to make textural observations because LMC textures evolve as the reaction proceed (Moshier and McManus, 1986). There is also a technical challenge to separate extremely fine material into definite ranges of crystal size. Papenguth (1991) used a 500 mesh (25 μm) sieve to separate fine material. Sediments that passed through the sieve with difficulty were denoted < 25 μm, whereas those that passed through easily were denoted ≪25 μm.

Deville de Periere et al. (2011) observed that LMC crystal size is controlled by both depositional and diagenetic facies. Coarser LMC microcrystals (> 2 μm) were found to be associated with rudist-rich bioclastic shoals and back shoal environments, whereas finer LMC microcrystals (< 2 μm) were found in association with sediments from a

protected inner platform. Additionally, the coarser LMC microcrystals were associated with intervals subjected to meteoric diagenesis. It was reasoned that selective dissolution of aragonite and HMC in meteoric fluids would create spaces between undissolved LMC crystals (Volery et al., 2010b; Deville de Periere et al., 2011), which enhances porosity, and the carbonate re-precipitates as cement overgrowths, leading to larger but fewer crystals (Deville de Periere et al., 2011). In contrast, finer LMC microcrystals experienced no observed leaching by meteoric fluids, but stabilization occurred in continuously supersaturated fluids (Deville de Periere et al., 2011).

### 5.5. Origin of LMC microcrystal textures

Early studies focused on the genetic origin of LMC microcrystals with little regard for textural variations (e.g., Bathurst, 1961; Folk, 1965; Bathurst, 1971; Pittman, 1971). More recent studies, however, document a wide variety of LMC microcrystal textures and have attempted to explain their diagenetic origins (Moshier, 1989a; Lambert et al., 2006; Deville de Periere et al., 2011).

In the preceding sections, various controls, such as mineralogy, texture, and diagenetic environment have been discussed in terms of their impact on the stabilization process. These controls not only affect the development of LMC microcrystals and associated micropores, but also the textures exhibited by LMC microcrystals that result from stabilization (Longman and Mench, 1978; Moshier, 1989a). In nature, the diagenetic history is often too complicated to discern the texture of the initial product formed during the mineralogical stabilization reaction. Moreover, experiments investigating the stabilization of carbonate sediments are limited and extremely controlled compared to natural settings (McManus and Rimstidt, 1982; Papenguth, 1991). Complicating matters further is the understanding that LMC microcrystals presumably undergo textural changes throughout their entire diagenetic history (Lambert et al., 2006; Deville de Periere et al., 2011; Hasiuk et al., 2016).

Moshier (1989a) suggested that higher porosity crystal-framework textures (Fig. 10) result from a mineralogical stabilization process that takes place in a closed system (i.e., high rock/water ratio), without substantial addition of carbonate material from an external source as cement. The lower porosity mosaic texture, conversely, was interpreted to form in an open system (i.e., low rock/water ratio) whereby additional carbonate is introduced from an outside source (Moshier, 1989a). Lambert et al. (2006) interpreted the rhombic LMC to result from mineralogical stabilization in seawater via dissolution of HMC and precipitation of LMC. They reasoned that the dissolution of aragonite would increase the Ca/Mg ratio, causing fluids to become undersaturated with respect to HMC and supersaturated with respect to LMC (Lambert et al., 2006). Lambert et al. (2006) interpreted anhedral compact textures to result from granular euhedral textures overprinted by further cementation induced by chemical compaction. The anhedral compact texture was observed in association with cemented facies (Lambert et al., 2006). Rounded LMC microcrystals have been interpreted to result from dissolution of granular euhedral LMC microcrystals (Lambert et al., 2006; Tavakoli and Jamalian, 2018). This dissolution process of LMC microcrystals was proposed to take place in the burial environment and is unrelated to dissolution of metastable sediments during mineralogical stabilization (Lambert et al., 2006). Lambert et al. (2006) observed the occurrence of rounded textures in the oil zone of Cretaceous limestones in Iraq and U.A.E., in the Middle East and suggested that they resulted from the dissolution at the edges and corners of rhombic crystals by acidic burial fluids. Lambert et al. (2006) argued that dissolution reduced the diameter of LMC microcrystals by > 1 μm and increased porosity by 8–13%. The rounded shape of crystals as well as channels observed between adjacent crystals were considered as evidence of dissolution. It was further reported that the porosity created by dissolution remained open and filled with hydrocarbons suggesting to Lambert et al. (2006) that acidic fluids were emplaced prior to or coeval with oil emplacement. Earlier, Moshier (1989a) reported the occurrence of smaller than average, and more rounded crystals along the edges of microchannels in Lower Cretaceous in age limestones from an undisclosed location in the Middle East. However, the SEM photomicrograph provided is of low resolution and does not clearly show rounded crystals (Moshier, 1989a, Fig. 8). Kaczmarek et al. (2015) found that crystals in the granular subhedral textures were slightly smaller than 2 μm, whereas crystals exhibiting the granular euhedral (their hypothesized precursor) were slightly larger than 2 μm, an observation that is consistent with the idea that dissolution reduced crystal size. However, Kaczmarek et al. (2015) reported that the granular subhedral crystals were not rounded, but rather polyhedral with well-defined crystal faces, an observation that is inconsistent with the dissolution model.

Upon reevaluating data from Lambert et al. (2006), Ehrenberg et al. (2012) argued that the amount of increase in porosity attributed to dissolution was unrealistic. They demonstrated that a reduction in crystal diameter from 4.5 μm (48 $\mu m^3$ volume) to 3 μm (14 $\mu m^3$ volume) would result in a 71% loss of solid material. They also showed that the published porosity and crystal size trends from Lambert et al. (2006), when extrapolated, would result in only 64% porosity when crystal size is equal to zero. This suggests that larger LMC crystals were ignored in the analysis, and that cementation likely occurred in other parts of the reservoir (Ehrenberg et al., 2012). Ehrenberg et al. (2012) further argued that acidic fluids would have likely caused extensive dissolution along the entire fluid migration pathway, not only along the structural crest of the reservoir as reported by Lambert et al. (2006).

Morad et al. (2018) argued that the dissolution hypothesis is incapable of explaining rounded LMC microcrystals because dissolution would produce etched and pitted anhedral crystals rather than smooth rounded crystals. It has been shown, however, that the mechanism by which dissolution occurs in carbonate minerals, largely depends on chemical variables, such as saturation state (Berner and Morse, 1974), and defect microstructure (Kaczmarek and Sibley, 2007). For example, in experiments conducted at pH = 3.9 and $P_{CO_2} = 10^{-2.5}$, Berner and Morse (1974) showed that rhombic LMC crystals dissolved to form rounded crystals. Alternatively, Morad et al. (2018) proposed that rounded (spheroidal) crystals can be associated with microbial precipitation of $CaCO_3$, though these forms are typically aragonite or HMC (e.g., Folk, 1993; Perri and Tucker, 2007; Maruthamuthu et al., 2010; Spadafora et al., 2010). Maruthamuthu et al. (2010) reported bacterial precipitation of LMC, yet crystals were mostly not rounded, but rather rod shaped. Mineralogy of the bacterially precipitated carbonates is important, because if the mineralogy is aragonite or HMC, then it will be subjected to mineralogical stabilization, and thus textural alteration.

Deville de Periere et al. (2011) observed that compact anhedral textures were accompanied by either micro-stylolitization or epitaxial overgrowth cement between LMC microcrystals. Additionally, clay contents were higher (10–20%) in the compact anhedral texture, compared to the microporous textures (0.1–10%) (Deville de Periere et al., 2011). These observations were interpreted to reflect pressure solution that led to subsequent cementation between LMC microcrystals. An association between stylolite abundance and fitted textures has been observed earlier by Moshier (1989a) from a Cretaceous reservoir in Middle East (Shuaiba Formation), and by Kaczmarek et al. (2015) in limestones from the Black Sea Region. Interestingly, the fitted textures and stylolites occurred approximately 10 m shallower than the limestones with stylolites exhibiting granular subhedral textures, suggesting that the relationship between LMC microtexture and burial depth is somewhat complicated.

## 6. Chalk microporosity

Despite being fundamentally different in terms of precursor mineralogy and texture (Hancock, 1975), chalk diagenesis is important to the discussion of limestone microporosity. Unlike shallow marine

carbonate sediments, which are characterized by wide array of carbonate minerals and textures, deep marine chalks are invariably LMC with a more straightforward diagenetic pathway (Scholle, 1977). Additionally, chalks serve as an analogue for shallow marine limestones deposited during times of calcite seas, which are hypothesized to have initial sediments dominated by LMC.

Chalks are regarded as deep marine deposits, mainly composed of calcareous nano- and micro-fossils, along with other, less common, siliceous, organic, and siliciclastic components (Scholle, 1977; Fabricius, 2007). Modern deep marine sediments (i.e., "ooze") consist of the skeletal remains of various calcareous planktic organisms, such as foraminifera, coccoliths, and pteropods, as well as siliceous organisms, such as radiolaria and diatoms (Milliman, 1974; James and Jones, 2015). Planktic organisms inhabit near-surface (upper 300 m) marine waters, but once they die they settle through the water column and accumulate as "pelagic rain" on the sea bottom (Ekdale and Bromley, 1984). The tests of planktic foraminifera are typically the main contributors to the sand-size fraction in the sediment, whereas skeletal fragments usually contribute to the silt-size fraction (Milliman, 1974). Coccoliths typically disintegrate into particles < 6 μm (Milliman, 1974). Both planktic foraminifera and coccolith are LMC, pteropods are aragonitic, whereas radiolarians and diatoms are siliceous (James and Jones, 2015). Contribution of the different planktic organisms to the pelagic sediments vary spatially and temporally (Bukry et al., 1971; Milliman, 1974). In modern oceans, planktic foraminifera are generally considered the significant contributor to deep marine sediments (Milliman, 1974). In the Mediterranean and the Black Seas, however, coccoliths are more dominant (e.g., Bukry et al., 1971). Based on measured coccolith abundances in several stratigraphic units, Bramlette (1958) proposed that contribution of coccoliths to calcareous oozes was greater during the Tertiary than its today.

Unlike the shallow marine sediments comprised of aragonite and HMC that stabilize to LMC microcrystals, deep marine sediments start out as mostly LMC (Schlanger and Douglas, 1974; Hancock, 1975; Scholle, 1977). Consequently, mineralogical stabilization is not a significant diagenetic process in chalk. Instead, chalk diagenesis is characterized by LMC-LMC recrystallization (Schlanger and Douglas, 1974; Fabricius, 2007; Hasiuk et al., 2016; Descamps et al., 2017), thought to be driven by either chemical equilibration between the solid phase and pore waters (Fabricius, 2007), or by Ostwald ripening (Schlanger and Douglas, 1974; Hasiuk et al., 2016). LMC recrystallization has been suggested to initiate after the organic coatings on carbonate skeletons are removed by bacterial activities (Henriksen et al., 2004; Fabricius, 2007).

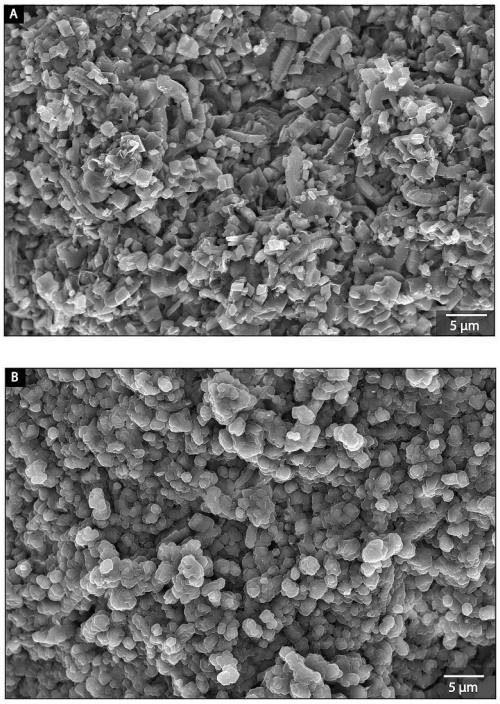


**Fig. 18.** SEM photomicrographs of chalk from the North Sea. A) Chalk characterized by micro- and nano-fossils. Micropores are hosted between these constituents. B) Recrystallized chalk that is, at the SEM level, undistinguishable from shallow marine microporous limestones.

Chalk constituents share the same particle size range as the LMC microcrystals in shallow marine microporous limestones (Hasiuk et al., 2016). At the SEM scale, textures in chalk are distinguishable from those of shallow marine microporous limestones by the presence of nano- and micro-fossils that host micropores if chalk has not experienced extensive recrystallization. Recrystallized chalk, on the other hand, may look very similar to shallow marine limestones (Fig. 18).

Calcareous oozes are documented to have ≥70% primary porosity (Scholle, 1977; Fabricius, 2007), which is present as interparticle and intraparticle micropores associated with skeletal remains (Fabricius, 2007). Porosity can decrease by more than 40% in the first few kilometers of burial (Cook and Cook, 1972; Scholle et al., 1974; Scholle, 1977; Fabricius and Borre, 2007), an observation attributed to mechanical compaction and/or chemical compaction and subsequent cementation (Schlanger and Douglas, 1974; Scholle, 1977; Fabricius, 2007). Mechanical compaction typically dominates during shallow burial, whereas chemical compaction dominates during deep burial (Schlanger and Douglas, 1974; Fabricius, 2007). Textural evidence for mechanical compaction includes broken, deformed, and reoriented allochems (Scholle, 1977). Experimental studies demonstrated that mechanical compaction of chalk can reduce porosity by up to 40% (Lind, 1993b; Fabricius, 2000, 2003). Schlanger and Douglas (1974) investigated the transition between deep sea oozes and lithified chalk in several pelagic cores spanning Recent to Upper Jurassic in age. They proposed that chalk porosity is reduced during a two-stage process. In the first stage, porosity reduction from 80% to 60% is observed in the upper 200 m of the core (Schlanger and Douglas, 1974). Sediments in the upper 200 m were characterized by intact, but etched foraminifera tests, and disaggregated coccoliths tests (Schlanger and Douglas, 1974). Porosity reduction during this stage was attributed mainly to mechanical compaction (Schlanger and Douglas, 1974). The second stage is characterized by a further 40% porosity reduction, which was attributed to dissolution-reprecipitation as evidenced by the presence of severely etched coccoliths fragments and foraminifera tests, as well as LMC void filling cements. The burial diagenetic history of chalk has been detailed by Fabricius (2003; Fig. 19).

## 7. Summary

Microporosity is a common attribute of ancient Phanerozoic limestones. The vast majority of limestone microporosity can be attributed to micropores hosted within a framework of LMC microcrystals, which typically measure < 10 μm and occur in matrix and grains. Less common types of micropores include microvugs, microchannels, and micropores between spar cement crystals.

Many hypotheses have been put forward to explain the origin of LMC microcrystals and associated micropores. The vast majority of data suggests that LMC microcrystals form through diagenetic stabilization, whereby a heterogeneous assortment of precursor sediments dominated by metastable aragonite and HMC are converted to a more homogeneous collection of LMC microcrystals. This is largely a constructive process in which LMC microcrystals precipitate in the pore spaces as cement. This transformation, which is driven, at least in part, by mineralogical stabilization is a common and fundamental process in nature. Importantly, porosity is not created during this process, but rather inherited from the precursor sediments. The pore system is simply rearranged.

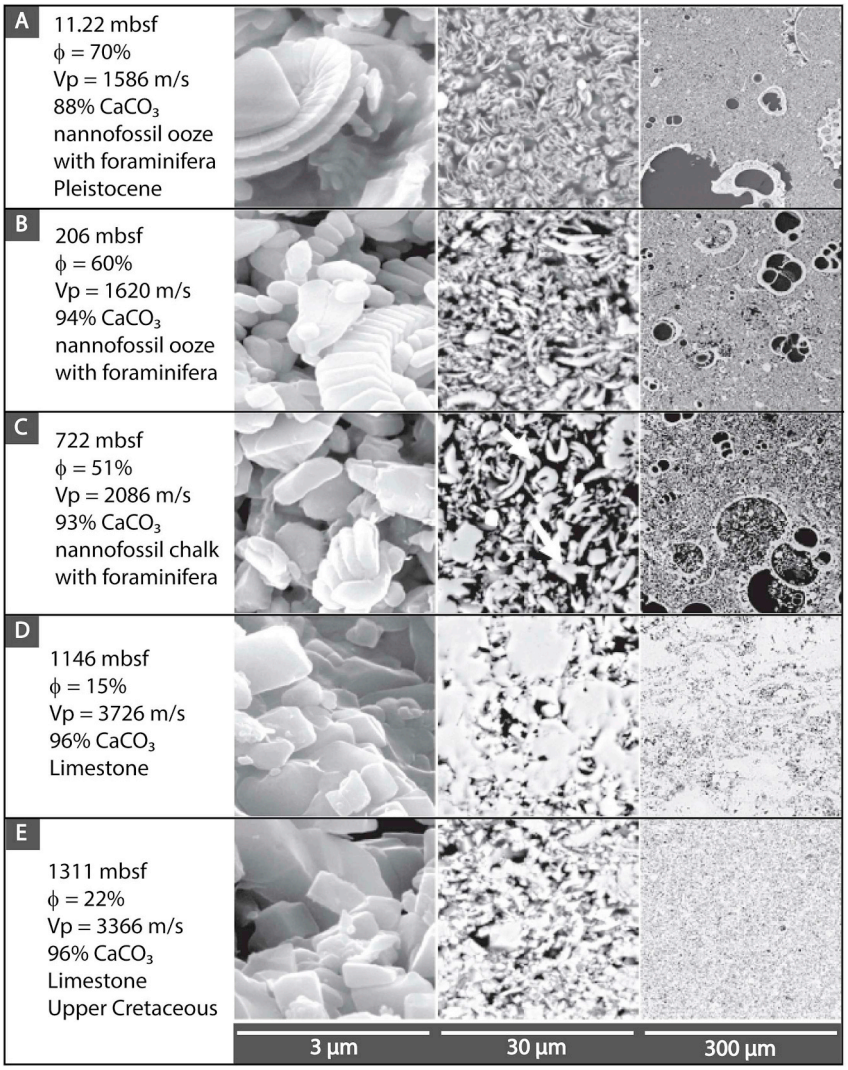


**Fig. 19.** SEM photomicrographs (left) and backscatter photomicrographs of epoxy-impregnated and polished thin sections (middle and right) from ODP Site 807 showing the development of chalk with depth. Modified after Fabricius (2003).

The diagenetic environment where mineralogical stabilization takes place is poorly understood. In modern Holocene sediments, LMC microcrystals have been observed among aragonitic mud in contact with meteoric fluids but not in the underlying mixing zone. Experimental investigations show that the presence of Mg inhibits mineralogical stabilization of aragonite to LMC. However, LMC microcrystals have been observed in Neogene-age rocks, interpreted to form in marine fluids and presumably never influenced by meteoric fluids. In ancient limestones, on the other hand, geochemical data suggest that LMC microcrystals form during burial diagenesis in marine-like fluids. If anything, these seemingly contradictory observations indicate the lack of robust understanding of two of the principle types of carbonate diagenesis.

LMC microcrystals exhibit various textures that have distinct porosities, permeabilities, and pore throat radii. The diagenetic origin of these textures has been attributed to various diagenetic processes. For example, granular-euhedral textures have typically been considered the product of stabilization process. Granular-subhedral (rounded) textures have been attributed to dissolution by corrosive fluids. Lastly, fitted textures have been interpreted to indicate cementation. Generally speaking, most of these interpretations are based on limited evidence.

Mineralogical stabilization is governed by various controls that determine the diagenetic product, and consequently, whether or not LMC microcrystals will develop. Some of these factors are depositional, such as precursor mineralogy, texture, and grain size, and some of them are diagenetic, such as fluid chemistry, temperature, and water/rock ratio. Diagenetic controls such as fluid chemistry and water/rock ratio are more important than depositional controls in lime mud. In contrast, depositional controls such as precursor mineralogy and microstructure are more important in carbonate grains.

While more than half a century of research on microporosity and lime mud diagenesis answered many questions and significantly improved our understanding, it also raised many other questions that need investigation in the future. Among these questions are:

1. Do diagenetic LMC microcrystals carry a depositional signature that indicates mineralogy and texture of precursor sediment?
2. What is the textural product of mineralogical stabilization?
3. How the different physiochemical factors such as temperature, fluid chemistry, precursor mineralogy, texture, and grain size affect textures of LMC microcrystals?
4. What is the role of the different diagenetic processes, such as dissolution, compaction, and cementation in modifying LMC microcrystal textures?

## Acknowledgements

This work was supported by a collaborative research grant from the U.S. National Science Foundation awarded to S. Kaczmarek (grant #1828880) and F. Hasiuk (grant #1828868). We would like to thank our colleagues Cameron Manche, Katharine Rose, and Brooks Ryan for reviewing earlier versions of this manuscript. Dr. Lars Reuning and an anonymous reviewer provided helpful comments that highly improved the manuscript. We also thank Romeo Akara for his assistance in translation from French to English in a few of the references cited.

## References

Ahr, W.M., 1989. Early diagenetic microporosity in the cotton valley limestone of east Texas. Sediment. Geol. 63 (3–4), 275–292.
Akbar, M., Vissapragada, B., Alghamdi, A.H., Allen, D., Herron, M., Carnegie, A., Dutta, D., Olesen, J.R., Chourasiya, R.D., Logan, D., Stief, D., 2000. A snapshot of carbonate reservoir evaluation. Oilfield Rev. 12 (4), 20–21.
Al-Aasm, I.S., Azmy, K.K., 1996. Diagenesis and evolution of microporosity of middle-upper devonian kee Scarp reefs; norman wells; northwest territories; Canada: petrographic and chemical evidence. AAPG (Am. Assoc. Pet. Geol.) Bull. 80, 82–100.
Al-Awar, A.A., Humphrey, J.D., 2000. Diagenesis of the Aptian Shuaiba Formation at Ghaba North Field, Oman.
Alexandersson, T., 1972. Intragranular growth of marine aragonite and Mg-calcite: evidence of precipitation from supersaturated seawater. J. Sediment. Res. 42 (2).
Alexandersson, T., 1979. Marine maceration of skeletal carbonates in the skagerrak, North Sea. Sedimentology 26 (6), 845–852.
Andrews, J.E., Christidis, S., Dennis, P.F., 1997. Assessing mineralogical and geochemical heterogeneity in the sub 63 micron size fraction of Holocene lime muds. J. Sediment. Res. 67 (3), 531–535.
Archie, G.E., 1952. Classification of carbonate reservoir rocks and petrophysical considerations. AAPG (Am. Assoc. Pet. Geol.) Bull. 36 (2), 278–298.
Arribas, M.E., Bustillob, A., Tsigec, M., 2004. Lacustrine chalky carbonates: origin, physical properties and diagenesis (Palaeogene of the Madrid Basin, Spain). Sediment. Geol. 166, 335–351.
Baechle, G.T., Colpaert, A., Eberli, G.P., Weger, R.J., 2008. Effects of microporosity on sonic velocity in carbonate rocks. Lead. Edge 27 (8), 1012–1018.
Bathurst, R.G.C., 1958. Diagenetic fabrics in some British Dinantian limestones. Liverp. Manch. Geol. J. 2, 11–36.
Bathurst, R.G.C., 1959b. The cavernous structure of some Mississippian Stromatactis reefs in Lancashire, England. J. Geol. 67 (5), 506–521.
Bathurst, R.G., 1971. Carbonate sediments and their diagenesis. Dev. Sedimentology 12, 620.
Bathurst, R.G., 1961. Diagenetic fabrics in some British Dinantian limestones. Geol. J. 2 (1), 11–36.
Bathurst, R.G.C., 1964. The replacement of aragonite by calcite in molluscan shell wall. Approaches Paleoecol. 357–367.
Bathurst, R.G.C., 1966. Boring algae, micrite envelopes and lithification of molluscan biosparites. Geol. J. 5 (1), 15–32.
Bathurst, R.G., 1972. Carbonate Sediments and Their Diagenesis, vol. 12 Elsevier.
Bathurst, 1975. Carbonate Sediments and Their Diagenesis, Developments in Sedimentology, vol. 12. Elsevier, pp. 658.
Berner, R.A., 1975. The role of magnesium in the crystal growth of calcite and aragonite from sea water. Geochem. Cosmochim. Acta 39 (4), 489–504.
Berner, R.A., Morse, J.W., 1974. Dissolution kinetics of calcium carbonate in sea water; IV, Theory of calcite dissolution. Am. J. Sci. 274 (2), 108–134.
Bischoff, J.L., 1969. Temperature controls on aragonite-calcite transformation in aqueous solution. Am. Mineral.: J. Earth Planet. Mater. 54 (1–2), 149–155.
Bischoff, J.L., Fyfe, W.S., 1968. Catalysis, inhibition, and the calcite-aragonite problem; [Part] 1, the aragonite-calcite transformation. Am. J. Sci. 266 (2), 65–79.
Borre, M.A.I., Fabricius, I.L., 1998. Chemical and mechanical processes during burial diagenesis of chalk: an interpretation based on specific surface data of deep-sea sediments. Sedimentology 45 (4), 755–769.
Boss, S.K., Neumann, A.C., 1993. Physical versus chemical processes of “whiting” formation in the Bahamas. Carbonates Evaporites 8 (2), 135.
Bramlette, M.N., 1958. Significance of coccolithophorids in calcium-carbonate deposition. Geol. Soc. Am. Bull. 69, 121–126.
Brand, U., 1989. Aragonite-calcite transformation based on Pennsylvanian molluscs. Geol. Soc. Am. Bull. 101, 377–390.
Brand, U., Veizer, J., 1980. Chemical diagenesis of a multicomponent system, 1. Trace elements. J. Sediment. Petrol. 50, 1219–1236.
Brigaud, B., Vincent, B., Durlet, C., Deconinck, J.-F., Blanc, P., Troullier, A., 2010. Acoustic properties of ancient shallow-marine carbonates: effects of depositional environments and diagenetic processes? J. Sediment. Res. 80, 791e807.
Broecker, W.S., Takahashi, T., 1966. Calcium carbonate precipitation on the Bahama banks. J. Geophys. Res. 71 (6), 1575–1602.
Budd, D.A., 1989. Micro-rhombic calcite and microporosity in limestones: a geochemical study of the Lower Cretaceous Thamama Group. UAE: Sediment. Geol. 63, 293–311. https://doi.org/10.1016/0037-0738(89)90137-1.
Budd, D.A., 1992. Dissolution of high-Mg calcite fossils and the formation of biomolds during mineralogical stabilization. Carbonates Evaporites 7 (1), 74.
Budd, D.A., Hiatt, E.E., 1993. Mineralogical stabilization of high-magnesium calcite; geochemical evidence for intracrystal recrystallization within Holocene porcellaneous foraminifera. J. Sediment. Res. 63 (2), 261–274.
Bukry, D., Douglas, R.G., Kling, S.A., Krasheninnikov, V., 1971. Planktonic microfossil biostratigraphy of the northwestern Pacific Ocean. Deep Sea Drilling Project Initial Repts 6, 1253–1300.
Burne, R.V., Moore, L.S., 1987. Microbialites: Organosedimentary Deposits of Benthic Microbial Communities. Palaios. pp. 241–254.
Bustos-Serrano, H., Morse, J.W., Millero, F.J., 2009. the formation of whitings on the little Bahama Bank. Mar. Chem. 113 (1–2), 1–8.
Cantrell, D.L., Hagerty, R.M., 1999. Microporosity in Arab Formation carbonates, Saudi Arabia. GeoArabia 4 (2), 129–154.
Carlson, W.D., 1983. The polymorphs of $CaCO_3$ and the aragonite-calcite transformation. Rev. Mineral. Geochem. 11 (1), 191–225.
Carozzi, A.V., 1962. Observations on algal biostromes in the great Salt Lake, Utah. J. Geol. 70 (2), 246–252.
Carpenter, S.J., Lohmann, K.C., Holden, P., Walter, L.M., Huston, T.J., Halliday, A.N., 1991. d18O values, 87Sr/86Sr and Sr/Mg ratios of Late Devonian abiotic marine calcite; implications for the composition of ancient seawater. Geochem. Cosmochim. Acta 55, 1991–2010.
Carpentier, C., Ferry, S., Lecuyer, C., Strasser, A., Géraud, Y., Trouiller, A., 2015. Origin of micropores in late jurassic (oxfordian) micrites of the eastern paris basin, France. J. Sediment. Res. 85, 660–682. https://doi.org/10.2110/jsr.2015.37.
Carter, J.G., 1990. Skeletal Biomineralization: Patterns, Processes and Evolutionary Trends, vol. 1 Springer.
Chafetz, H.S., Butler, J.C., 1980. Petrology of recent caliche pisolites, spherulites, and speleothem deposits from central Texas. Sedimentology 27 (5), 497–518.
Chave, K., 1964. Skeletal durability and preservation. In: Imbrie, J., Newell, N.D. (Eds.), Approaches to Paleoecology. Wiley, New York, pp. 377–387.
Chilingar, G.V., 1962. Dependence on temperature of Ca/Mg ratio of skeletal structures of organisms and direct chemical precipitates out of sea water. Bull. South Calif. Acad. Sci. 61 (1), 45–60.
Choquette, P.W., Pray, L.C., 1970. Geologic nomenclature and classification of porosity in sedimentary carbonates. AAPG Bull. 54 (2), 207–250.
Clark Jr., S.P., 1957. A Note on Calcite-Aragonite Equilibrium.
Clerke, E.A., 2009a. Permeability, relative permeability, microscopic displacement efficiency and pore geometry of M-1 bimodal pore systems in Arab D limestone. Soc. Petrol. Eng. 14, 524–531.
Clerke, E.A., 2009b. Permeability, relative permeability, microscopic displacement efficiency and pore geometry of M-1 bimodal pore systems in Arab D limestone. Soc. Petrol. Eng. 14, 524–531.
Clerke, E.A., Mueller, H.W., Phillips, E.C., Eyvazzadeh, R.Y., Jones, D.H., Ramamoorthy, R., Srivastava, A., 2008. Application of thomeer hyperbolas to decode the pore systems, facies and reservoir properties of the upper jurassic Arab D limestone, ghawar field, Saudi Arabia: a “rosetta stone” approach. GeoArabia 13 (4), 113–160.
Cloud Jr., P.E., Blackmon, P.D., Sisler, F.D., Kramer, H., Carpenter, J.H., Robertson, E.C., Sykes, L.R., Newell, M., 1962. Environment of Calcium Carbonate Deposition West of Andros Island, Bahamas, with Sections on Mechanical Characteristics of the Sediments; Microbiology and Biochemistry of Sediments and Overlying Water; Chemical Analyses of the Water; the Problem of Calcium Determination in Sea Water and Experimental Consolidation of Calcium Carbonate Sediment (No. 350). US Govt. Print. off.
Coalson, E.B., Hartmann, D.J., Thomas, J.B., 1985. Productive characteristics of common reservoir porosity types. Bull. S. Tex. Geol. Soc. 15 (6), 35–51.
Coimbra, R., Immenhauser, A., Olóriz, F., 2009. Matrix micrite δ13C and δ18O reveals synsedimentary marine lithification in upper jurassic ammonitico rosso limestones (betic cordillera, SE Spain). Sediment. Geol. 219 (1–4), 332–348.
Cook, F.M., Cook, H.E., 1972. Physical Properties Synthesis: Initial Reports of the Deep Sea Drilling Project, vol. IX. U. S. Government Printing Office, Washington, pp. 945–946.
Cox, P.A., Wood, R.A., Dickson, J.A.D., Rougha, Al, H.B., Shebl, H., Corbett, P.W.M., 2010. Dynamics of cementation in response to oil charge: evidence from a Cretaceous carbonate field. UAE: Sediment. Geol. 228, 246–254. https://doi.org/10.1016/j.sedgeo.2010.04.016.
da Silva, A.C., Loisy, C., Cerepi, A., Toullec, R., Kiefer, E., Humbert, L., Razin, P., 2009. Variations in stratigraphic and reservoir properties adjacent to Mid-Paleocene sequence boundary, Campo section, Pyrenees, Spain. Sediment. Geol. 219, 237e251.
Davis, B.L., Adams, L.H., 1965. Kinetics of the calcite⇌ aragonite transformation. J. Geophys. Res. 70 (2), 433–441.
Debenay, J.-P., André, J.-P., Lesourd, M., 1999. Production of lime mud by breakdown of foraminiferal tests. Mar. Geol. 157, 159–170.
Descamps, F., Faÿ-Gomord, O., Vandycke, S., Schroeder, C., Swennen, R., Tshibangu, J.P., 2017. Relationships between Geomechanical Properties and Lithotypes in NW European Chalks. Geological Society, vol. 458. Special Publications, London, pp. SP458–S459.
Deville de Periere, M., Durlet, C., Vennin, E., Lambert, L., Caline, B., Bourillot, R., Poli, E., 2011. Morphometry of micrite particles in cretaceous microporous limestones of the Middle East: influence on reservoir properties. Mar. Petrol. Geol. 28, 1727–1750. https://doi.org/10.1016/j.marpetgeo.2011.05.002.
Dewever, B., Breesch, L., Mezini, A., Swennen, R., 2007. Sedimentological and marine eogenetic control on porosity distribution in Upper Cretaceous carbonate turbidites (central Albania). Sedimentology 54 (2), 243–264.
Dickson, J.A.D., Kenter, J.A.M., 2014. Diagenetic evolution of selected parasequences across a carbonate platform: late Paeozoic, Tengiz reservoir, Kazakhstan. J. Sediment. Res. 84 (8), 664–693.
Dierssen, H.M., Zimmerman, R.C., Burdige, D.J., 2009. Optics and remote sensing of Bahamian carbonate sediment whitings and potential relationship to wind-driven

Langmuir circulation. Biogeosciences 6, 1–14.
Dravis, J.J., 1989. Deep-burial microporosity in Upper Jurassic Haynesville oolitic grainstones, east Texas. Sediment. Geol. 63, 325–341. https://doi.org/10.1016/0037-0738(89)90139-5.
Dunham, R.J., 1962. Classification of Carbonate Rocks According to Depositional Textures.
Eardley, A.J., 1938. Sediments of great Salt Lake, Utah. AAPG (Am. Assoc. Pet. Geol.) Bull. 22 1305 1411.
Eberli, G.P., Baechle, G.T., Anselmetti, F.S., Incze, M.L., 2003. Factors controlling elastic properties in carbonate sediments and rocks. Lead. Edge 22 (7), 654–660.
Ehrenberg, S.N., Walderhaug, O., Bjorlykke, K., 2012. Carbonate porosity creation by mesogenetic dissolution: reality or illusion? AAPG Bull. 96 (2), 217–233.
Ekdale, A.A., Bromley, R.G., 1984. Comparative ichnology of shelf-sea and deep-sea chalk. J. Paleontol. 58, 322–332.
Elf-Aquitai, 1977. Essai de caractérisation sédimentologique des dépôts carbonatés. 2. Eléments d'interprétation. Thechnip, pp. 231p.
Ellis, J.P., Milliman, J.D., 1985. Calcium carbonate suspended in Arabian Gulf and Red Sea waters; biogenic and detrital, not" chemogenic. J. Sediment. Res. 55 (6), 805–808.
Enos, P., Sawatsky, L.H., 1981. Pore networks in Holocene carbonate sediments. J. Sediment. Res. 51 (3), 961–985.
Fabricius, I.L., 2000. Interpretation of burial history and rebound from loading experiments and the occurrence of microstylolites in the mixed sediments of the Caribbean Sites 999 and 1001. Proc. Ocean Drill. Progr. Sci. Results 165, 177–190.
Fabricius, I.L., 2003. How burial diagenesis of chalk sediments controls sonic velocity and porosity. AAPG (Am. Assoc. Pet. Geol.) Bull. 87, 1755–1778.
Fabricius, I.L., 2007. Chalk: composition, diagenesis and physical properties. Geol. Soc. Denmark. Bull. 55, 97–128.
Fabricius, I.L., Borre, M.K., 2007. Stylolites, porosity, depositional texture, and silicates in chalk facies sediments. Ontong Java Plateau–Gorm and Tyra fields, North Sea. Sedimentology 54 (1), 183–205.
Fabricius, I.L., Gommesen, L., Krogsboll, A., Olsen, D., 2008. Chalk porosity and sonic velocity versus burial depth: influence of fluid pressure, hydrocarbons, and mineralogy. AAPG (Am. Assoc. Pet. Geol.) Bull. 92, 201–223. https://doi.org/10.1306/10170707077.
Faÿ-Gomord, O., Soete, J., Katika, K., Galaup, S., Caline, B., Descamps, F., Lasseur, E., Fabricius, I.L., Saïag, J., Swennen, R., Vandycke, S., 2016. New insight into the microtexture of chalks from NMR analysis. Mar. Petrol. Geol. 75, 252–271.
Fegley Jr., B., 2012. Practical Chemical Thermodynamics for Geoscientists. Academic Press.
Feary, D.A., Hine, A.C., Malone, M.J., Andres, M., Betzler, C., Brooks, G.R., Brunner, C.A., Fuller, M., Garza, R.S.M., Holbourn, E.A., Huuse, M., Isern, A.R., James, N.P., Ladner, B.C., Li, Q., Machiyama, H., Mallinson, D.J., Matsuda, H., Mitterer, R.M., Robin, C., Russell, J.L., Shafik, S., Simo, J.A., Smart, P.L., Spence, G.H., Surlyk, F.C., Swart, P.K., Wortmann, U.G., 2000. In: Proceedings of the Ocean Drilling Program, Initial Reports, 182 [CD-ROM]. Ocean Drilling Program, Texas A&M University, College Station, TX, USA.
Ferguson, J., Ibe, A.C., 1982 Jan. Some aspects of the occurrence of proto-kerogen in Recent ooids. Journal of Petroleum Geology 4 (3), 267–285.
Flügel, E., 2004. Microfacies of Carbonate Rocks: Analysis, Interpretation and Application. Springer 976 pp.
Flügel, E., 2013. Microfacies of Carbonate Rocks: Analysis, Interpretation and Application. Springer Science & Business Media.
Flügel, E., Franz, H.E., Ott, W.F., 1968. Review on electron microscope studies of limestones. In: Recent Developments in Carbonate Sedimentology in Central Europe. Springer, Berlin, Heidelberg, pp. 85–97.
Folk, R.L., 1959. Practical petrographic classification of limestones. AAPG (Am. Assoc. Pet. Geol.) Bull. 43 (1), 1–38.
Folk, R.L., 1962. Spectral Subdivision of Limestone Types.
Folk, R.L., 1965. Some aspects of recrystallization in ancient limestones. In: Pray, L.C., Murray, R.C. (Eds.), Dolomitization and Limestone Diagenesis, SEPM Spec. Pub. 13, pp. 14–48.
Folk, R.L., 1974. The natural history of crystalline calcium carbonate; effect of magnesium content and salinity. J. Sediment. Res. 44 (1), 40–53.
Folk, R.L., 1993. SEM imaging of bacteria and nannobacteria in carbonate sediments and rocks. J. Sediment. Res. 63 (5), 990–999.
Fournier, F., Borgomano, J., 2009. Critical porosity and elastic properties of microporous mixed carbonate-siliciclastic rocks. Geophysics 74, 93–109.
Frank, T.D., Bernet, K.H., 2000. Isotopic signature of burial diagenesis and primary lithologic contrasts in periplatform carbonates (Miocene, Great Bahama Bank). Sedimentology 47 (6), 1119–1134.
Friedman, G.M., 1964. Early diagenesis and lithification in carbonate sediments. J. Sediment. Res. 34 (4), 777–813.
Friedman, G.M., 1965. Terminology of crystallization textures and fabrics in sedimentary rocks. J. Sediment. Petrol. 35 (3), 643–655.
Friedman, G.M., 1993. Biochemical and uitrastructural evidence for the origin of whitings: a biologically induced calcium carbonate precipitation mechanism: comment and Reply. J. Earth Sci. 14, 79–85.
Frost, S.H., Bliefnick, D.M., Harris, P.M., 1983. Deposition and porosity evolution of a lower cretaceous rudist buildup, Shuaiba Formation of eastern arabian peninsula. In: In: Harris, P.M. (Ed.), Carbonate Buildups-A Core Workshop. Soc. Econ. Paleontol. Mineral, Core Workshop, vol. 4. pp. 381–410.
Fullman, R.L., 1952. Metal Interfaces. American Society for Metals, Metals Park, OH.
Fullmer, S.M., Guidry, S.A., Gournay, J., Bowlin, E., Ottinger, G., Neyadi, Al, A., Gupta, G., Gao, B., Edwards, E., 2014. Microporosity: characterization, distribution, and influence on oil recovery. In: International Petroleum Technology Conference.
Fyfe, W.S., Bischoff, J.L., 1965. The calcite-aragonite problem. In: Pray, L.C., Murray, R.C. (Eds.), Dolomitization and Limestone Diagenesis: Society of Economic Paleontologists and Mineralogists Special Publication 13, pp. 3–13.
Gannon, M.E., Pérez-Huerta, A., Aharon, P., Street, S.C., 2017. A biomineralization study of the Indo-Pacific giant clam Tridacna gigas. Coral Reefs 36 (2), 503–517.
Gebelein, C.D., 1974. Guidebook for Modern Bahaman Platform Environments: Field Trip. Geological Society of America, Annual Meeting 1974 (No. 3). Bermuda Biological Station.
Gee, H., et al., 1932. Calcium equilibrium in sea water: scripps Inst. Oceanography Bull., Tech. Ser. 3, 145–190.
Geno, K.R., Chafetz, H.S., 1982. Petrology of Quaternary fluvial low-magnesian calcite coated grains from central Texas. J. Sediment. Res. 52 (3), 833–842.
Gischler, E., Zingeler, D., 2002. The origin of carbonate mud in isolated carbonate platforms of Belize, Central America. Int. J. Earth Sci. 91 (6), 1054–1070.
Gischler, E., Dietrich, S., Harris, D., Webster, J.M., Ginsburg, R.N., 2013. A comparative study of modern carbonate mud in reefs and carbonate platforms: mostly biogenic, some precipitated. Sediment. Geol. 292, 36–55.
Golubic, S., Seong-Joo, L., Browne, K.M., 2000. Cyanobacteria: architects of sedimentary structures. In: Microbial Sediments. Springer, Berlin, Heidelberg, pp. 57–67.
Gomberg, D.N., Bonatti, E., 1970. High-magnesian calcite: leaching of magnesium in the deep sea. Science 168 (3938), 1451–1453.
Grabau, A.W., 1904. On the Classification of Sedimentary Rocks.
Hancock, J.M., 1975. The petrology of the chalk. Proc. Geol. Assoc. 86, 499–535.
Hardie, L.A., 1990. The roles of rifting and hydrothermal $CaCl_2$ brines in the origin of potash evaporites: an hypothesis. Am. J. Sci. 290, 43–106.
Hardie, L.A., 1996. Secular variation in seawater chemistry: an explanation for the coupled secular variation in the mineralogies of marine limestones and potash evaporites over the past 600 my. Geology 24 (3), 279–283.
Harland, S.R., Wood, R.A., Curtis, A., Van Dijke, M.I.J., Stratford, K., Jiang, Z., Kallel, W., Sorbie, K., 2015. Quantifying flow in variably wet microporous carbonates using object-based geological modeling and both lattice-Boltzmann and pore-network fluid flow simulations. AAPG (Am. Assoc. Pet. Geol.) Bull. 99, 1827–1860. https://doi.org/10.1306/04231514122.
Harris, P.M., Frost, 5. H., 1984. Middle cretaceous carbonate reservoirs, fahud field and northwestern Oman. AAPG (Am. Assoc. Pet. Geol.) Bull. 68, 649–658.
Harris, P.M., Frost, 5. H., Seiglle, 6. A., Schnelderman, N., 1985. Regional unconformities and depositional cycles, cretaceous of the arabian peninsula. In: In: Schlee, J.S. (Ed.), Interregional Unconformities and Hydrocarbon Accumulation: Am. Assoc. Petroleum Geologists Mem, vol. 36. pp. 67–80.
Hasiuk, F.J., Kaczmarek, S.E., Fullmer, S.M., 2016. Diagenetic origins of the calcite microcrystals that host microporosity in limestone reservoirs. J. Sediment. Res. 86 (10), 1163–1178.
Hathaway, J.C., Robertson, E.C., 1961. Microtexture of artificially consolidated aragonite mud. U. S. Geol. Surv. Prof. Pap. C 424, 301–304.
Heasley, E.C., Worden, R.H., Hendry, J.P., 2000. Cement distribution in a carbonate reservoir: recognition of a palaeo oil–water contact and its relationship to reservoir quality in the Humbly Grove field, onshore, UK. Mar. Petrol. Geol. 17 (5), 639–654.
Henriksen, K., Stipp, S.L.S., Young, J.R., Marsh, M.E., 2004. Biological control on calcite crystallization: AFM investigation of coccolith polysaccharide Function. Am. Mineral. 89, 1709–1716.
Hoffmann, H., 1983. X-ray Diffraction Analysis of Mineralogy in Recent Lime Muds, Florida Bay. Unpublished B.S. Thesis, University of Illinois, Urbana, IL 72 pp.
Holail, H., Lohmann, K.C., 1994. The role of early lithification in development of chalky porosity in calcitic micrites: upper Cretaceous chalks, Egypt. Sediment. Geol. 88, 193–200. https://doi.org/10.1016/0037-0738(94)90061-2.
Horowitz, A.S., Potter, P.E., 2012. Introductory Petrography of Fossils. Springer Science & Business Media.
Hoskin, C.M., 1963. Recent Carbonate Sedimentation of Alacran Reef, Yucatan, Mexico (No. 19). National Academies.
Hover, V.C., Walter, L.M., Peacor, D.R., 2001. Early marine diagenesis of biogenic aragonite and Mg-calcite: new constraints from high-resolution STEM and AEM analyses of modern platform carbonates. Chem. Geol. 175 (3–4), 221–248.
Humbert, L., 1976. Eléments de pétrologie dynamique des systèmes calcaires. Description macroscopique et microscopique, diagenèse, applications. Technip Eds, pp. 213.
Husseini, S.I., Matthews, R.K., 1972. Distribution of high-magnesium calcite in lime muds of the Great Bahama Bank; diagenetic implications. J. Sediment. Res. 42 (1), 179–182.
Illing, L.V., Wood, G.V., Fuller, G.N., 1967. January. Reservoir rocks and stratigraphic traps in non-reef carbonates. In: 7th World Petroleum Congress. World Petroleum Congress.
Ings, S.J., MacRae, R.A., Shimeld, J.W., Pe-Piper, G., 2005. Diagenesis and porosity reduction in the late cretaceous wyandot formation, offshore nova scotia: a comparison with Norwegian North Sea chalks. Bull. Can. Petrol. Geol. 53, 237–249.
Irwin, H., Curtis, C., Coleman, M., 1977. Isotopic evidence for source of diagenetic carbonates formed during burial of organic-rich sediments. Nature 269, 209–213.
James, N.P., Choquette, P.W., 1984. Diagenesis 9. Limestones-the meteoric diagenetic environment. Geosci. Can. 11 (4).
James, N.P., Jones, B., 2015. Origin of Carbonate Rocks. John Wiley & Sons.
Jameson, J., 1994. Models of porosity formation and their impact on reservoir description, Lisburne field, Prudhoe Bay, Alaska. AAPG (Am. Assoc. Pet. Geol.) Bull. 78, 1651–1678.
Janjuhah, H.T., Alansari, A., Vintaned, J.A.G., 2019. Quantification of microporosity and its effect on permeability and acoustic velocity in Miocene carbonates, Central Luconia, offshore Sarawak, Malaysia. J. Pet. Sci. Eng. 175, 108–119.
Joachimski, M.M., 1994. Subaerial exposure and deposition of shallowing upward sequences: evidence from stable isotopes of Purbeckian peritidal carbonates (basal

Cretaceous), Swiss and French Jura Mountains. Sedimentology 41 (4), 805–824.
Jodry, R.L., 1972. Pore geometry of carbonate rocks (basic geologic concepts). Oil Gas Product. Carbonate Rocks 35–82.
Johnson, J.H., 1971. An introduction to the study of organic limestones. Quart. Colorado School of Mines 66 (2), 185.
Kaczmarek, S.E., Sibley, D.F., 2007. A comparison of nanometer-scale growth and dissolution features on natural and synthetic dolomite crystals: implications for the origin of dolomite. J. Sediment. Res. 77 (5), 424–432.
Kaczmarek, S.E., Fullmer, S.M., Hasiuk, F.J., 2015. A universal classification scheme for the microcrystals that host limestone microporosity. J. Sediment. Res. 85, 1197–1212. https://doi.org/10.2110/jsr.2015.79.
Kaczmarek, S.E., Gregg, J.M., Bish, D.L., Machel, H.G., Fouke, B.W., MacNeil, A., Lonnee, J., Wood, R., 2017. Dolomite, very-high magnesium calcite, and microbes: implications for the microbial model of dolomitization. SEPM (Soc. Sediment. Geol.) Spec. Publ. 109, 1–14.
Kahle, C.F., 1974. Ooids from Great Salt Lake, Utah, as an analogue for the genesis and diagenesis of ooids in marine limestones. J. Sediment. Res. 44 (1), 30–39.
Kaldi, J., 1989. Diagenetic microporosity (chalky porosity), middle devonian kee Scarp reef complex, norman wells, northwest territories, Canada. Sediment. Geol. 63, 241–252.
Keith, B.D., Pittman, E.D., 1983. Bimodal porosity in oolitic reservoir–effect on productivity and log response, rodessa limestone (lower cretaceous), east Texas basin. AAPG (Am. Assoc. Pet. Geol.) Bull. 67 (9), 1391–1399.
Kieke, E.M., Hartmann, D.J., 1974. Detecting microporosity to improve formation evaluation. J. Pet. Technol. 26 (10), 1–080.
Kominz, M.A., Patterson, K., Odette, D., 2011. Lithology dependence of porosity in slope and deep marine sediments. J. Sediment. Res. 81, 730–742. https://doi.org/10.2110/jsr.2011.60.
Lambert, L., Durlet, C., Loreau, J.P., Marnier, G., 2006. Burial dissolution of micrite in Middle East carbonate reservoirs (Jurassic-Cretaceous): keys for recognition and timing. Mar. Petrol. Geol. 23, 79–92.
Land, L.S., 1979. Chert-chalk diagenesis: the Miocene Island slope of North Jamaica. J. Sediment. Res. 49, 223–232.
Land, L.S., MacKenzie, F.T., Gould, S.J., 1967. Pleistocene history of Bermuda. Geol. Soc. Am. Bull. 78 (8), 993–1006.
Land, L.S., Behrens, E.W., Frishman, S.A., 1979. The ooids of Baffin Bay, Texas. J. Sediment. Res. 49 (4), 1269–1277.
Larson, E.B., Mylroie, J.E., 2014. A review of whiting formation in the Bahamas and new models. Carbonates Evaporites 29 (4), 337–347.
Lasemi, Z., Sandberg, P.A., 1983. Recognition of original mineralogy in micrites. AAPG (Am. Assoc. Pet. Geol.) Bull. 67 (3), 499–500.
Lasemi, Z., Sandberg, P.A., 1984. Transformation of aragonite-dominated lime muds to microcrystalline limestones. Geology 12 (7), 420–423.
Lasemi, Z., Sandberg, P., 1993. Microfabric and compositional clues to dominant mud mineralogy of micrite precursors. In: Carbonate Microfabrics. Springer, New York, NY, pp. 173–185.
Leighton, M.W., Pendexter, C., 1962. Carbonate Rock Types, vol. I. American Association of Petroleum Geologists Memoir, pp. 33–61.
Léonide, P., Fournier, F., Reijmer, J.J., Vonhof, H., Borgomano, J., Dijk, J., Rosenthal, M., van Goethem, M., Cochard, J., Meulenaars, K., 2014. Diagenetic patterns and pore space distribution along a platform to outer-shelf transect (Urgonian limestone, Barremian–Aptian, SE France). Sediment. Geol. 306, 1–23.
Lind, I.L., 1993. Loading Experiments on Carbonate Ooze and Chalk from Leg 130, Ontong Java Plateau.
Lippman, Friedrich, 1960. Versuche zur Aufklarung der Bildungsbedingungen yon Calcit und Aragonit: Fortschr. Miner 38, 156–161.
Logan, B.W., Cebulski, D.E., 1970. Sedimentary Environments of Shark Bay, Western Australia.
Longman, M.W., 1977. Factors controlling the formation of microspar in the Bromide Formation. J. Sediment. Petrol. 47, 347–350.
Longman, M.W., Mench, P.A., 1978. Diagenesis of Cretaceous limestones in the Edwards aquifer system of south-central Texas: a scanning electron microscope study. Sediment. Geol. 21 (4), 241–276.
Lønøy, A., 2006. Making sense of carbonate pore systems. AAPG (Am. Assoc. Pet. Geol.) Bull. 90, 1381–1405.
Loreau, J.-P., 1969. Vltrastructures et diageneses des oolithes marines anciennes (Jurassiques). C.R. Acad. Sci. Paris 269, 819–822.
Loreau, J.P., 1972. Pétrographie de calcaires fins au microscope électronique à balayage: introduction à une classification des "micrites. Comptes rendu de l'Académie des Sciences, Paris 274, 810–813.
Loreau, J.P., 1982. Sediments aragonitiques et leur gene 'se. Muse ′um d'Histoire Naturelle Memoir 47 312 pp.
Loreau, J.P., Purser, B.H., 1973. Distribution and ultrastructure of Holocene ooids in the Persian Gulf. In: The Persian Gulf. Springer, Berlin, Heidelberg, pp. 279–328.
Loucks, R.G., Kerans, C., Zeng, H., Sullivan, P.A., 2017 Jan 1. Documentation and characterization of the Lower Cretaceous (Valanginian) Calvin and Winn carbonate shelves and shelf margins, onshore northcentral Gulf of Mexico. AAPG Bulletin 101 (1), 119–142.
Loucks, R.G. and Ulrich, M., Origin and characterization of the nanopore/micropore network in the leonardian clear fork reservoirs in the goldsmith field in ector Co., Texas. In AAPG Annual Convention and Exhibition.
Loucks, R.G., Moody, R.T.J., Bellis, J.K., Brown, A.A., 1998. Regional depositional setting and pore network systems of the el garia formation (metlaoui Group, lower eocene), offshore Tunisia. Geol. Soc., Lond., Spec. Publ. 132, 355–374. https://doi.org/10.1144/GSL.SP.1998.132.01.20.
Loucks, R.G., Lucia, F.J., Waite, L.E., 2013. Origin and description of the micropore network within the lower cretaceous stuart city trend tight-gas limestone reservoir in pawnee field in south Texas. GCAGS J. 2, 29–41.
Lowenstam, H.A., 1955. Aragonite needles secreted by algae and some sedimentary implications. J. Sediment. Res. 25 (4), 270–272.
Lowenstam, H.A., 1963. Biologic Problems Relating to the Composition and Diagenesis of Sediments. University of Chicago Press, Chicago, pp. 137–195.
Lowenstam, H.A., Epstein, S., 1957. On the origin of sedimentary aragonite needles of the Great Bahama Bank. J. Geol. 65 (4), 364–375.
Lowenstam, H.A., Weiner, S., 1989. On Biomineralization. Oxford University Press on Demand.
Lowenstein, T.K., Timofeeff, M.N., Brennan, S.T., Hardie, L.A., Demicco, R.V., 2001. Oscillations in Phanerozoic seawater chemistry: evidence from fluid inclusions. Science 294 (5544), 1086–1088.
Lucia, F.J., 1995. Rock-fabric/petrophysical classification of carbonate pore space for reservoir characterization. AAPG (Am. Assoc. Pet. Geol.) Bull. 79, 1275–1300.
Lucia, F.J., 2007. Carbonate Reservoir Characterization: an Integrated Approach. Springer, Berlin; New York 337 pp.
Lucia, F.J., 2017. Observations on the origin of micrite crystals. Mar. Petrol. Geol. 86, 823–833.
Lucia, F.J., Loucks, R.G., 2013. Micropores in carbonate mud: early development and petrophysics. GCAGS J. 2, 1–10.
MacDonald, G.J., 1956. Experimental determination of calcite-aragonite equilibrium relations at elevated temperatures and pressures. Am. Mineral.: J. Earth Planet. Mater. 41 (9–10), 744–756.
Macintyre, I.G., Reid, R.P., 1992. Comment on the origin of aragonite needle mud: a picture is worth a thousand words. J. Sediment. Res. 62 (6).
Macintyre, I.G., Reid, R.P., 1995. Crystal alteration in a living calcareous alga (Halimeda); implications for studies in skeletal diagenesis. J. Sediment. Res. 65 (1a), 143–153.
Mackenzie, F.T., Pigott, J.D., 1981. Tectonic controls of Phanerozoic sedimentary rock cycling. J. Geol. Soc. 138 (2), 183–196.
Majewske, O.P., 1974. Recognition of Invertebrate Fossil Fragments in Rocks and Thin Sections, vol. 13 Brill Archive.
Maliva, R.G., Missimer, T.M., Clayton, E.A., Dickson, J.A.D., 2009. Diagenesis and porosity preservation in Eocene microporous limestones, South Florida, USA. Sediment. Geol. 217, 85–94. https://doi.org/10.1016/j.sedgeo.2009.03.011.
Martin, G.D., Wilkinson, B.D., Lohmann, K.C., 1986. The role of skeletal porosity in aragonite neomorphism - strombus and montastrea from the Pleistocene key largo limestone, Florida. J. Sediment. Petrol. 56, 194–203.
Maruthamuthu, S., Dhandapani, P., Ponmariappan, S., Sathiyanarayanan, S., Muthukrishnan, S., Palaniswamy, N., 2010. Scale formation by calciumprecipitating bacteria in cooling water system. J. Fail. Anal. Prev. 10, 416–426.
Marzouk, I., Takezaki, H., Suzuki, M., 1998. New Classification of Carbonate Rocks for Reservoir Characterization. Society of Petroleum Engineers, pp. 49475.
Mathews, R.K., 1966. Genesis of Recent lime mud in southern British Honduras. J. Sediment. Res. 36 (2), 428–454.
McManus, K.M., 1982. The Aqueous Aragonite to Calcite Transformation: Rate, Mechanisms, and its Role in the Development of Neomorphic Fabrics. Doctoral dissertation, Virginia Polytechnic Institute and State University.
McManus, K.M., Rimstidt, J.D., 1982. Aqueous aragonite to calcite transformation: a geometry controlled dissolution-precipitation reaction (abstract). Geol. Soc. Am. Abstr. Progr. 14, 562.
Melim, L.A., 1996. Limitations on lowstand meteoric diagenesis in the Pliocene-Pleistocene of Florida and Great Bahama Bank: implications for eustatic sea-level models. Geology 24, 893–896.
Melim, L.A., Masaferro, J.L., 1997. Geology of the Bahamas: subsurface geology of the Bahamas banks. In: In: Vacher, H.L., Quinn, T.M. (Eds.), Geology and Hydrogeology of Carbonate Islands, vol. 54. Elsevier, Amsterdam, pp. 161–182 Dev. Sedimentol.
Melim, L.A., Swart, P.K., Maliva, R.G., 1995. Meteoric-like fabrics forming in marine waters: implications for the use of petrography to identify diagenetic environments. Geology 23, 755–758.
Melim, L.A., Anselmetti, F.S., Eberli, G.P., 2001a. The importance of pore type on permeability of Neogene carbonates, Great Bahama Bank. In: In: Ginsburg, R.N. (Ed.), Subsurface Geology of a Prograding Carbonate Platform Margin, Great Bahama Bank, vol. 70. SEPM Spec. Publ., pp. 217–240.
Melim, L.A., Swart, P.K., Maliva, R.G., 2001b. Meteoric and marine burial diagenesis in the subsurface of the Great Bahama Bank. In: In: Ginsburg, R.N. (Ed.), Subsurface Geology of a Prograding Carbonate Platform Margin, Great Bahama Bank, vol. 70. SEPM Spec. Publ., pp. 137–162.
Melim, L.A., Westphal, H., Swart, P.K., Eberli, G.P., Munnecke, A., 2002. Questioning carbonate diagenetic paradigms: evidence from the Neogene of the Bahamas. Mar. Geol. 185 (1–2), 27–53.
Milliken, K.L., Curtis, M.E., 2016. Imaging pores in sedimentary rocks: foundation of porosity prediction. Mar. Petrol. Geol. 73, 590–608.
Milliken, K.L., Pigott, J.D., 1977. Variation of oceanic Mg/Ca ratio through time-implications for the calcite sea. In: Geological Society of America, Abstracts with Programs, vol. 9. pp. 345–367.
Milliman, J.D., 1974. Marine Carbonates, Part I. Heidelberg Springer-Verlag, Berlin, Heidelburg.
Milliman, J.D., Müller, J., 1973. Precipitation and lithification of magnesian calcite in the deep-sea sediments of the eastern Mediterranean Sea. Sedimentology 20 (1), 29–45.
Milliman, J.D., Hook, J.A., Golubic, S., 1985. Meaning and usage of micrite cement and matrix-reply to discussion. J. Sediment. Petrol. 55 (5), 776–777.
Milliman, J.D., Freile, D., Steinen, R.P., Wilber, R.J., 1993. Great Bahama Bank aragonitic muds; mostly inorganically precipitated, mostly exported. J. Sediment. Res. 63 (4), 589–595.
Moore, C.H., Wade, W.J., 2013. Carbonate Reservoirs: Porosity and Diagenesis in a

Sequence Stratigraphic Framework, vol. 67 Newnes.
Morad, D., Paganoni, M., Al Harthi, A., Morad, S., Ceriani, A., Mansurbeg, H., Al Suwaidi, A., Al-Aasm, I.S., Ehrenberg, S.N., 2018. Origin and evolution of microporosity in packstones and grainstones in a Lower Cretaceous carbonate reservoir, United Arab Emirates. Geol. Soc., Lond., Spec. Publ. 435 (1), 47–66.
Morad, S., Al Suwaidi, M., Mansurbeg, H., Morad, D., Ceriani, A., Paganoni, M., Al-Aasm, I., 2019. Diagenesis of a limestone reservoir (lower cretaceous), abu dhabi, United Arab Emirates: comparison between the anticline crest and flanks. Sediment. Geol. 380, 127–142.
Morse, J.W., Casey, W.H., 1988. Ostwald processes and mineral paragenesis in sediments. Am. J. Sci. 288 (6), 537–560.
Morse, J.W., Mackenzie, F.T., 1990. Geochemistry of Sedimentary Carbonates, vol. 48 Elsevier.
Morse, J.W., Mackenzie, F.T., 1993. Geochemical constraints on $CaCO_3$ transport in subsurface sedimentary environments. Chem. Geol. 105 (1–3), 181–196.
Morse, J.W., Millero, F.J., Thurmond, V., Brown, E., Ostlund, H.G., 1984. The carbonate chemistry of Grand Bahama Bank waters: after 18 years another look. J. Geophys. Res.: Oceans 89 (C3), 3604–3614.
Morse, J.W., Gledhill, D.K., Millero, F.J., 2003. $CaCO_3$ precipitation kinetics in waters from the great Bahama bank: implications for the relationship between bank hydrochemistry and whitings. Geochem. Cosmochim. Acta 67 (15), 2819–2826.
Morse, J.W., Wang, Q., Tsio, M.Y., 1997. Influences of temperature and Mg: Ca ratio on CaCO3 precipitates from seawater. Geology 25 (1), 85–87.
Moshier, S.O., 1987. On the Nature and Origin of Microporosity in Micritic Limestones.
Moshier, S.O., 1989a. Microporosity in micritic limestones: a review. Sediment. Geol. 63 (3–4), 191–213.
Moshier, S.O., 1989b. Development of microporosity in a micritic limestone reservoir, Lower Cretaceous, Middle East. Sediment. Geol. 63, 217–240. https://doi.org/10.1016/0037-0738(89)90133-4.
Moshier, S.O., McManus, K.M., 1986. Textural evolution during experimental lime-mud diagenesis. Am. Assoc. Petrol. Geol. Bull. 70 (CONF-860624).
Munnecke, A., Westphal, H., Reijmer, J.J.G., Samtleben, C., 1997. Microspar development during early marine burial diagenesis: a comparison of Pliocene carbonates from the Bahamas with Silurian limestones from Gotland (Sweden). Sedimentology 44, 977–990.
Munnecke, A., Westphal, H., Kölbl-Ebert, M., 2008. Diagenesis of plattenkalk: examples from the Solnhofen area (Upper Jurassic, southern Germany). Sedimentology 55 (6), 1931–1946.
Neev, D., 1963. Recent Precipitation of Calcium Salts in the Dead Sea 11G Research Council Israel Bull.
Neilson, J.E., Oxtoby, N.H., Simmons, M.D., 1998. The relationship between petroleum emplacement and carbonate reservoir quality: examples from Abu Dhabi and the Amu Darya Basin. Mar. Petrol. Geol. 15, 57–72. https://doi.org/10.1016/S0264-8172(97)00033-0.
Neumann, A.C., Land, L.S., 1975. Lime mud deposition and calcareous algae in the Bight of Abaco, Bahamas; a budget. J. Sediment. Res. 45 (4), 763–786.
Newell, N.D., 1955. Depositional fabric in Permian reef limestones. J. Geol. 63 (4), 301–309.
Newell, N.D., Rigby, J.K., 1957. Geological Studies on the Great Bahama Bank.
Njiekak, G., Schmitt, D.R., Kofman, R.S., 2018. Pore systems in carbonate formations, Weyburn field, Saskatchewan, Canada: micro-tomography, helium porosimetry and mercury intrusion porosimetry characterization. J. Pet. Sci. Eng. 171, 1496–1513.
O'Connell, L.G., James, N.P., 2015. Composition and genesis of temperate, shallow-marine carbonate muds: Spencer Gulf, South Australia. J. Sediment. Res. 85 (10), 1275–1291.
Oldershaw, A.E., 1972. Microporosity control in microcrystalline carbonate rocks, southern Ontario, Canada. 24th Int. Geol. Congr., Sect. 6, 198–207.
Ostwald, W., 1887. Lehrbuch der Allgemeinen Chemie. Verlag von Wilhelm Engelmann, Leipzig, pp. 909.
Oti, m., Müller, g., 1985. Textural and mineralogical changes in coralline algae during meteoric diagenesis-an experimental approach. neues jahrbuch fur mineralogie-abhandlungen 151 (2), 163–195.
Papenguth, H.W., 1991. Experimental Diagenesis of Lime Mud. Doctoral dissertation, University of Illinois at Urbana-Champaign.
Perdikouri, C., Kasioptas, A., Putnis, C.V., Putnis, A., 2008. The effect of fluid composition on the mechanism of the aragonite to calcite transition. Mineral. Mag. 72 (1), 111–114.
Perkins, R.D., 1989. Origin of micro-rhombic calcite matrix within cretaceous reservoir rock, west stuart city trend, Texas. Sediment. Geol. 63, 313–321. https://doi.org/10.1016/0037-0738(89)90138-3.
Perri, E., Tucker, M., 2007. Bacterial fossils and microbial dolomite in Triassic stromatolites. Geology 35 (3), 207–210.
Perri, E., Borrelli, M., Spadafora, A., Critelli, S., 2017. The role of microbialitic facies in the micro-and nano-pore system of dolomitized carbonate platforms (Upper Triassic–Southern Italy). Mar. Petrol. Geol. 88, 1–17.
Perri, E., Tucker, M.E., Słowakiewicz, M., Whitaker, F., Bowen, L., Perrotta, I.D., 2018. Carbonate and silicate biomineralization in a hypersaline microbial mat (Mesaieed sabkha, Qatar): roles of bacteria, extracellular polymeric substances and viruses. Sedimentology 65 (4), 1213–1245.
Perry, C.T., Salter, M.A., Harborne, A.R., Crowley, S.F., Jelks, H.L., Wilson, R.W., 2011. Fish as major carbonate mud producers and missing components of the tropical carbonate factory. Proc. Natl. Acad. Sci. Unit. States Am. 108, 3865–3869.
Pilkey, O.H., 1964. Mineralogy of the fine fraction in certain carbonate cores. Bull. Mar. Sci. 14 (1), 126–139.
Pingitore, N.R., 1976. Vadose versus phreatic diagenesis: processes, products and their recognition in corals. J. Sediment. Petrol. 46, 985–1006.
Pittman, E.D., 1971. Microporosity in carbonate rocks. AAPG (Am. Assoc. Pet. Geol.) Bull. 55, 1873–1878.
Plummer, L.N., Mackenzie, F.T., 1974. Predicting mineral solubility from rate data; application to the dissolution of magnesian calcites. Am. J. Sci. 274 (1), 61–83.
Purdy, E.G., 1968. Carbonate diagenesis: an environmental survey. Geol. Rom. 7, 183–228.
Purdy, E.G., Imbrie, J., Laporte, L.F., Rigby, J.K., 1964. Carbonate Sediments, Great Bahama Bank. Geological Society of America Convention.
Purkis, S., Cavalcante, G., Rohtla, L., Oehlert, A.M., Harris, P.M., Swart, P.K., 2017. Hydrodynamic control of whitings on great Bahama Bank. Geology 45 (10), 939–942.
Purser, B.H., 1969. Syn-sedimentary marine lithification of middle jurassic limestones in the paris basin. Sedimentology 12, 205–230.
Queen, J.M., 1977. Carbonate Sedimentology and Ecology of Some Pelleted Muds West of Andros Island. Great Bahama Bank. Ph. D. dissert. Stony Brook, State University of, New York.
Reid, R.P., Macintyre, I., 1998. Carbonate Recrystallization in Shallow Marine Environments: A Widespread Diagenetic Process Forming Micritized Grains. vol. 68. pp. 928–946.
Reid, R.P., Macintyre, I.G., 2000. Microboring versus recrystallization: further insight into the micritization process. J. Sediment. Res. 70 (1), 24–28.
Reid, R.P., Macintyre, I.G., Post, J.E., 1992. Micritized skeletal grains in northern Belize Lagoon; a major source of Mg-calcite mud. J. Sediment. Res. 62 (1), 145–156.
Reitner, J., 1993. Modern cryptic microbialite/metazoan facies from Lizard Island (Great Barrier Reef, Australia) formation and concepts. Facies 29 (1), 3–39.
Reitner, J., Thiel, V., Zankl, H., Michaelis, W., Wörheide, G., Gautret, P., 2000. Organic and biogeochemical patterns in cryptic microbialites. In: Microbial Sediments. Springer, Berlin, Heidelberg, pp. 149–160.
Reuning, L., Reijmer, J.J., Mattioli, E., 2006 Aug. Aragonite cycles: diagenesis caught in the act. Sedimentology 53 (4), 849–866.
Richard, J., Sizun, J.P., Machhour, L., 2007. Development and compartmentalization of chalky carbonate reservoirs: the Urgonian Jura-Bas Dauphiné platform model (Génissiat, southeastern France). Sediment. Geol. 198, 195–207.
Richter, D.K., 1979. Die stufen der meteorisch-vadosen umwandlung von Mg-calcit in calcit in Rezenten bis Pliozanen biogenen Greichenlands. Neues Jahrbuch fur Geologie und Palaontologie Abhandlungen 158, 277–333.
Ries, J.B., 2006. Aragonitic algae in calcite seas: effect of seawater Mg/Ca ratio on algal sediment production. J. Sediment. Res. 76 (3), 515–523.
Ries, J.B., 2010. Geological and experimental evidence for secular variation in seawater Mg/Ca (calcite-aragonite seas) and its effects on marine biological calcification. Biogeosciences 7 (9), 2795.
Ries, J.B., Stanley, S.M., Hardie, L.A., 2006. Scleractinian corals produce calcite, and grow more slowly, in artificial Cretaceous seawater. Geology 34 (7), 525–528.
Riding, R., 1993 Nov 1. Phanerozoic patterns of marine CaCO 3 precipitation. Naturwissenschaften 80 (11), 513–516.
Robbins, L.L., Blackwelder, P.L., 1992. Biochemical and ultrastructural evidence for the origin of whitings: a biologically induced calcium carbonate precipitation mechanism. Geology 20 (5), 464–468.
Robie, R.A., Hemingway, B.S., 1995. Thermodynamic Properties of Minerals and Related Substances at 298.15 K and 1 Bar (105 Pascals) Pressure and at Higher Temperatures, vol. 2131 US Government Printing Office.
Rivers, J.M., Kurt Kyser, T., James, N.P., 2012 Feb. Salinity reflux and dolomitization of southern Australian slope sediments: the importance of low carbonate saturation levels. Sedimentology 59 (2), 445–465.
Roniewicz, E., 1996. The key role of skeletal microstructure in recognizing high-rank scleractinian taxa in the stratigraphical record. Paleontol. Soc. Pap. 1, 187–206.
Saller, A.H., 1984. Diagenesis of Cenozoic Limestones on Enewetak Atoll. Ph.D. Dissertation. Louisiana State University, Baton Rouge, La., pp. 363 (unpublished).
Saller, A.H., Moore Jr., C.H., 1989. Meteoric diagenesis, marine diagenesis, and microporosity in Pleistocene and Oligocene limestones, Enewetak Atoll, Marshall Islands. Sediment. Geol. 63, 253–272. https://doi.org/10.1016/0037-0738(89)90135-8.
Salter, M.A., Perry, C.T., Wilson, R.W., 2012. Production of mud-grade carbonates by marine fish: crystalline products and their sedimentary significance. Sedimentology 59, 2172–2198.
Sandberg, P.A., 1975. New interpretation of great Salt Lake ooids and of ancient non-skeletal carbonate mineralogy. Sedimentology 25, 673–702.
Sandberg, P.A., 1983 Sep. An oscillating trend in Phanerozoic non-skeletal carbonate mineralogy. Nature 305 (5929), 19.
Sandberg, P., 1985. Aragonite Cements and Their Occurrence in Ancient Limestones.
Sandberg, P.A., Hudson, J.D., 1983. Aragonite relic preservation in Jurassic calcite-replaced bivalves. Sedimentology 30 (6), 879–892.
Sandberg, P.A., Schneidermann, N., Wunder, S.J., 1973. Aragonitic ultrastructural relics in calcite-replaced Pleistocene skeletons. Nat. Phys. Sci. (Lond.) 245 (148), 133.
Sanders, J.E., Friedman, G.M., 1967. Origin and occurrence of limestones. In: Chilingar, G.V., Bissell, H.J., Fairbridge, R.W. (Eds.), Carbonate Rocks: Origin, Occurrence and Classijication. Elsevier, Amsterdam, pp. 169–265 Developments in Sedimentology, 9A.
Schlanger, S.O., Douglas, R.G., 1974. The pelagic ooze-chalk-limestone transition and its implications for marine stratigraphy. Special Publ. Int. Assoc. Sedimentol. 1, 117–148.
Scholle, P.A., 1977. Chalk diagenesis and its relation to petroleum exploration: oil from chalks, a modern miracle? AAPG (Am. Assoc. Pet. Geol.) Bull. 61, 982–1009.
Scholle, P.A., Kinsman, D.J., 1974. Aragonitic and high-Mg calcite caliche from the Persian Gulf-a modern analog for the Permian of Texas and New Mexico. J. Sediment. Res. 44 (3), 904–916.
Scholle, P.A., Hsu, K.J., Jenkyns, H.C., 1974. Diagenesis of upper cretaceous chalks from england, northern Ireland and the north sea. In: Pelagic Sediments: on Land and

under the Sea, vol. 1. Spec. Publs int. Ass. Sediment, pp. 177–210.
Schroeder, J.H., 1969. Experimental dissolution of calcium, magnesium, and strontium from recent biogenic carbonates: a model of diagenesis. J. Sediment. Petrol. 39, 1057–1073.
Schroeder, J.H., 1979. Carbonate diagenesis in Quaternary beachrock of Uyombo, Kenya: sequences of processes and coexistence of heterogenic products. Geol. Rundsch. 68, 894–919.
Scholle, P.A., Ulmer-Scholle, D.S., 2003. A Color Guide to the Petrography of Carbonate Rocks: Grains, Textures, Porosity, Diagenesis. In: AAPG Memoir 77 AAPG.
Schultz, L.N., Dideriksen, K., Mueter, D., Hakim, S.S., Stipp, S.L.S., 2013. Early stage Ostwald ripening of submicrometer calcite. Mineral. Mag. 77 (5), 2168.
Sellwood, B.W., Beckett, D., 1991. Ooid microfabrics: the origin and distribution of high intra-ooid porosity; Mid-Jurassic reservoirs, S. England. Sediment. Geol. 71, 189–193. https://doi.org/10.1016/0037-0738(91)90101-I.
Shinn, E.A., Steinen, R.P., Lidz, B.H., Swart, P.K., 1989. Whitings, a sedimentologic dilemma. J. Sediment. Res. 59 (1), 147–161.
Simkiss, K., 1964. Variations in the crystalline form of calcium carbonate precipitated from artificial sea water. Nature 201, 492–493.
Simone, L., 1980. Ooids: a review. Earth Sci. Rev. 16, 319–355.
Skalinski, M., Kenter, J.A., 2015. Carbonate petrophysical rock typing: integrating geological attributes and petrophysical properties while linking with dynamic behaviour. Geol. Soc., Lond., Spec. Publ. 406 (1), 229–259.
Slowakiewicz, M., Perri, E., Tucker, M.E., 2016. Micro-and nanopores in tight Zechstein 2 carbonate facies from the southern Permian Basin, NW Europe. J. Pet. Geol. 39 (2), 149–168.
Smith, C.L., 1940. The Great Bahama Bank, 1. General hydrographic and chemical factors; 2. Calcium carbonate precipitation. J. Mar. Res. 3 (1–31), 147–189.
Sorby, H.C., 1879. The structure and origin of limestones. Pop. Sci. Rev. 3 (9), 134–137.
Spadafora, A., Perri, E., McKenzie, J.A., Vasconcelos, C., 2010. Microbial biomineralization processes forming modern Ca: Mg carbonate stromatolites. Sedimentology 57 (1), 27–40.
Stanley Jr., G.D., 2003. The evolution of modern corals and their early history. Earth Sci. Rev. 60 (3–4), 195–225.
Stearn, C.W., Webby, B.D., Nestor, H., Stock, C.W., 1999. Revised classification and terminology of Palaeozoic stromatoporoids. Acta Palaeontol. Pol. 44 (1).
Steinen, R.P., 1978. On the diagenesis of lime mud; scanning electron microscopic observations of subsurface material from Barbados, WI. J. Sediment. Res. 48 (4), 1139–1148.
Steinen, R.P., 1982. SEM observations on the replacement of Bahamian aragonitic mud by calcite. Geology 10, 471–475.
Steinen, R.P., Swart, P.K., Shinn, E.A., Lidz, B.H., 1988. Bahamian Lime Mud: the Algae Didn't Do it. Geol. Soc. America, Abstr. w. Progr., pp. A209.
Stockman, K.W., Ginsburg, R.N., Shinn, E.A., 1967. The production of lime mud by algae in south Florida. J. Sediment. Res. 37 (2), 633–648.
Swart, P.K., 2000. The oxygen isotopic composition of interstitial waters: evidence for fluid flow and recrystallization in the margin of great Bahama Bank. In: In: Swart, P.K., Eberli, G.P., Malone, M. (Eds.), Proceedings of the Ocean Drilling Program, College Station, TX, vol. 166. Ocean Drill. Prog. Sci. Results, pp. 91–98.
Swart, P.K., Burns, S.J., 1990. Pore-water chemistry and carbonate diagenesis in sediments from Leg 115: Indian Ocean. In: Proc., scientific results, ODP, Leg 115, Mascarene Plateau. ODP, Texas A&M University, College Station; UK distributors, IPOD Committee, NERC, Swindon, pp. 629–645.
Swart, P.K., Melim, L.A., 2000. The origin of dolomites in Tertiary sediments from the margin of Great Bahama Bank. J. Sediment. Res. 70, 738–748.
Swinchatt, J.P., 1965. Significance of constituent composition, texture, and skeletal breakdown in some recent carbonate sediments: Jour. Sed. Petrol. 35 (1), 71–90.
Taft, W.H., 1967. Physical chemistry of formation of carbonates. In: Chillingar, G.V., Bissel, H.J., Fairbridge, R.W. (Eds.), Developments ilzSedimentology, 9B, Carbonate Rocks. Elsevier, pp. 151–168.
Tavakoli, V., Jamalian, A., 2018. Microporosity evolution in Iranian reservoirs, Dalan and Dariyan formations, the central Persian Gulf. J. Nat. Gas Sci. Eng. 52, 155–165.
Thorp, E.M., 1936 Aug 1. The sediments of the Pearl and Hermes reef [Hawaii]. Journal of Sedimentary Research 6 (2), 109–118.
Tonietto, S.N., Smoot, M.Z., Pope, M., 2014. PS Pore Type Characterization and Classification in Carbonate Reservoirs.
Towe, K.M., Hemleben, C., 1976. Diagenesis of magnesian calcite: evidence from miliolacean foraminifera. Geology 4 (6), 337–339.
Trower, E.J., Lamb, M.P., Fischer, W.W., 2019. The origin of carbonate mud. Geophys. Res. Lett. 46 (5), 2696–2703.
Tucker, M.E. (Ed.), 2009. Sedimentary Petrology: an Introduction to the Origin of Sedimentary Rocks. John Wiley & Sons.
Turner, R.V., Anderson, T.F., Sandberg, P.A., Goldstein, S.I., 1986. Isotopic, chemical and textural relations during the experimental alteration of biogenic high-magnesian calcite. Geochem. Cosmochim. Acta 50, 495–506.
Turpin, M., Emmanuel, L., Renard, M., 2008. Nature and origin of carbonate particles along a transect on the western margin of Great Bahama Bank (Middle Miocene): sedimentary processes and depositional model. Bull. Soc. Geol. Fr. 179 (3), 231–244.
Turpin, M., Emmanuel, L., Reijmer, J.J.G., Renard, M., 2011. Whiting-related sediment export along the middle-miocene carbonate ramp of the great Bahama Bank. Int. J. Earth Sci. 100, 1875–1893.
Turpin, M., Gressier, V., Bahamonde, J.R., Immenhauser, A., 2014. Component-specific petrographic and geochemical characterization of fine-grained carbonates along Carboniferous and Jurassic platform-to-basin transects. Sediment. Geol. 300, 62–85. https://doi.org/10.1016/j.sedgeo.2013.11.004.
Van Simaeys, S., Rendall, B., Lucia, F.J., Kerans, C., Fullmer, S., 2017. Facies-independent reservoir characterization of the micropore-dominated word field (edwards formation), lavaca county, Texas. AAPG (Am. Assoc. Pet. Geol.) Bull. 101 (1), 73–94.
Vaughan, T.W., 1917. Chemical and organic deposits of the sea. Bull. Geol. Soc. Am. 28 (1), 933–944.
Volery, C., Davaud, E., Foubert, A., Caline, B., 2009. Shallow-marine microporous carbonate reservoir rocks in the Middle East: relationship with seawater Mg/Ca ratio and eustatic sea level. J. Pet. Geol. 32 (4), 313–325.
Volery, C., Davaud, E., Foubert, A., Caline, B., 2010a. Lacustrine microporous micrites of the madrid basin (late Miocene, Spain) as analogues for shallow-marine carbonates of the mishrif reservoir formation (cenomanian to early turonian, Middle East). Facies 56 (3), 385–397.
Volery, C., Davaud, E., Durlet, C., Clavel, B., Charollais, J., Caline, B., 2010b. Microporous and tight limestones in the Urgonian Formation (late Hauterivian to early Aptian) of the French Jura Mountains: focus on the factors controlling the formation of microporous facies. Sediment. Geol. 230, 21–34. https://doi.org/10.1016/j.sedgeo.2010.06.017.
Walter, L.M., 1983. The Dissolution Kinetics of Shallow Water Carbonate Grains: Effects of Mineralogy, Microstructure and Solution Chemistry. unpublished Ph.D. dissertation. University of Miami, pp. 320.
Walter, L.M., Morse, J.W., 1985. The dissolution kinetics of shallow marine carbonates in seawater: a laboratory study. Geochem. Cosmochim. Acta 49 (7), 1503–1513.
Wells, A.J., Illing, L.V., 1964. Present-day precipitation of calcium carbonate in the Persian Gulf. In: Developments in Sedimentology, vol. 1. Elsevier, pp. 429–435.
Wendt, J., 1990. The first aragonitic rugose coral. J. Paleontol. 64 (3), 335–340.
Westphal, H., 1998. Carbonate Platform Slopes—A Record of Changing Conditions. Lecture Notes in Earth Sciences, vol. 75 Springer-Verlag, New York.
Westphal, H., Munnecke, A., 1997. Mechanical compaction versus early cementation in fine-grained limestones: differentiation by the preservation of organic microfossils. Sediment. Geol. 112 (1–2), 33–42.
Westphal, H., Reijmer, J.J.G., Head, M.J., 1999. Input and diagenesis on a carbonate slope (Bahamas): response to morphology evolution and sea-level fluctuations. In: In: Harris, P.M., Saller, A.H., Simo, J.A., Handford, R. (Eds.), Advances in Carbonate Sequence Stratigraphy - Application to Reservoirs, Outcrops and Models, vol. 63. Spec. Publ. SEPM, pp. 247–274.
Westphal, H., Head, M.J., Munnecke, A., 2000. Differential diagenesis of rhythmic limestone alternations supported by palynological evidence. J. Sediment. Res. 70, 715–725.
Wiggins, W.D., 1986. Geochemical signatures in carbonate matrix and their relation to deposition and diagenesis, Pennsylvanian Marble Falls Limestone, Central Texas. J. Sediment. Petrol. 56, 771–783.
Wilkinson, B.H., 1979. Biomineralisation, paleoceanography and the evolution of calcareous marine organisms. Geology 7, 524–527.
Wilkinson, B.H., Given, R.K., 1986. Secular variation in abiotic marine carbonates: constraints on Phanerozoic atmospheric carbon dioxide contents and oceanic Mg/Ca ratios. J. Geol. 94 (3), 321–333.
Wilkinson, B.H., Owen, R.M., Carroll, A.R., 1985. Submarine hydrothermal weathering, global eustasy, and carbonate polymorphism in Phanerozoic marine oolites. J. Sediment. Res. 55 (2), 171–183.
Wilson, J.L., 1975. Carbonate Facies in Geologic History. Springer-Verlag 471 pp.
Wood, A., 1941. “Algal dust” and the finer-grained varieties of Carboniferous limestone. Geol. Mag. 78 (3), 192–200.
Wray, J.L., 1977. Calcareous Algae (Developments in Paleontology and Stratigraphy No. 4). Elsevier, New York 185 pp.
Wright, V.P., Zarza, A.A., Sanz, M.E., Calvo, J.P., 1997. Diagenesis of late Miocene micritic lacustrine carbonates, Madrid Basin, Spain. Sediment. Geol. 114 (1–4), 81–95.
Yates, K.K., Robbins, L.L., 1998. Production of carbonate sediments by a unicellular green alga. Am. Mineral. 83 (11), 1503–1509.
Zharkov, M.A., 1984. Paleozoic Salt Bearing Formations of the World. Springer Verlag, New York.